INFORMATION TO USERS

This manuscript has been reproduced from the microfilm master. UMI films the text directly from the original or copy submitted. Thus, some thesis and dissertation copies are in typewriter face, while others may be from any type of computer printer.

The quality of this reproduction is dependent upon the quality of the copy submitted. Broken or indistinct print, colored or poor quality illustrations and photographs, print bleedthrough, substandard margins, and improper alignment can adversely affect reproduction.

In the unlikely event that the author did not send UMI a complete manuscript and there are missing pages, these will be noted. Also, if unauthorized copyright material had to be removed, a note will indicate the deletion.

Oversize materials (e.g., maps, drawings, charts) are reproduced by sectioning the original, beginning at the upper left-hand corner and continuing from left to right in equal sections with small overlaps.

Photographs included in the original manuscript have been reproduced xerographically in this copy. Higher quality 6" x 9" black and white photographic prints are available for any photographs or illustrations appearing in this copy for an additional charge. Contact UMI directly to order.

Bell & Howell Information and Learning
300 North Zeeb Road, Ann Arbor, MI 48106-1346 USA
800-521-0600

UMI®

METALLOGENY OF EPITHERMAL GOLD AND BASE METAL VEINS OF THE SOUTHERN DAWSON RANGE, YUKON

by

Katherine A. Smuk

Department of Earth and Planetary Sciences
McGill University
Montréal, Québec, Canada

March, 1999

A thesis submitted to the Faculty of Graduate Studies and Research in partial fulfilment of the requirements of the degree of Master of Science

Abstract

Epithermal veins of the southern Dawson Range, Yukon, are hosted by a wide range of lithologies, ranging from Proterozoic metasedimentary rocks to Late Cretaceous volcanic rocks. Both the 105 Ma calc-alkaline Mount Nansen volcanic group and the 70 Ma shoshonitic Carmacks volcanic group also host small Au-Cu(±Mo) porphyry deposits. Although the structurally-controlled mineralized veins are spatially associated with Mount Nansen felsic dykes, K/Ar dates for sericitically and argillically altered dykes proximal to mineralization are ~70 Ma, indicating thermal resetting by a Carmacks-age hydrothermal event. These altered dykes are depleted in Na, Pb, Zn, and Cu, but enriched in As and Sb, relative to unaltered dykes.

The base metal-rich epithermal veins are transitional between classic low and high sulphidation deposit types. They were deposited by a Na^+-dominated fluid with an average salinity of ~6 wt.% NaCl equiv., a temperature of ~300°C, a high S^{2-} (0.20 *m*) concentration, and significant CO_2 (~1 mol.%). The isotopic composition of inclusion fluids ($\delta^{18}O$=~-10 ‰; δD=~-95 ‰) indicate that the hydrothermal fluid was dominantly meteoric, but a magmatic fluid contribution is suggested by the heavy $\delta^{18}O$, $\delta^{34}S$ values close to zero, and the high temperatures, salinities, ΣS, and CO_2. The isotopic compositions of Pb in galena correlate well with initial whole rock values for Carmacks volcanic rocks, suggesting that much of the Pb, and other base metals, were leached from the Carmacks volcanics. As and Sb, and by inference Au, are not locally derived.

The log $fO2$ and pH conditions of mineralization were between -34 and -36, and 3-5, respectively. The deposition of base metal sulphides appears to have been caused by an increase in pH due to the consumption of H^+ during the alteration of the host rocks. The decrease in ΣS caused by sulphide precipitation destabilized $Au(HS)_2^-$ complexes, precipitating native gold. The mineralization was caused by the hydrothermal circulation of acidic, meteoric water, probably driven by Carmacks magmatism.

Résumé

Les veines épithermales du sud de la chaîne de Dawson au Yukon sont contenues dans un large éventail de lithologies, allant d'assemblages métasédimentaires Protérozoïques à des roches volcaniques du Crétacé. Les deux groupes volcaniques du Crétacé, le groupe calco-alcalin de Mount Nansen daté à 105 Ma et le groupe shoshonitique de Carmacks daté à 70 Ma, contiennent également de petits gisements porphyriques de Au-Cu (±Mo). Bien que les veines minéralisées et controllées structuralement soient associées spatialement aux dykes felsiques du groupe de Mount Nansen, les datations K/Ar des dykes les plus argilitisés et séricitisés proches des veines donnent des âges d'environ 70 Ma, semblant indiquer un 'reset' thermique par un événement hydrothermal d'âge équivallent à celui du groupe de Carmacks. Ces dykes altérés sont appauvris en Na, Pb, Zn et Cu et enrichis en As et Sb.

Les veines épithermales riches en métaux de base ont des caractéristiques intermédiaires entre les types classiques de sulfuration faible et élevée. Elles ont été déposées à partir d'un fluide dominé par Na^+ ayant une salinité moyenne d'environ 6% en poids de NaCl équivalent, une température de 300°C, de fortes concentrations en Cl^- (1 *m*) et en S^{2-} (0.2 *m*), et une quantité significative de CO_2 (~ 1 % molaire). La composition isotopique des inclusions fluides ($\delta^{18}O$=~-10 ‰; δD=~-95 ‰) indique que le fluide était principalement d'origine météorique, mais les valeurs élevées en $\delta^{18}O$, en isotopes du soufre ($\delta^{34}S$=~-1.0 ‰), en température, en salinité, en ΣS et en CO_2 suggèrent la contribution d'un fluide magmatique. Les compositions isotopiques en Pb des galènes sont bien corrélées avec les valeurs isotopiques initiales de la roche totale du groupe de Carmacks, suggérant que le Pb et les autres métaux de base ont été lessivés des roches volcaniques du groupe de Carmacks. Les éléments As et Sb, et par déduction Au, ont été introduits par le fluide hydrothermal.

Les conditions de log $fO2$ et de pH de minéralisation sont respectivement comprises entre –34 et –36, et <5. La déposition de sulfures de métaux de base à partir de complexes chlorés semble être due à une augmentation de pH causée par la

consommation d'ions H^+ au cours de l'altération des roches encaissantes. La diminution en ΣS causée par la précipitation de sulfates a déstabilisé les complexes $Au(HS)_2^-$. La minéralisation semble être liée à la circulation d'un fluide hydrothermal dominé par de l'eau météorique, certainement apporté par le groupe de Carmacks.

Preface

This thesis consists of five chapters. The third chapter has been published, in 1997, as an unrefereed paper in "Yukon Geology and Exploration 1996". The fourth chapter is also in manuscript format, and is intended for submission to a refereed journal. Both manuscripts have been integrated as chapters formatted to the general layout of the thesis.

The following is excerpted from Guidelines for Thesis Preparation, Faculty of Graduate Studies and Research, McGill University:

> "Candidates have the option of including, as part of the thesis, the text of one or more papers submitted for publication, or the clearly-duplicated text of one or more published papers. These texts must be bound as an integral part of the thesis.
>
> If this option is chosen, connecting texts that provide logical bridges between the different papers are mandatory. The thesis must be written in such a way that it is more than a mere collection of manuscripts; in other words, results of a series of papers must be integrated.
>
> The thesis must still conform to all other requirements of the "Guidelines for Thesis Preparation". The thesis must include: A Table of Contents, an abstract in English and French, an introduction which clearly states the rationale and objectives of the study, a review of the literature, a final conclusion and summary, and a thorough bibliography or reference list.
>
> Additional material must be provided where appropriate (e.g. in appendices) and in sufficient detail to allow a clear and precise judgement to be made of the importance and originality of the research reported in the thesis.
>
> In the case of manuscripts co-authored by the candidate and others, the candidate is required to make an explicit statement in the thesis as to who contributed to such work and to what extent. Supervisors must attest to the accuracy of such statements at the doctoral oral defence. Since the task of the examiners is made more difficult in these cases, it is in the candidate's interest to make perfectly clear the responsibilities of all the authors of the co-authored papers."

Sampling, petrography, fluid inclusion work, gas chromatography, scanning electron microscopy, and electron microprobe analyses were performed by the author. XRF whole rock analyses were performed by T. Ahmedali at the Department of Earth and Planetary Sciences, McGill University. $^{40}Ar/^{39}Ar$ age determinations were obtained by D. Lux at the University of Maine. Oxygen and hydrogen isotopic analyses were performed by Dr. K. Kyser at Queen's University, sulphur isotopic analyses by N. Morriset at the Ottawa-Carlton Geoscience Centre Stable Isotope Facility, and lead isotopes by Dr. C. Gariépy at GEOTOP at the Université du Québec à Montréal.

Contributions of Authors

Funding for this project was provided by an NSERC strategic grant to Drs. D. Francis and A. E. Williams-Jones, and comprises a complementary part of an ongoing study by D. Francis focussing on the Carmacks volcanic group. The thesis author, K. Smuk, is responsible for all the new scientific data on the mineral deposits and alteration of the host rocks of the southern Dawson Range.

Drs. Williams-Jones and Francis acted as research supervisors and advised the author during the critical evaluation of data and the logical development of the scientific concepts expressed in the thesis.

Acknowledgements

Several individuals made additional important contributions to the preparation of this thesis: at McGill University, G. Panagiotidis prepared thin sections, Drs. W. Halter and E. Sakoma assisted with gas chromatographic analyses, G. Poirier guided microprobe analyses, D. Palmer assisted with the SEM and microprobe, and A.-C. Abraham prepared a French translation of the abstract. C. Hart of the Yukon Geology Program provided fluid inclusion data and valuable discussion.

Drs. D. Francis and A. E. Williams-Jones are thanked for their ideas and their tolerance.

Table of Contents

List of Figures

List of Tables

Chapter 1
General Introduction

1.1 General Statement

Numerous detailed studies have shown that epithermal vein deposits throughout the Cordillera of North and South America share many common characteristics. These common features include: a shallow depth of formation (<1500 metres), an association with igneous activity, and economic concentrations of gold and silver typically with only subordinate base metals (e.g. Hayba et al., 1985; Panteleyev, 1986; Heald et al., 1987). These epithermal deposits are believed to be deeper expressions of surface hot springs, in which predominantly meteoric hydrothermal fluids deposit metals in veins or breccias at temperatures up to 400°C, as a result of changes in fluid physicochemistry.

Epithermal deposits can be divided into high sulphidation, or acid-sulphate, and low sulphidation, or adularia-sericite, types based on alteration and ore mineralogy (Hayba et al., 1985; Heald et al., 1987). High sulphidation epithermal deposits contain sulphide minerals with a high sulphur to metal ratio, such as enargite, luzonite, and covellite, associated with characteristic argillic alteration assemblages dominated by alunite or pyrophyllite (Sillitoe, 1993). High sulphidation deposits are thought to form from acidic, sulphur-rich, oxidized fluids, generated by the condensation of SO_2-rich magmatic volatiles (Heald et al., 1987). Low sulphidation epithermal deposits contain sulphide minerals with lower sulphur to metal ratios and are associated with potassic, sericitic, argillic, or chloritic alteration. They are thought to form from near-neutral, sulphur-poor, reduced fluids dominated by meteoric water (Sillitoe, 1993) (Table 1.1).

Sillitoe (1989) demonstrated that low sulphidation, adularia-sericite deposits are found in the peripheries and upper parts of porphyry molybdenum deposits, whereas both low sulphidation and high sulphidation gold deposits form in the upper parts of porphyry copper-gold, copper-molybdenum, and tin systems. Building on the proposed relationship of epithermal gold deposits with underlying porphyry systems, Panteleyev (1986) proposed a "Canadian Cordilleran Epithermal Model", based on the Toodoggone camp of British Columbia, which infers the existence of a continuum from porphyry

Table 1.1 Brief comparison of epithermal deposit types. Dawson Range epithermal vein characteristics are indicated in italicized type.

LOW SULPHIDATION (ADULARIA-SERICITE)	HIGH SULPHIDATION (ACID-SULPHATE)
Ore Characteristics	**Ore Characteristics**
high base metal proportion 1/3 of known deposits	common high base metal proportion
high Ag:Au (due to Ag-sulphides, sulphosalts)	high Au:Ag
variable Cu	high Cu
texture: veins, cavity filling, breccias - highly variable	texture: replacement, breccias, veins - little variation
Au, Ag, Zn, Pb (Cu, Sb, As, Hg, Se)	Cu, Au, Ag, As (Pb, Hg, Sb, Te, Sn, Mo, Bi)
pyrite, electrum, Au, sphalerite, galena, (arsenopyrite)	*pyrite, enargite, chalcopyrite, tennantite,* covellite, Au, tellurides
no specific characteristic assemblage	typical assemblage of enargite-luzonite + pyrite ± covellite
rare: *enargite-luzonite, tennantite*, covellite	rare: *electrum, pyrargyrite, arsenopyrite*
Alteration	**Alteration**
characteristic adularia + *sericite*	characteristic alunite + *kaolinite*
quartz, chalcedony, calcite, adularia, illite, *carbonate*	*quartz*, alunite, *barite, kaolinite, pyrophyllite*
no alunite (except supergene)	*no adularia (Dawson Range?)*
chlorite	*no chlorite*
± selenides, rhodochrosite, fluorite	*no selenides, rhodochrosite, fluorite*
zoning: K-feldspar + quartz + chlorite with ore -> sericitic ± argillite further -> propylitic furthest	zoning: *advanced argillic + quartz with ore -> argillic ± sericitic further -> propylitic furthest*
common reaction: plagioclase -> montmorillonite ->kaolinite	common reaction: *K-spar -> sericite -> kaolinite* -> alunite
Fluid Characteristics	**Fluid Characteristics**
near neutral pH (4-7)	*very low pH (2-4)*
predominantly meteoric (5-10% magmatic?)	magmatic-meteoric
low fS_2 (0.01 *m* range), no magmatic SO_2	*high fS_2 (0.1 m range)*, magmatic SO_2
low CO_2 (~ 0.15-0.40 mol.%)	*higher CO_2 (~ 0.15-14 mol.%)*
Cl-rich	*S-rich*
Pb from older country rocks	*Pb from volcanics* or magmatic fluids
reduced	oxidized
higher FeS in sphalerite (~ 1-4 mol.% or >)	low FeS in sphalerite (<1 mol.%)
Geology	**Geology**
volcanic association unclear, usually much later	*common close volcanic association*
highly variable host lithologies	common volcanic host lithology
andesite-rhyolite association (also shoshonitic + alkalic suites)	andesite-dacite association
Cu-porphyry link unclear	*possible Cu-porphyry link*
extensive, high lateral flow	restricted area and extent

Compiled from Hedenquist et al., 1996; Heald et al., 1987; Hayba et al., 1985; and Graney and Kesler, 1995.
Note that these are general and common epithermal deposit characteristics, but are by no means invariable or absolute. Dawson Range deposit characteristics are similarly variable.

copper and skarn through transitional (mesothermal) deposits, to epithermal veins, and hot spring discharge deposits (see also Dawson et al., 1991). Similar continuum models have been proposed by Bonham (1989) and Sillitoe (1993) for epithermal deposits in the western United States, and Sillitoe (1989) and Mitchell and Balce (1990) for epithermal deposits in western Pacific island arcs.

Additional important features of both types of epithermal deposits include a ubiquitous association in space and time with calc-alkaline igneous activity, and thus an inferred correlation with subduction-related magmatism, and a possible genetic relationship with felsic intrusive rocks (Sawkins, 1972). The epithermal deposits of the Circum-Pacific are predominantly Tertiary in age (some later Mesozoic), and typically occur at elevations 2000 to 4000 metres above sea level, and are commonly removed by erosion (Sawkins, 1972; Sillitoe, 1989; Table 1.2). An alternate sub-class of epithermal gold deposits is the "alkalic-type" (typically low sulphidation), associated with potassic or shoshonitic ("alkalic") magmatism (Richards, 1995).

The northernmost portion of the western Cordillera, in the Yukon Territory and British Columbia, hosts numerous porphyry, mesothermal, and epithermal deposits. Typically the epithermal deposits are attractive exploration targets because they generally have high precious-to-base metal ratios (Panteleyev, 1986), for example, the Jurassic Toodoggone (Thiersch et al, 1997), and Eocene Mount Skukum (Love, 1989) camps. Table 1.2 briefly summarizes the main features of a selection of Canadian Cordilleran epithermal deposits, and includes several mesothermal, or transitional (Nesbitt et al., 1986; Panteleyev, 1986; Nesbitt and Muehlenbachs, 1989) Cordilleran deposits for comparison.

The gold-bearing polymetallic vein deposits of the southern Dawson Range, Yukon Territory, comprise an extensive series of structurally controlled gold-rich base-metal sulphide veins hosted by a wide variety of local rock types. They are thought to be

Table 1.2 Summary of selected Canadian Cordilleran vein deposits

Name	Ore	Ag/Au	% S[1]	Deposit Type	Deposit Age	Host Rock	Mineralogy [2]	Alteration
Epithermal								
Dusty Mac, B.C.	Ag, Au, (Cu, Pb)	21	<15	adularia-sericite	Eocene	sandstone, shale, Tertiary andesite and pyroclastics of White Lake Fm.	py, (cpy, bn, gal, sph, Ag)	Si, Ch, Cb
Blackdome, B.C.	Ag, Au	3	minor	adularia-sericite transitional	Eocene	calc-alkaline rhyolitic to andesitic volcanics and volcaniclastic sediments	Au + Ag, el, ac, frb, Ag-ss, aguilarite, naumannite, (py, po, mc, cpy, bn, aspy, sph, gal, tte)	Si, P, A, Pr
Equity Silver, B.C.	Ag, Cu, Au, Sb	210-128	present	adularia-sericite (acid-sulphate?) transitional	Eocene	dacite, tuff, volcanic conglomerate of Goosly Sequence	py, cpy, mt, po, hm, tte, sph, mc, aspy, Au, gal, ss	A, Ph
Cinola, B.C.	Au	21	<10	adularia-sericite hotspring (Carlin-type?)	Miocene	conglomerate, sandstone, shale of Skonun Fm.	py, mc, (rt, po, hm, mt, sph, cpy, gal, Au, cn, tiemannite)	Si, A, Ph, Pr
Silbak-Premier, Stewart-Iskut Camp, B.C.	Au, (Ag, Pb, Zn, Cu)	112-5 (23)	5-45	adularia-sericite	Jurassic	andesite, dacite, Hazelton volcanic conglomerates and tuffs	py, sph, gal, cpy, po, ac, tte, Pb/Ag-ss, sb, el, Au, Ag, Hg, cc, bar, ad	Si, P, Ph, Pr
Shasta Toodoggone Camp, B.C.	Au, Ag		minor	quartz-kaolinite-alunite	E. Jurassic	high-K andesite-dacite lapilli tuffs and flows of Toodoggone Fm.	ac, el, Ag, (cpy, sph, gal)	P
Mount Skukum, Y.T.	Au, Ag	0.9	<1	adularia-sericite	Eocene	andesites of Mt. Skukum complex, Sloko Volcanic Province	1) ch + py, po,sph, cpy, very low Au-Ag 2) el qtz-carb-ser veins	P, Si, Ph, Pr
Venus, Y.T.	Ag	26	15-60	adularia-sericite (mesothermal?)	Paleocene	andesite of Hutshi Grp., bt-quartz monzonite	aspy, py, sph, gal, (pyr, cpy, frb, rlg, orp, jm, sb, ag)	Si, Ph, A
Mt. Nansen, Y.T.	Ag, Au	39 (13-21)	>60	adularia-sericite	Cretaceous	metaseds, intrusives, and Mt. Nansen volcanic rocks	py, aspy, sph, gal, cpy, sb, various ss	Ph, A, (P)
Laforma, Y.T.	Au, Ag	2	present	adularia-sericite	Cretaceous	granodiorite, quartz syenite	cc, ank, cpy, sph, bar, gal, aspy, ss	Ph
Sixtymile River Area, Y.T.	Au Ag		present	adularia-sericite	Cretaceous ?	andesite of Carmacks (?) Gp.	1) py, aspy, gal, sph, cpy, mo, Au 2) gal, sph, py, po, aspy, cpy, gal, ss	A
Mesothermal								
Fairview Camp, B.C.	Au, Ag		<1	quartz vein	Eocene ?	Carboniferous schists of Kobau Gp.	py, gal, sph, cpy, (bn, tte, ac, bl), Au	Si, (Cb, Ph)
Erickson Cassiar District, B.C.	Au	1-0.1	3-15	quartz vein	E. Cretaceous	Sylvester Gp. mafic volcanic, sedimentary, ultramafic rocks	py, po, aspy, cpy, gal, sph, tte, Au	Cb, (Si, A)
Sixtymile River Area, Y.T.	Au		minor	qtz-carb-sulphide veins	Eocene ?	Precambrian to Paleozoic metamorphic rocks	py, aspy, po; py, aspy, gal, py, sph, cpy, frb	Ph, P, Pr
Klondike Area, Y.T.	Au		trace	quartz vein	E. Cretaceous	meta sedimentary and meta-igneous lithologies of Yukon-Tanana terrane	gal +/- sph, aspy, po, tte, Au, bar	Cb (py, Ph)

[1] Approximate proportion of sulphide minerals in mineralized zones
[2] Where known, listed in approximate order of abundance; bracketed are minor phases

Mineral Abbreviations: ac=acanthite/argentite, ad=adularia, ank=ankerite, aspy=arsenopyrite, bar=barite, bl=boulangerite, bn=bornite, carb=carbonate, cc=calcite, ch=chlorite, cn=cinnabar, cpy=chalcopyrite, el=electrum, frb=freibergite, gal=galena, hm=hematite, jm=jamesonite, mc=marcasite, mo=molybdenite, mt=magnetite, orp=orpiment, po=pyrrhotite, py=pyrite, pyr=pyrargyrite, rlg=realgar, rt=rutile, sb=stibnite, sph=sphalerite, ss=sulphosalts, tte=tetrahedrite/tenantite
Alteration Abbreviations: A=argillic, Cb=carbonate, Ch=chloritic, P=potassic, Ph=phyllic, Pr=propyltic, Si=silicic

Table 1.2 *continued*

Name	Temp. (°C)	NaCl (wt.%)	Depth	$\delta^{18}O$	δD	Reference
Epithermal						
Dusty Mac, B.C.	230-250	<1	140-460 m	-7 to -9	-133	Taylor, 1996; Zhang et al., 1989; Nesbitt et al., 1986
Blackdome, B.C.	285	~1.2	0.3-1.4 km	-6.8 to -8.8	-125 to -134	Taylor, 1996; Dawson et al., 1991; Vivian et al., 1987
Equity Silver, B.C.	220-300	>5	1 km			Taylor, 1996; Panteleyev, 1986; Schroeter and Panteleyev, 1986; Cyr et al., 1984; Wojdak and Sinclair, 1984; Barr, 1980
Cinola, B.C.	160, 270	0.5	1.1-1.8 km	+13 to +16	~-70	Taylor, 1996; Champigny and Sinclair, 1982; Shen et al., 1982
Silbak-Premier, Stewart-Iskut Camp, B.C.	250	<1-4				Taylor, 1996, Grove, 1971; Panteleyev, 1986
Shasta	225	1.5	295-775 m	-1.6 to -1.4	-148 to -171	Thiersch et al., 1997; Diakow et al., 1991
Toodoggone Camp, B.C.	280			-4 to -3.5		
Mount Skukum, Y.T.	313	0.7	470 m	-11 to -14	~-160	McDonald, 1990; Love, 1989; McDonald et al., 1986; Nesbitt et al., 1986
	330	4.1				
	250	0.9				
Venus, Y.T.	180-240	5-9		+5	-160	Taylor, 1996; Nesbitt and Muehlenbachs, 1989; Walton and Nesbitt, 1986; McFaull, 1981; Morin, 1981
Mt. Nansen, Y.T.	~290	5-10	~1 km	-10 to -13	-85 to -100	Hart and Langdon, 1997; Sawyer and Dickinson, 1986; Saager and Bianconi, 1971; this study
Laforma, Y.T.	185	2-4.5	1-1.5 km	-18.4	-138	McInnes et al., 1990; McInnes, 1987
	(165-430)	(4-43)				
Sixtymile River Area, Y.T.	200-300	2-2.5				Glasmacher and Friedrich, 1992a; Glasmacher, 1990
	165-275	<8.6				
Mesothermal						
Fairview Camp, B.C.	280-330	3-6	<1 km	+4 to +6	-121 to -148	Zhang et al., 1989
Erickson	350		~2 km	+1 to +6	-160 to -130	Sketchley and Sinclair, 1991; Anderson and Hodgson, 1989; Nesbitt et al., 1986; Sketchley et al., 1986
Cassiar District, B.C.						
Sixtymile River Area, Y.T.	~330	6-18				Glasmacher, 1992b
Klondike Area, Y.T.	200-350	3.5-6	1-7 km	+8.3	-150	Rushton et al., 1993; Mortensen et al., 1992

genetically related to one of the two volcanic suites preserved in this area: the mid-Cretaceous, high-K calc-alkaline Mount Nansen group or the Late Cretaceous, shoshonitic Carmacks volcanic group. They exhibit many of the features of adularia-sericite, low sulphidation epithermal deposits (Hayba et al., 1985; Heald et al., 1987), which comprise virtually all epithermal deposits in the Canadian Cordillera, although they also share some characteristics of acid-sulphate, high sulphidation deposits (Table 1.1). The following study investigates the occurrence of gold in the numerous atypical adularia-sericite epithermal vein deposits of the southern Dawson Range, and attempts to place them in the context of a regional metallogenic event.

1.2 Dawson Range Gold Belt: Exploration History and Previous Work

The Yukon Territory is host to many types of mineralization, including porphyry copper deposits, epithermal vein deposits, and, perhaps most famously, placer gold deposits. One area of extensive placer gold production is the Dawson Range of south central Yukon, commonly referred to as the "Dawson Range gold belt" (Hart et al., 1998). This belt comprises a 60 km-long north-westerly trend of placer gold occurrences, porphyry copper-gold showings, and gold-bearing polymetallic epithermal veins. During the time of the Klondike gold rush around Dawson City, placer gold was also discovered in the Dawson Range around Mount Nansen and Freegold Mountain, approximately 50 kilometres west of the town of Carmacks (Figure 2.1). The first placer claims in the Dawson Range were staked on Discovery Creek in the Mt. Nansen area in 1910 (Cairnes, 1917), while the first lode claim was staked nearby in 1917 (Sawyer and Dickinson, 1976). Since the 1940s, the southern Dawson Range has enjoyed considerable exploration and small-scale production. An examination of the angular morphology of placer gold deposits in the Mount Nansen camp (LeBarge, 1995) has confirmed that the sources of placer gold are local lode deposits.

The Dawson Range was first mapped by Cairnes (1917) and then by Bostock (1936) who first noted the close correlation of gold showings with felsic dykes, and by Johnston (1937). The first published 1:30,000 scale maps were completed by Carlson (1987) and Payne et al. (1987). Assessment reports by prospectors and exploration companies also provide more detailed maps, albeit of limited coverage. The Yukon Minfile (1996) describes approximately 35 gold and base metal vein and porphyry prospects in the Dawson Range, from the Mount Nansen area in the south to the Prospector Mountain camp in the north (Figure 2.2). Two deposits have been mined in the past, the Mt. Nansen and the Laforma deposits. The Mt. Nansen gold mine operated briefly in 1968-1969 and was reopened in 1996 (Hart and Langdon, 1998; Sawyer and Dickinson, 1976) using a cyanide circuit on oxide ore. The Laforma gold mine operated in 1939-1940 and is currently being re-evaluated because of the rehabilitation of the nearby Mt. Nansen mill.

Several mineral deposits of the southern Dawson Range have been the subjects of scientific study. McInnes et al. (1987, 1988, 1990) conducted a study of the Laforma gold deposit, and two nearby prospects, the Antoniuk gold-bearing porphyry/breccia and the Emmons Hill polymetallic vein gold deposit, all in the Freegold Mountain camp (Figure 2.2, Table 1.2). They also studied the petrology of the plutonic host rocks and Mount Nansen rhyolitic dykes. The Frog and Lilypad prospects of the Prospector Mountain area have been investigated by Glasmacher (1990). He and Grond et al. (1984) also provided a description of the Carmacks volcanic group. Hart and Langdon (1998) completed a study of the geology and mineral occurrences of the Mount Nansen camp, and Anderson and Stroshein (1998) mapped the geology of the Flex vein system in the Mount Nansen camp.

There has been considerable confusion in the past over the physicochemical differences between, and the ages of, the Mount Nansen and the Carmacks volcanic groups of the Dawson Range. Consequently, an understanding of the association of mineralization with either volcanic group has been difficult. Mineralization has generally

been attributed to the Mount Nansen volcanic event due to the proximity of mineralized veins to felsic dykes, which have been assigned to the Mount Nansen group on the basis of field relationships (Carlson, 1987; McInnes, 1987). McInnes (1987, 1988) determined an age of 77.5 ± 3.1 Ma from a single altered rhyolitic dyke at the Laforma deposit using the K/Ar method, and interpreted this date, along with dates from the Carmacks volcanic group from Grond et al. (1984) (68 to 73 Ma), as the age of the Mt. Nansen volcanics. More recent radiometric dating has, however, established an average age of 70 Ma for the Carmacks group volcanics (Stevens et al., 1982; Templeman-Kluit, 1984; Johnston, 1995; Johnston et al., 1996; Wynne et al., 1998; this study), and an average age of 105 Ma for the Mount Nansen Group (Templeman-Kluit, 1984; Carlson, 1987; Hunt and Roddick, 1991; this study). Because of this confusion, a clearer understanding of the relationship between these two volcanic groups and gold metallogeny is needed in the Dawson Range.

2.3 Objectives

This study comprises a detailed investigation of five mineral deposits in the Dawson Range Gold Belt: the Huestis and Tawa properties in the Mount Nansen camp, the Tinta Hill and Emmons Hill properties in the Freegold Mountain camp, and the Frog prospect at Prospector Mountain. Data collected from the mineral deposits include petrography, fluid inclusion microthermometry and gas chromatography, oxygen and hydrogen, sulphur, and lead isotopes. In a parallel study, whole-rock analyses and $^{40}Ar/^{39}Ar$ age determinations were conducted on samples of the Mount Nansen and Carmacks volcanics collected from a large number of widely spaced localities in order to: chemically differentiate them, to obtain reliable ages of emplacement, and to constrain chemical change associated with hydrothermal alteration related to ore deposition. The objective of this study is to use the above geochemical data to highlight the similarities and differences between the five studied epithermal deposits of the southern Dawson Range in order to: characterize the controls on gold and base metal deposition, and

determine whether the mineralization is related to the Mount Nansen or the Carmacks magmatic events.

2.5 References

Anderson, F., and Stroshein, R., 1998, Geology of the Flex gold-silver vein system, Mount Nansen area, Yukon: Yukon Exploration and Geology 1997, Exploration and Geological Services Division, Yukon, Indian and Northern Affairs Canada, p. 139-143.

Anderson, P. G., and Hodgson, C. J., 1989, The structure and geological development of the Erickson gold mine, Cassiar District, British Columbia, with implications for the origin of mother-lode-type gold deposits: Canadian Journal of Earth Sciences, v. 26, p. 2645-2660.

Barr, D. A., 1980, Gold in the Canadian Cordillera: Canadian Institute of Mining and Metallurgy Bulletin, v. 73, no. 818, p. 59-76.

Bonham, Jr., H. F., 1989, Bulk Mineable Gold Deposits of the Western United States: Economic Geology Monograph 6, p. 193-207.

Bostock, H. S., 1936, Carmacks District, Yukon: Geological Survey of Canada Memoir 189, 67 p.

Cairnes, D. D., 1917, Investigations and Mapping in Yukon Territory: Geological Survey of Canada, Memoir 284.

Carlson, G. G., 1987, Geology of Mount Nansen (115-I/3) and Stoddart Creek (115-I/6) Map Areas, Dawson Range, Central Yukon: Indian and Northern Affairs Canada, Northern Affairs: Yukon Region Open File 1987-2.

Champigny, N., and Sinclair, A. J., 1982, The Cinola Gold Deposit, Queen Charlotte Islands, British Columbia: Geology of Canadian Gold Deposits, Canadian Institute of Mining and Metallurgy Special Volume 24, p. 243-254.

Cyr, J. B., Pease, R. P., and Schroeter, T. G., 1984, Geology and Mineralization at Equity Silver Mine: Economic Geology, v. 79, p. 947-968.

Dawson, K. M., Panteleyev, A., Sutherland-Brown, A., and Woodsworth, G. J., 1991, Regional Metallogeny, Chapter 19: Geology of the Canadian Cordillera, (ed.) H. Gabrielse, C.J. Yorath, Geological Survey of Canada, Geology of Canada, No. 4, p. 707-768.

Diakow, L. J., Panteleyev, A., and Schroeter, T. G., 1991, Jurassic Epithermal Deposits in the Toodoggone River Area, Northern British Columbia: Examples of Well-Preserved, Volcanic-Hosted, Precious Metal Mineralization: Economic Geology, v. 86, p. 529-554.

Glasmacher, U., 1990, Petrogenetische und metallogeneitsche Entwicklung ausgewahlter Gebiete im 'Yukon – Tanana Terrane' und 'Stikine Terrane', (Yukon Territorium, Kanada) wahrend der Oberkreide und des Alttertiars: Mitteilungen zur Mineralogie und Lagerstattenkunde, Nr. 38, Aachen University Ph.D. Thesis, 605 p.

Glasmacher, U., and Friedrich, G., 1992a, Volcanic-hosted epithermal gold-sulphide mineralization and associated enrichment processes, Sixtymile River area, Yukon Territory, Canada: Yukon Geology, v. 3, Exploration and Geological Services Division, Yukon, Indian and Northern Affairs Canada, p. 271-291.

Glasmacher, U., and Friedrich, G., 1992b, Gold-sulphide enrichment processes in mesothermal veins of the Sixtymile River area, Yukon Territory, Canada: Yukon Geology, v. 3, Exploration and Geological Services Division, Yukon, Indian and Northern Affairs Canada, p. 292-311.

Grond, H. C., Churchill, S. J., Armstrong, R. L., Harakal, J. E., and Nixon, G. T., 1984, Late Cretaceous age of the Hutshi, Mount Nansen, and Carmacks groups, southwestern Yukon Territory and northwestern British Columbia: Canadian Journal of Earth Sciences, v. 21, p. 554-558.

Grove, E. W., 1971, Geology and Mineral Deposits of the Stewart Area, Northwestern British Columbia: British Columbia Department of Mines and Petroleum Resources, Bulletin No. 58, 219 p.

Hart, C. J. R., and Langdon, M., 1998, Geology and mineral deposits of the Mount Nansen camp, Yukon: Yukon Exploration and Geology 1997, Exploration and Geological Services Division, Yukon, Indian and Northern Affairs Canada, p. 129-138.

Hayba, D. O., Bethke, P. M., Heald, P., and Foley, N.K., 1985, Geologic, Mineralogic, and Geochemical Characteristics of Volcanic-Hosted Epithermal Precious-Metal

Deposits: Geology and Geochemistry of Epithermal Systems, Reviews in Economic Geology, v. 2, p. 129-167.

Heald, P., Foley, N. K., and Hayba, D. O., 1987, Comparative Anatomy of Volcanic-Hosted Epithermal Deposits: Acid-Sulfate and Adularia-Sericite Types: Economic Geology, v. 82, p. 1-26.

Hedenquist, J. W., Izawa, E., Arribas, A., and White, N. C., 1996, Epithermal gold deposits: Styles, characteristics, and exploration: Resource Geology Special Publication Number 1, 16 p.

Hunt, P. A., and Roddick, J. C., 1991, A Compilation of K-Ar Ages, Report 20: Radiogenic Age and Isotopic Studies: Report 4, Geological Survey of Canada, Paper 90-2, p. 113-143.

Johnston, J. R., 1937, Geology and mineral deposits of Freegold Mountain, Carmacks District, Yukon: Geological Survey of Canada, Memoir 214, 21 p.

Johnston, S. T., 1995, Geological Compilation with Interpretation from Geophysical Surveys of the Northern Dawson Range, Central Yukon (115 J/9 and 10, 115 I/12, 1:100 000 Scale Map): Exploration and Geological Services Division, Department of Indian and Northern Affairs Open File 1995-2(G).

Johnston, S. T., Wynne, P. J., Francis, D., Hart, C. J. R., Enkin, R. J., and Engebretson, D. C., 1996, Yellowstone in Yukon: The Late Cretaceous Carmacks Group: Geology, v. 26, p. 997-1000.

LeBarge, W. P., 1995, Sedimentology of Placer Gravels Near Mt. Nansen, Central Yukon Territory: Bulletin 4, Exploration and Geological Services Division, Indian and Northern Affairs Canada, Yukon Region, 155 p.

Love, D.A., 1989, Geology of the Epithermal Mount Skukum Gold Deposit, Yukon Territory: Geological Survey of Canada Open File 2123, 47 p.

McDonald, B. W. D., 1990, Geology and genesis of the Mount Skukum epithermal gold-silver deposits, southwestern Yukon Territory (NTS 105D 3, 6): Exploration and Geological Services Division, Yukon Region, Bulletin 2, 65 p.

McDonald, B. W. R., Stewart, E. B., and Godwin, C. I., 1986, Exploration geology of the Mt. Skukum epithermal gold deposit, southwestern Yukon: Yukon Geology, v. 1,

Exploration and Geological Services Division, Yukon, Indian and Northern Affairs Canada, p. 11-18.

McFaull, J., 1981, The Geology and Mineralization of the Venus Pb-Zn-Ag Mine, Yukon Territory (abstract): Paper 46, Canadian Institute of Mining and Metallurgy Bulletin, v. 74, No. 833, p. 64.

McInnes, B. I. A., 1987, Geological and precious metal evolution at Freegold Mountain, Dawson Range, Yukon: unpublished M.Sc. thesis, McMaster University, 230 p.

McInnes, B. I. A., Goodfellow, W. D., Crocket, J. H., and McNutt, R. H., 1988, Geology, geochemistry and geochronology of subvolcanic intrusions associated with gold deposits at Freegold Mountain, Dawson Range, Yukon: Current Research, Part E, Geological Survey of Canada, Paper 88-1E, p. 137-151.

McInnes, B. I. A., Crocket, J. H., and Goodfellow, W. D., 1990, The Laforma deposit, an atypical epithermal-Au system at Freegold Mountain, Yukon Territory, Canada: Epithermal Gold Mineralization of the Circum-Pacific: Geology, Geochemistry, Origin and Exploration, II, (ed.) J.W. Hedenquist, N.C. White, and G. Siddeley, Journal of Geochemical Exploration, v. 36, p. 73-102.

Mitchell, A. H. G., and Balce, G. R., 1990, Geological features of some epithermal gold systems, Philippines: Epithermal Gold Mineralization of the Circum-Pacific: Geology, Geochemistry, Origin and Exploration, II, (ed.) J.W. Hedenquist, N.C. White, and G. Siddeley, Journal of Geochemical Exploration, v. 35, p. 241-296.

Morin, J. A., 1981, Element distribution in Yukon gold-silver deposits: Yukon Geology and Exploration 1979-80, Exploration and Geological Services Division, Yukon, Indian and Northern Affairs Canada, p. 68-84.

Mortensen, J. K., Nesbitt, B. E., and Rushton, R., 1992, Preliminary observations on the geology and geochemistry of quartz veins in the Klondike district, West-Central Yukon: Yukon Geology, v. 3, Exploration and Geological services Division, Indian and Northern Affairs Canada, p. 260-270.

Nesbitt, B. E., and Muehlenbachs, K., 1989, Geology, Geochemistry, and Genesis of Mesothermal Lode Gold Deposits of the Canadian Cordillera: Evidence for Ore

Formation from Evolved Meteoric Water: Economic Geology Monograph 6, p. 553-563.

Nesbitt, B. E., Murowchick, J. B., and Muehlenbachs, K., 1986, Dual origins of lode gold deposits in the Canadian Cordillera: Geology, v. 14, p. 506-509.

Panteleyev, A., 1986, A Canadian Cordilleran Model for Epithermal Gold-Silver Deposits: Geoscience Canada, v. 13, p. 101-111.

Payne, J. G., Gonzalez, R. A., Akhurst, K., and Sisson, W. G., 1987, Geology of Colorado Creek (115-J/10), Selwyn River (115-J/9), and Prospector Mountain (115-I/5) Map Areas, Western Dawson Range, West-Central Yukon: Indian and Northern Affairs Canada, Northern Affairs: Yukon Region Open File 1987-3.

Richards, J. P., 1995, Alkalic-type epithermal gold deposits – a review: Magmas, Fluids, and Ore Deposits, MAC Short Course, (ed.). J.F.H. Thompson, p. 367-400.

Rushton, R. W., Nesbitt, B. E., Muehlenbachs, K., and Mortensen, J. K., 1993, A Fluid Inclusion and Stable Isotope Study of Au Quartz Veins in the Klondike District, Yukon Territory, Canada: A Section through a Mesothermal Vein System: Economic Geology, v. 88, p. 647-678.

Saager, K., and Bianconi, F., 1971, The Mount Nansen Gold-Silver Deposit, Yukon Territory, Canada: Mineralium Deposita, v. 6, p. 209-224.

Sawkins, F. J., 1972, Sulfide ore deposits in relation to plate tectonics: Journal of Geology, v. 80, p. 377-397.

Sawyer, J. P. B., and Dickinson, R. A., 1976, Mount Nansen: Paper 34, Part B - Porphyry Copper and Copper-Molybdenum deposits of the Calc-Alkaline Suite: Porphyry Deposits of the Canadian Cordillera, Canadian Institute of Mining and Metallurgy Special Volume 15, p. 336-343.

Schroeter, T. G., and Panteleyev, A., 1986, Lode gold-silver deposits in northwestern British Columbia: Mineral Deposits of Northern Cordillera, Canadian Institute of Mining and Metallurgy Special Volume 37, p. 178-190.

Shen, K., Champigny, N., and Sinclair, A. J., 1982, Fluid Inclusion and Sulphur Isotope Data in Relation to Genesis of the Cinola Gold Deposit, Queen Charlotte

Islands, B.C.: Geology of Canadian Ore Deposits, Canadian Institute of Mining and Metallurgy Special Volume 24, p. 255-257.

Sillitoe, R. H., 1989, Gold Deposits in Western Pacific Island Arcs: The Magmatic Connection: Economic Geology Monograph 6, p. 274-290.

Sillitoe, R. H., 1993, Epithermal Models: Genetic Types, Geometric Controls and Shallow Features: Mineral Deposit Modeling, (ed.) R. V. Kirkham, W. D. Sinclair, R. I. Thorpe, J. M. Duke, Geological Association of Canada, Special Paper 40, p. 403-417.

Sketchley, D. A., and Sinclair, A. J., 1991, Carbonate Alteration in Basalt, Total Erickson Gold Mine, Cassiar, Northern British Columbia, Canada: Economic Geology, v. 86, p. 570-587.

Sketchley, D. A., Sinclair, A. J., and Godwin, C. I., 1986, Early Cretaceous gold-silver mineralization in the Sylvester allochton, near Cassiar, north central British Columbia: Canadian Journal of Earth Sciences, v. 23, p. 1455-1458.

Stevens, R. D., Delabio, R. N., and Lachance, G. R., 1982, Age determinations and geological studies; K-Ar isotopic ages, Report 16: Geological Survey of Canada, Paper 82-2, 52 p.

Taylor, B., 1996, Epithermal gold deposits: Geology of Canadian Mineral Deposit Types, (ed.) O.R. Eckstrand, W.D. Sinclair, and R.I. Thorpe, Geological Survey of Canada, Geology of Canada, no. 8, p. 329-350.

Tempelman-Kluit, D. J., 1984, Geology of the Lebarge and Carmacks Map Sheets: Geological Survey of Canada, Open File 1101, map sheets with legends.

Thiersch, P. C., Williams-Jones, A. E., and Clark, J. R., 1997, Epithermal mineralization and ore controls of the Shasta Au-Ag deposit, Toodoggone District, British Columbia, Canada: Mineralium Deposita, v. 32, p. 44-57.

Vivian, G., Morton, R. D., Changkakoti, A., and Gray, J., 1987, Blackdome Eocene epithermal Ag-Au deposit, British Columbia, Canada – nature of ore fluids: Transactions of the Institution of Mining and Metallurgy (Section B: Applied earth science), v. 96, p. B9-B14.

Walton, L., and Nesbitt, B. E., 1986, Evidence for late-stage Au-galena mineralization in the Venus arsenopyrite-pyrite-quartz vein, southwest Yukon (abstract): Program with Abstracts, Geological Association of Canada – Mineralogical Association of Canada, Annual Meeting, Ottawa, 1986, v. 11, p. 141.

Wojdak, P. J., and Sinclair, A. J., 1984, Equity Silver Silver-Copper-Gold Deposit: Alteration and Fluid Inclusion Studies: Economic Geology, v. 79, p. 969-990.

Wynne, P. J., Enkin, R. J., Baker, J., Johnston, S. T., and Hart, C. J. R., 1998, The big flush: paleomagnetic signature of a 70 Ma regional hydrothermal event in displaced rocks of the northern Canadian Cordillera: Canadian Journal of Earth Sciences, v. 35, p. 657-671.

Yukon Minfile, 1996. Version 2.05, May 31, 1996: Exploration and Geological Services Division, Indian and Northern Affairs Canada.

Zhang, X., Nesbitt, B. E., and Muehlenbachs, K., 1989, Gold Mineralization in the Okanagan Valley, Southern British Columbia: Fluid Inclusion and Stable Isotope Studies: Economic Geology, v. 84, p. 410-424.

Chapter 2

Geology of the Southern Dawson Range

2.1 Tectonic Setting

The southern end of the Dawson Range study area is located at approximately 62°N in southwest-central Yukon, within the northern Canadian Cordillera. The Canadian Cordillera can be divided into five tectonic belts comprised of allochthonous terranes accreted onto the ancestral North American craton along the Tintina fault (Fig. 2.1), a structure which preserves a strike-slip motion of over 400 km (Gabrielse, 1985). The Dawson Range, a volcano-plutonic mountain range floored by meta-sedimentary assemblages, straddles the Yukon-Tanana (Kootenay and Nisling) and Stikinia Terranes. The Yukon-Tanana terrane has been recently divided into the Kootenay terrane, a pericratonic terrane derived from contiguous North American basement, and the Nisling terrane, a displaced continental margin sequence comprising metamorphosed Proterozoic to Paleozoic passive continental margin strata and partly metamorphosed carbonaceous and siliceous off-shelf sedimentary rocks (Clowes, 1997). The Stikinia terrane consists of Devonian to Lower Jurassic platform carbonates, island arc volcanic rocks and comagmatic plutons, and volcaniclastic rocks (Clowes, 1997). By the mid-Cretaceous, terrane accretion was essentially complete, and Late Cretaceous and younger magmatic events throughout the belt are thought to be related to terrane dislocation and deformation (Yorath, 1991). Gold mineralization in the southern Dawson Range postdates completion of terrane accretion, occurring in epithermal veins hosted by a variety of country rocks belonging to both the Yukon-Tanana and the Stikinia terranes. Past authors have linked the golf mineralization to either the mid-Cretaceous Mount Nansen or the Late Cretaceous Carmacks magmatic events (e.g. Carlson, 1987; McInnes, 1987; Glasmacher, 1990; Hart and Langdon, 1998). The diversity of sedimentary and volcanic country rocks implies a large range of possible sources for gold and base metal mineralization.

Paleomagnetic evidence consistently suggests that the Canadian Cordilleran terranes originated at considerable distances south of their present latitudes. Umhoefer (1987), Irving and Wynne (1990), and Engebretson et al. (1985) have suggested that the northern Cordillera was at the latitude of Baja California at 100-90 Ma, and has

Figure 2.1 Regional tectonic setting of south-central Yukon and location of the southern Dawson Range study area (outlined area refers to Fig. 2.2). Terrane boundaries are interpreted from Journeay and Williams (1995). Y-T - Yukon-Tanana Terrane; N.A. - North America; SK - Stikine Terrane; CC - Cache Creek Terrane; CPB - Coast Plutonic Belt.

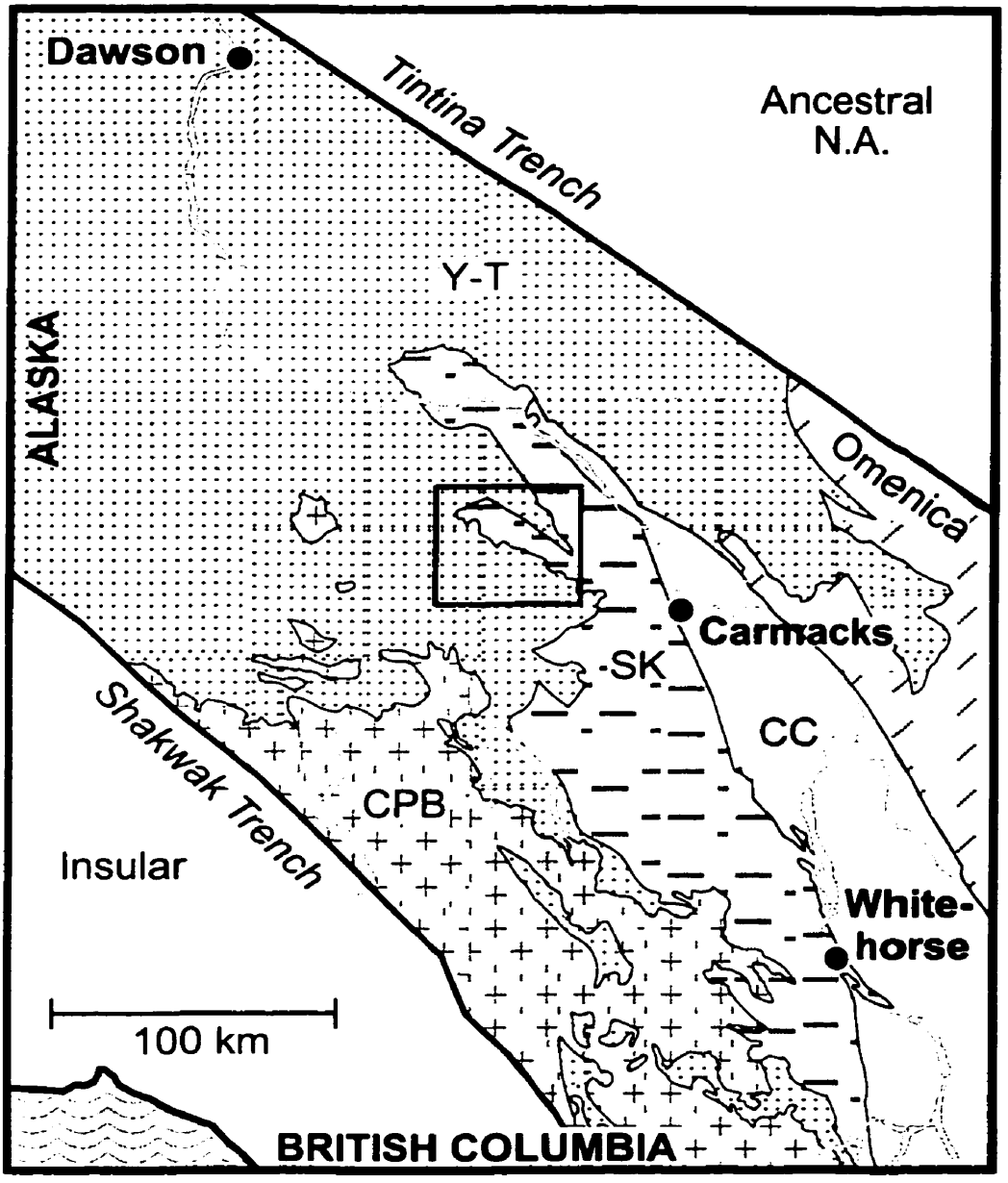
Dawson
Tintina Trench
Ancestral
N.A.
Y-T
ALASKA
Omenica
Carmacks
SK
CC
Shakwak Trench
CPB
Insular
White-
horse
100 km
BRITISH COLUMBIA

dislocated northwards a distance of some 2000 km by about 55 Ma with respect to the North American continent. Wynne et al. (1998), Johnston et al. (1996), and Marquis and Globerman (1988) suggest that the Carmacks group was erupted 1900 ± 700 km south of its present latitude on the basis of paleomagnetic studies, around present-day Oregon at 70 Ma. Mineralization in the Dawson Range is thus interpreted to have developed in the amalgamated Yukon-Tanana and Stikinia terranes between about 105 and 70 Ma, a minimum of 2000 kilometres south of the present latitude. This invites comparisons with metallogenic regions associated with the Yellowstone hotspot in the Western American Cordillera. For example, Oppliger et al. (1997) have related the Carlin gold trend in Nevada to the 40-30 Ma position of the Yellowstone hotspot.

2.2 Physiography and Glacial History

The Dawson Range is part of the Yukon Plateau Physiographic Province (Carlson, 1987), which is characterized by a moderately rugged topographic expression with elevations ranging from 900 to over 2000 metres (3000-6500 feet) above sea level. The highest peak is Apex Mountain, which reaches an elevation of 2022 metres (6634 feet). Treeline is at approximately 1400 metres elevation, below which thick, low brush is the dominant vegetation type, down to the valleys that are wooded with coniferous forest. North-facing slopes at or below treeline are generally covered with thick moss, due to permafrost, while south-facing slopes are drier and often grassy.

Four glacial events have been recognized in the central Yukon: the Nansen and Klaza (1.08-0.84 Ma), Reid (150-42.9 Ka) and McConnell (29.6-10.3 Ka) advances (LeBarge, 1995). The Dawson Range study area escaped the Reid and McConnell glaciations, and as a result the area is deeply weathered and has assumed a smoothed profile in which ridges are generally continuous, connected by narrow saddles, and valleys are "U" shaped. Outcrop is rare except for castellated outcrops at ridge tops. Mapping has been facilitated by the observation that talus or felsenmeer on slopes has travelled only short distances (metre-scale), and thus is a fairly accurate indication of the

underlying bedrock. Prospecting and exploration mapping is generally accomplished by bulldozer trenching.

2.3 Local Structure

The general structural fabric in the Dawson Range runs approximately north-northwest - south-southeast, reflecting the trend of the Dawson Range and the Tintina fault. The largest structure in the Dawson Range study area is the Big Creek fault, a normal fault with southwest side down motion (Carlson, 1987), which appears to follow the valley of Big Creek in the northern part of the study area. According to McInnes (1987) there is also a dextral displacement of at least 14 kilometres on the Big Creek fault. An incision in the valley side just south of Big Creek, and Carlson's (1987) observation that geological characteristics south of the creek are observed for a short distance to the north, puts the exact location of the Big Creek fault into question. The Big Creek fault continues, or splays, to the southeast, through or just north of Freegold Mountain (possibly equivalent to the Camp fault (McInnes, 1987)).

The principal stress direction during Cretaceous deformation in the northern Cordillera was 160° (Gabrielse, 1985), and numerous smaller faults parallel to the general northwest orientation of the Big Creek fault are found throughout the study area, and exhibit both normal and dextral strike-slip motion (McInnes et al., 1988; Hart and Langdon, 1998) (Figure 2.2). The majority of felsic dykes and mineralized veins also follow this dominant trend. A second set of smaller-scale, sinistral faults oriented at 020° host ore blow-outs in the Mt. Nansen vein system, where they intersect the earlier northwest-trending faults and (Hart and Langdon, 1998). The Laforma gold vein is hosted by one of these 020° structures. A final set of east-northeast-trending (050°-080°) sinistral faults is prominent in geological maps of the study area (Carlson, 1997; Payne et al., 1997), but does not appear to be related to mineralization. Felsic dyke and mineralized vein orientations are dominantly northwest in the Mount Nansen camp, while north-northeast trends are most common at Freegold and Prospector Mountains.

Figure 2.2 Geology map of the southern Dawson Range, modified from Carlson (1987) and Payne et al. (1987). Indicated on the map are the three main exploration camps (Mount Nansen, Freegold Mountain, and Prospector Mountain) and all gold and base metal deposits or prospects (Yukon Minfile, 1996).

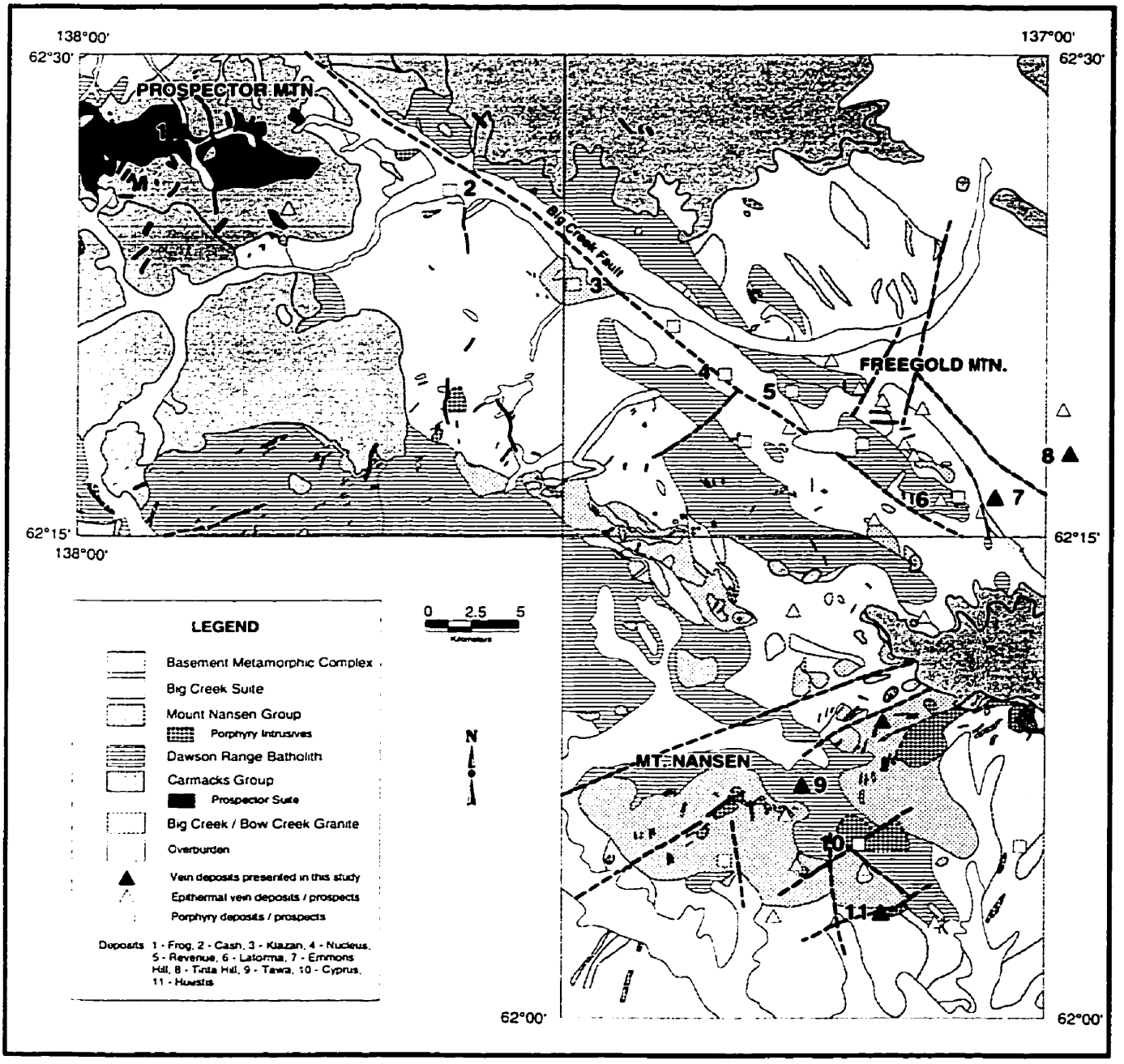
138°00'
137°00'
62°30'
62°15'
62°00'
PROSPECTOR MTN.
FREEGOLD MTN.
MT. NANSEN
Big Creek Fault
1
2
3
4
5
6
7
8
9
10
11
LEGEND
Basement Metamorphic Complex
Big Creek Suite
Mount Nansen Group
Porphyry Intrusives
Dawson Range Batholith
Carmacks Group
Prospector Suite
Big Creek / Bow Creek Granite
Overburden
Vein deposits presented in this study
Epithermal vein deposits / prospects
Porphyry deposits / prospects
Deposits 1 - Frog, 2 - Cash, 3 - Klazan, 4 - Nucleus, 5 - Revenue, 6 - Latorma, 7 - Emmons Hill, 8 - Tinta Hill, 9 - Tawa, 10 - Cyprus, 11 - Huestis
0 2.5 5
Kilometers
N

2.4 Dawson Range Lithologies

This section provides a detailed description of the lithologies that make up the southern Dawson Range and host the numerous mineral occurrences therein and addresses the discrepancies between the historic assignment of ages and names to these units.

2.4.1 Basement Metamorphic Complex

Basement rocks outcrop primarily in the Mount Nansen area, where they exhibit a north-striking structural grain and northeasterly-trending fold axes (Sawyer and Dickinson, 1976). The Basement Metamorphic Complex comprises a lower metasedimentary unit of quartzite, quartz-feldspar-mica schist, quartz-feldspar gneiss, and limestone, and an upper "schist and gneiss" unit comprising a foliated plutonic unit of intermediate composition, a granitic gneiss, a layered gneissic unit, and amphibolite (Carlson, 1987). Payne et al. (1987) recognized igneous protoliths to many of the metamorphosed rock types within these two units. The Complex is Paleozoic to Proterozoic in age (Tempelman-Kluit and Wanless, 1980), and the grade of metamorphism varies from greenschist to lower amphibolite facies (Payne et al., 1987). The rocks are characterized by a well-developed gneissic foliation generally metamorphic in origin, although original bedding is locally recognizable (Carlson, 1987).

2.4.2 Big Creek Meta-Plutonic Suite

The Big Creek meta-plutonic Suite is a prominent unit that outcrops on both sides of the Big Creek fault, and is covered to the northwest and the southeast by later volcanics. The suite is dominated by the weakly foliated Big Creek Syenite, which is characterized by very coarse, pink, tabular K-feldspar in a matrix of hornblende, plagioclase and quartz and should properly be classified as a monzonite. A second intrusive rock type in the Big Creek Suite consists of plagioclase, hornblende and quartz,

and lacks the K-feldspar megacrysts (Carlson, 1987). A hornblendite has been included as a third subunit, but is likely just a hornblende-rich phase or segregation of the main intrusive unit (Payne et al., 1987). The Suite was emplaced at approximately 184 Ma (Tempelman-Kluit, 1984), and locally preserves a strong tectonic foliation interpreted to be due to Late Jurassic uplift (Carlson, 1987).

Included in the Big Creek Meta-Plutonic Suite is Carlson's (1987) Klotassin Meta-Plutonic Suite, or "Granite Batholith" (Tempelman-Kluit, 1984). The Granite Batholith is dated at approximately 192 Ma (Tempelman-Kluit, 1984), and is essentially a foliated, coarse-grained, hornblende-biotite diorite to granodiorite. Major phases in this lithology include 50-75% plagioclase, with lesser quartz, K-feldspar, hornblende, and biotite (Carlson, 1987). The Klotassin Batholith may be a distinct unit of the Big Creek Meta-Plutonic Suite, but has commonly been considered to be part of the Dawson Range Batholith because plutonic units with the name "Klotassin" have yielded ages ranging from 200 Ma down to 95 Ma (Godwin, 1975; Tempelman-Kluit and Wanless, 1975; Le Couteur and Tempelman-Kluit, 1976). One interpretation for these conflicting ages is that the ages of the Jurassic Klotassin units have been reset by a mid-Cretaceous magmatic event represented by the Coffee Creek Granite (see Section 2.4.4) (Tempelman-Kluit and Wanless, 1975; Le Couteur and Tempelman-Kluit, 1976). The name "Granite Batholith" will be used preferentially for this Jurassic granodiorite unit.

2.4.3 Mount Nansen Group

The Mount Nansen group is a high-potassium volcanic and plutonic suite that was probably emplaced in a volcanic arc environment related to convergence of the Pacific Plate with the Cordilleran Insular Superterrane (Souther, 1991). Volcanic rocks of the Mount Nansen group, now relatively isolated in and around the Mount Nansen mining camp, consist largely of coarse volcanic breccia and small felsite flows and/or high-level domes. Previous workers have documented a few andesite lava flows (Carlson, 1987; Payne et al., 1987), and mafic flows occur on Klaza Mountain. The volcanic breccias are

typically bimodal, consisting of rounded andesite and rhyolite fragments. The andesite is typically dark green to grey, with sparse phenocrysts of feldspar, pyroxene, hornblende and/or biotite, now variably chloritized and epidotized as a result of recrystallization under greenschist facies metamorphic conditions. Rhyolite fragments are very fine-grained, rarely porphyritic, and consist primarily of quartz and feldspar that is generally altered to sericite and clay.

The Mount Nansen group also includes a prominent swarm of felsic, porphyritic dykes found throughout the study area. These dykes have an average age of 105 Ma (Chapter 3; Tempelman-Kluit, 1984; Carlson, 1987; Hunt and Roddick, 1991) obtained from both U/Pb and K/Ar methods on relatively unaltered samples from areas peripheral to the mining camps. Dykes which have been dated by K/Ar near areas of known mineralization appear to record an alteration age of approximately 70-75 Ma (Chapter 3; Stevens et al., 1982; Grond et al., 1984; McInnes et al., 1985; Hunt and Roddick, 1991). The dykes are typically quartz- and feldspar-phyric, and are commonly sericitically and argillically altered. These Mount Nansen felsic dykes have previously been thought to be genetically as well as spatially related to lode gold mineralization in the southern Dawson Range (Carlson, 1987; McInnes, 1987; Yukon Minfile, 1996; Hart and Langdon, 1998).

2.4.4 Dawson Range Batholith

The Dawson Range Batholith is believed to be essentially comagmatic with the Mount Nansen suite, although it ranges in age from 105 to 90 Ma (Tempelman-Kluit and Wanless, 1975; 1980; Le Couteur and Tempelman-Kluit, 1976). This unit is exposed almost continuously from Carmacks northwest to Alaska, and is believed to have intruded the Yukon-Tanana Terrane as extensive sheet-like sills (Hart and Langdon, 1998). The exposure of such a large area of plutonic rock implies a large degree of erosion since mid-Cretaceous time (Souther, 1991). The Dawson Range Batholith includes the Casino Granodiorite, a prominent unit throughout the study area dated at 106 Ma (Carlson, 1987). This unfoliated biotite-hornblende granodiorite is generally weakly altered, and is

locally segregated into biotite- and hornblende-rich varieties. The Coffee Creek Granite appears to be closely related to the Casino Granodiorite and outcrops primarily along the Big Creek fault. This coarse-grained unit ranges in composition from granite to quartz monzonite and has an age of approximately 95 Ma (Tempelman-Kluit and Wanless, 1975; Le Couteur and Tempelman-Kluit, 1976).

The Dawson Range Batholith has included the Klotassin Suite Granodiorite, which, according to Godwin (1975) and Tempelman-Kluit and Wanless (1975), has an average age of 95 Ma. However, because this unit is more likely originally of Jurassic age (Section 2.4.2), the term "Klotassin" is not here applied to the Dawson Range Batholith, although the term "Klotassin Suite Granodiorite" has been used in Chapter 3 for part of the Dawson Range Batholith.

2.4.5 Carmacks Group

The Carmacks group is a widespread volcanic series characterized by localized thick lower units of andesitic tuffs and breccias, succeeded by an upper unit of extensive basaltic flows. The Carmacks group outcrops in large isolated exposures from Whitehorse to Dawson, and is believed to have covered most of southwest-central Yukon at one time (Johnston et al., 1996). The Carmacks volcanic group has an average age of 70 Ma (Stevens et al., 1982; Grond et al., 1984; Tempelman-Kluit, 1984; Johnston, 1995; Lowey et al., 1986; this study), with individual age determinations from widespread localities ranging from 65 to 71 Ma.

The Carmacks volcanic group appears to have been deposited over a surface with appreciable relief (Souther, 1991), and the contact of the lower volcaniclastic Carmacks unit with underlying lithologies is defined by a slight (<10°) angular unconformity (Johnston et al., 1996). The Carmacks volcaniclastic unit can be divided into a lower succession (200-500 metres) of volcanic breccias, tuffs, and minor thin flows, largely of andesitic composition, which grades into a 400-500 metre-thick unit of interbedded

ankaramitic basalt, tuffs and flows. This lower unit is overlain by a 500-metre upper succession of thick, extensive, basaltic flows. All the lava flows of the Carmacks group in the Dawson Range area are shoshonitic in character, being highly potassic, enriched in large ion lithophile and light rare earth elements, and depleted in the high field strength elements. The ankaramitic flows are strongly olivine- and clinopyroxene-phyric, contain up to 15 wt.% MgO, with MgO peaking at the transition between the lower and upper volcanic successions. The lavas are commonly amygdaloidal, with amygdules up to 10 cm in diameter filled with chalcedonic and rarely drusy quartz or carbonate, reflecting zeolite facies metamorphic conditions.

There was little intrusive activity associated with the Carmacks event compared to the Mount Nansen event. Two small intrusions have been shown to be contemporaneous with the Carmacks group; the Prospector Suite, a granitic plug exposed at Prospector Mountain, and the Patton Porphyry at the Casino deposit, north of the study area (Godwin, 1975; Tempelman-Kluit, 1984; Selby and Nesbitt, 1998). A swarm of feldspar-phyric (± mafic phenocrysts such as biotite and pyroxene), mafic to intermediate dykes is also found throughout the southern Dawson Range, with similar orientations to the felsic dykes of the Mount Nansen group. These dykes are typically sericitized and carbonatized, especially in the three mining camps. The alteration and significance of dykes of the Carmacks group will be discussed further in Chapter 3.

The Carmacks group had been interpreted previously as having formed in a subduction-related arc or transtensional, pull-apart environment (Souther, 1991). Grond et al. (1984) interpreted the potassic character of the Carmacks group as being representative of an arc-distal or back-arc tectonic setting. However, several lines of evidence suggest that the Carmacks group may have affinities with flood basalts, including: the absence of coeval volcanism along the rest of the Canadian Cordillera, the paucity of contemporaneous felsic intrusive rocks, the extensive flat-lying upper basalt flows, and the primitive compositions of the ankaramitic lavas (Francis and Johnston, 1998; Johnston et al., 1996). Wynne et al. (1998) and Johnston et al. (1996) present

paleomagnetic data showing the remagnetization of older units in the south-central Yukon to a remanent direction identical to that obtained from the Carmacks group, suggesting that the Carmacks group may be a Late Cretaceous expression of the Yellowstone hotspot, which is believed to have caused large-scale, regional hydrothermal circulation.

2.4.6 Big Creek / Bow Creek Granite

This intrusion comprises medium- to fine-grained biotite quartz monzonite to granite, fine-grained alaskitic granophyre, and a very fine-grained, porphyritic border phase. The border phase has been dated at approximately 60 Ma (Carlson, 1987), although an earlier biotite K/Ar date of 85 Ma was obtained by Tempelman-Kluit (1984). This unit is spatially associated with Mount Nansen volcanic rocks, and outcrops north of Mount Nansen and Victoria Mountain. Tempelman-Kluit (1984) originally correlated the Bow Creek Granite with the Mount Nansen group based on age and location, but Carlson (1987) relates it to the Carmacks group volcanics because of its Paleocene age and similarity to glassy felsites and felsic pyroclastics at the base of the Carmacks group.

2.5 Mineralization

Few epithermal veins in the southern Dawson Range are hosted by volcanic rocks, but rather by the plutonic rocks of the Big Creek Suite and the Dawson Range Batholith, or by meta-sedimentary basement rocks. The notable exception to this generalization is the Frog deposit at Prospector Mountain, which is hosted by the lower succession of the Carmacks volcanic group. The Big Creek porphyry deposits, however, are hosted by Mount Nansen stocks, while the Casino porphyry deposit is hosted by the Patton Porphyry of the Carmacks group. This observation appears to indicate the existence of two separate metallogenic events, and poses the problem of the volcanic association of the mineralized epithermal veins in non-volcanic host rocks.

The Huestis, Tawa, Tinta Hill, Emmons Hill, and Frog deposits are the main focus of this thesis, and are discussed in detail in Chapter 4. The purpose of this following section is to detail the geology and mineralization of other deposits found in the southern Dawson Range in order to provide context for a discussion of the regional metallogeny.

2.5.1 Mount Nansen Camp

Mount Nansen Vein Mineralization

The "Mount Nansen trend" (Hart and Langdon, 1998) comprises a series of gold-bearing veins that stretches for approximately 12 kilometres in a northwest-southeast trending horst immediately east and southeast of Mount Nansen. The rocks are dominated by granites of the Dawson Range Batholith and schists and gneisses of the Basement Metamorphic Complex. Andesitic volcaniclastic rocks of the Mount Nansen group are also present, but do not host the majority of the vein mineralization. From southeast to northwest, the Mount Nansen trend includes: the Brown-McDade zone, the Huestis-Flex-Webber vein system, the Spud and Orloff-King zones, the Goulter showing (now Willow Creek, Eliza North, Eliza South, and Eliza Extension), the Cyprus, Kelly and Etzel porphyries, and the Dic and Tawa veins (Yukon Minfile, 1996; Hart and Langdon, 1998). The Tawa or Esansee prospect on the northeastern flank of Mount Nansen is the inferred northwesternmost extension of the Mount Nansen vein system.

The Mount Nansen trend is gold-rich; Saager and Bianconi (1971) report a gold fineness of approximately 800 from the Huestis deposit, while Lister (1989) reports a fineness of 750 from the Brown-McDade zone. This study concentrates on the Huestis and Tawa veins, as representatives of the Mount Nansen epithermal camp, which are detailed in Chapter 4.

Cyprus Porphyry

The Cyprus copper-molybdenum porphyry deposit occurs in Mount Nansen group quartz- and feldspar-phyric felsic stocks and associated quartz-tourmaline breccias. The host rocks are part of the Mount Nansen porphyry complex, a three-kilometre long zone following the Mount Nansen trend characterized by porphyritic dykes, small plugs of quartz monzonite and quartz diorite, and associated breccia pipes. Hypogene mineralization in the porphyry complex includes, in order of decreasing abundance; disseminated pyrite and chalcopyrite, and veinlet molybdenite, galena, sphalerite and gold, with chalcocite and covellite occurring as supergene minerals (Sawyer and Dickinson, 1976). The deep hypogene zone averages 0.1 to 0.15 wt.% Cu and 0.01 wt.% MoS_2, with sporadic higher grades of up to 0.6 wt.% Cu and 0.06 wt.% MoS_2 (Sawyer and Dickinson, 1976). These grades double in the overlying, 150 metre-thick supergene zone. Leaching of the porphyry has completely oxidized the primary sulphides to depths of 70 metres below surface. Gold grades ranging up to 0.99 g/t Au (Yukon Minfile, 1996) are associated with quartz fracture fillings not affected by leaching.

The Cyprus porphyry deposit exhibits four types of alteration (Sawyer and Dickinson, 1976). Quartz-tourmaline alteration is present in breccia bodies, and is characterized by the mineral assemblage of quartz, tourmaline and sericite, and accessory kaolinite and apatite. The breccia clasts are silicified, sericitized, and variably kaolinitized, and the tourmaline occurs disseminated in the breccia matrix. Potassic alteration is also reported in the central brecciated part of the porphyry system (Hart and Langdon, 1998). These brecciated centres are surrounded by haloes of phyllic alteration, composed of quartz, sericite, pyrite and kaolinite. Outside the phyllic zone, a widespread argillic alteration zone has been developed, characterized by kaolinite, quartz, and minor sericite. Propylitic alteration, recognized by the assemblage epidote, clinozoisite, albite, chlorite, leucoxene, carbonate, pyrite, and minor sericite and clay minerals, has affected most of the host Dawson Range Batholith, and is attributed to supergene processes by Sawyer and Dickinson (1976) but may reflect greenschist facies metamorphism. Hart and

Langdon (1998) propose a controversial mineralization model in which the Mount Nansen porphyry complex is the deep magmatic portion of a porphyry to epithermal magmatic-hydrothermal system, linking the Cyprus deposit with the Huestis and Tawa vein systems. The porphyry deposits are also thought to be the source of the extensive placer gold deposits in the Mount Nansen area (Hart and Langdon, 1998).

2.5.2 Freegold Camp (including Big Creek Trend)

Tinta Hill

The Tinta Hill deposit lies 6.4 kilometres east of Freegold Mountain, on the flank of Granite Mountain. The prospect comprises a series of quartz-sulphide veins that occur in a near vertical, northwest-trending (300°) shear zone that is at least 3500 metres long (Bostock, 1936; INAC, 1990) and up to 30 metres wide (Yukon Minfile, 1996), and is still open at both ends. Morin (1981) reports high values of Pb, Zn, Cu, Ag, Cd, Mo, Sb and Hg, and lower values of Mn, As, Tl and B, associated with Tinta Hill veins. The Tinta Hill deposit is described in detail in Chapter 4.

Emmons Hill

The Emmons Hill quartz-barite-carbonate-sulphide vein and breccia zone is hosted by the Basement Metamorphic Complex in a window in the Big Creek meta-plutonic Suite. Morin (1981) found unspecified concentrations of Au, Ag, Hg, As, Sb, Zn, Pb, and $BaSO_4$ in the vein material, and the Yukon Minfile (1996) reports barite, stibnite, cinnabar, orpiment, ferroan carbonates and chalcedonic quartz (McInnes, 1987, also reports the presence of marcasite), suggestive of a high-level "hot-spring"-type hydrothermal system.

McInnes (1987) has classified the Emmons Hill deposit as a high-level vein/breccia system. He reported fluid inclusion homogenization temperatures of

140°-185°C and salinities of 0-0.5 wt.% NaCl equivalent in samples of barite. Barite (δD_{H_2O}) and calcite ($\delta^{18}O$) from the deposit recorded non-meteoric water isotopic signatures, and sulphur isotopic values of 2-3‰ implied a magmatic sulphur source. The deposit was thought to have been emplaced in a near-surface, oxidizing environment from a low-temperature, low-pH boiling hydrothermal fluid. McInnes (1987) interpreted the Emmons Hill deposit as a fossil hot spring system coeval with Mount Nansen rhyolite volcanism, preserved as a result of a remarkably slow rate of denudation since the time of emplacement. Chapter 4 will show that our data and interpretation for the Emmons Hill deposit that differ somewhat from those presented by McInnes (1987).

Laforma

The Laforma deposit at Freegold Mountain comprises a gold-bearing quartz vein in a north-northeast-trending shear zone that cuts granodiorite of the Dawson Range Batholith. The Laforma vein is approximately 300 metres deep, 300 metres long, and up to one metre wide (McInnes et al., 1990). Numerous rhyolite dykes of the Mount Nansen group are found around the Laforma vein, oriented either northwest, parallel to the local Pal fault, or following the trend of the Laforma vein. Andesite dykes, possibly belonging to the Carmacks group, are also found crosscutting the rhyolite dykes, and trending generally northwest. McInnes (1987) reports that rhyolite dykes have been hydrothermally altered preferentially compared to the andesite dykes, perhaps suggesting that ore formation post-dated rhyolite dyke emplacement and was associated with andesite dyke intrusion. However, McInnes (1987) also notes that the shear structure that hosts the Laforma vein has sinistrally displaced an andesite dyke by 75 metres, suggesting the possibility of an even later tectonic, ore-forming event.

Alteration of the granodiorite wall rocks is dominantly sericitic (McInnes et al., 1990), although silicification and carbonatization are locally developed. The alteration is typically stronger in the hanging wall than in the footwall. Argillic alteration is also

present in a narrow zone accompanying the most intensely sheared component of the vein-fault, but may be unrelated to the ore-forming event.

The Laforma vein is largely massive white quartz, with barite and calcite as late-stage fracture-filling minerals. The central part of the vein has a cockscomb texture, with Fe-Mg carbonate, sericite, and euhedral sulphide minerals filling vugs. The multi-stage quartz texture of the vein at surface is indicative of brecciation and silicification (McInnes et al., 1990). Sulphide minerals include arsenopyrite, pyrite, tourmaline, gold, galena, sphalerite, chalcopyrite, and tennantite. The vein is divided into the Upper Ore Zone, from the surface to approximately 100 metres depth, the Boiling Zone, which extends from 100 to 200 metres below the surface, and the Deep Ore Zone, below 200 metres (McInnes et al., 1990). The vein mineralogy is vertically zoned. Tourmaline, galena, Fe-rich sphalerite and chalcopyrite occur only at depths greater than 175 metres and are most abundant in the Deep Ore Zone, as are Fe-Mg carbonate and sericite intergrown with quartz. By contrast, tennantite is only found above the 175-metre level, while arsenopyrite and pyrite occur throughout the vein. Gold occurs as microscopic inclusions in arsenopyrite and as isolated fine grains, rarely large enough to be visible. SEM-EDS analyses (McInnes et al., 1990) of the gold indicate an Ag content of less than 5 wt.%, and reserves have been calculated at over 150,000 tonnes grading 5.62 g/t Au (Yukon Minfile, 1996).

McInnes (1987) and McInnes et al. (1988; 1990) concluded that gold mineralization at Freegold Mountain was temporally and spatially related to Mount Nansen rhyolitic volcanism, an observation that has been echoed by most workers in the area (Johnston, 1937; Sawyer and Dickinson, 1976). The Laforma gold-quartz vein is thought to be formed by meteoric water of moderately low temperatures (175° - 195° C) and salinities (2-4.5 wt.% NaCl equivalent) (McInnes, 1987; McInnes et al., 1990). The deposit has a well-defined boiling zone, and is believed to have been formed at an approximate depth of 1 km. Based on hydrogen isotopic values, McInnes (1987) and

McInnes et al. (1988; 1990) estimated that the deposit formed approximately 350-450 km south of its present location.

Big Creek Porphyries

The Big Creek trend includes four porphyry deposits along the south rim of Big Creek, south of the Big Creek fault. These comprise, from southeast to northwest, the Revenue, Nucleus, Klazan, and Cash deposits. All the Big Creek porphyry deposits are hosted by felsic porphyry stocks analogous in appearance and composition to felsic porphyry dykes of the Mount Nansen group. A possible exception to this is the stock hosting the Cash deposit, which has a chemical affinity lying between that of the Mount Nansen and the Carmacks group, and differs in its more mafic phenocryst mineralogy.

The Revenue gold-copper porphyry deposit occurs in breccia and stockwork zones within a sheared and brecciated quartz monzonite intrusion of the Dawson Range Batholith, with associated Mount Nansen porphyry dykes that cut Mount Nansen (?) lapilli tuff-breccias. Hydrothermal alteration is generally weak, although local zones of strong propylitic and argillic, and lesser phyllic, alteration have been found (Yukon Minfile, 1996). Carlson (1987) reports a broad zone of silicification and pyritization with associated weak argillic alteration that surrounds a stronger phyllic zone adjacent to the intrusive breccia unit. Chalcopyrite, pyrite, and minor scheelite are the only minerals reported to be present (Yukon Minfile, 1996), although samples collected for this study consist of early disseminated sphalerite (5.2-9.2 mol.% FeS) and later galena in argillically-altered, feldspar-phyric, felsic intrusive stock of the Mount Nansen group. Carlson (1987) describes the occurrence of native silver, and reports grades of up to 5 g/t Au, 20 g/t Ag, and 1 wt.% Cu in breccia zones. Exploration drilling in 1991 defined a sulphide zone grading 0.14-0.27 g/t Au and 0.18-0.20 wt% Cu, a supergene sulphide zone grading 1.00 g/t Au and 0.66 wt% Cu, and an oxide cap grading 1.03 g/t Au and 0.28% Cu (Yukon Minfile, 1996).

Preliminary results from a small set of two-phase fluid inclusions in sphalerite indicate the existence of three different fluid episodes: a high-temperature population that homogenizes at temperatures >500°C; a lower-temperature population that homogenizes at approximately 330°C; and a third population that homogenizes at temperatures around 150°C. Cryogenic data was not obtained for the Revenue sphalerite samples. These different fluids could represent different hydrothermal events in the southern Dawson Range, with the highest temperature fluid reflecting early porphyry-style mineralization, the 300°C fluids representing later epithermal-type fluids, and the coolest fluids representing a late-stage waning fluid as preserved in secondary inclusions in epithermal veins (see Chapter 4 for full fluid inclusion details). Clearly more data is needed to confirm this scenario, but a full study of the porphyry mineralization is beyond the scope of this study.

The Nucleus gold-copper-molybdenum deposit occurs in a highly fractured, argillically-altered and silicified porphyry of the Mount Nansen group, microgranite or granodiorite of the Big Creek Suite, and schist of the Basement Metamorphic Complex. It is localized between two north-trending quartz-feldspar porphyry dykes of the Mount Nansen group (Carlson, 1987; Yukon Minfile, 1996), but soil geochemistry suggests that the deposit may be connected with the adjacent Revenue property (Yukon Minfile, 1996). The reported sulphide minerals include chalcopyrite, molybdenite, and tetrahedrite. Anomalous Au soil values are accompanied by anomalous values of As, Cu, W, and Ag. Trenching and drilling has discovered an oxidized gold-bearing zone overlain by a supergene sulphide zone, covered by a 60-100 metre gold-bearing leached cap. Exploration drilling in 1991 encountered grades of about 0.9 g/t Au in the oxide zone, 0.9 g/t Au and 0.24 wt.% Cu in the supergene zone, and 1.0 g/t Au and 0.04 wt.% Cu in the leached cap (Yukon Minfile, 1996). Combined reserves are estimated at 4.2 million tonnes grading 1.0 g/t Au (Yukon Minfile, 1996).

The Klazan prospect consists of quartz veins in brecciated and leached rhyolite surrounding a stock of altered orthoclase porphyry of the Mount Nansen group, which is

anomalous in Mo, Cu, Pb, Zn, Ag, Au, and As (Carlson, 1987; Yukon Minfile, 1996). Pyrite and rare molybdenite, galena, and sphalerite mineralization have been reported from surface trenches in gossanous rhyolite. Grades range up to 0.17 wt.% Cu over 44.2 metres, and 0.16 wt.% Cu and 0.68 wt.% MoS_2 over 3.0 metres (Yukon Minfile, 1996).

The Cash copper-molybdenum deposit is reported to occur in association with feldspar-phyric dykes and plugs of the Mount Nansen group (Yukon Minfile, 1996). The mineralized zone is centred on two small stocks of feldspar (andesine and minor orthoclase) porphyry of quartz monzonitic to granodioritic composition (Sinclair et al., 1981) that intrude the Basement Metamorphic Complex and the Big Creek Suite (Payne et al., 1987). In addition to feldspar, biotite and hornblende are common phenocryst phases in the porphyry, in contrast to typical quartz- and feldspar-porphyry stocks or dykes of the Mount Nansen group found throughout the southern Dawson Range. A recent abstract by Selby (1998) indicates that Cash may have an age of 70 Ma, although no evidence is provided. Hydrothermal alteration of the stocks has resulted in roughly concentric potassic, phyllic, and propylitic zones, with local late argillic zones (Sinclair et al., 1981). Primary sulphide minerals include pyrite, chalcopyrite, molybdenite and bornite, which occur along fractures, in quartz veinlets, and disseminated in the feldspar porphyry and related rocks. Galena and sphalerite are inferred to occur in this deposit due to the presence of anomalous lead and zinc values in soil. The Yukon Minfile (1996) reports a 20-year old reserve estimate of 36.3 million tonnes grading 0.17 wt.% Cu and 0.018 wt.% MoS_2, with 0.2 g/t Au and 0.4 to 9.0 g/t Ag.

2.5.3 Prospector Mountain Camp

Frog

The Frog, or Lilypad, prospects occur in a series of discrete quartz veins on the western flank of Prospector Mountain. Mineralization consists of gold- and silver-bearing sulphosalts, galena, and chalcopyrite in a pyrite-quartz-carbonate gangue (Payne

et al., 1987). Although total ore grades are not reported, one galena sample assayed 3361 g/t Ag, and soil sampling over the veins has encountered grades of up to 5 g/t Au (Payne et al, 1987).

Glasmacher (1990) has determined a temperature of 320°C for gold-sulphide vein formation on the basis of arsenopyrite thermometry, in approximate agreement with fluid inclusion homogenization temperatures from four generations of quartz that indicate a main deposition temperature of 310°C. Successive fluid populations yield temperatures of 270°C, 200°C, and 170°C. He reports the salinity of the primary mineralizing fluid to average 23 wt.% NaCl equivalent, and to decrease with decreasing temperature, leading him to propose mixing between high-temperature, high-salinity, magmatic fluid, and low-temperature, low-salinity meteoric water. Glasmacher (1990) also calculated a fluid pH of between 3 and 5, and a log fO_2 of approximately –30 for the main-stage mineralization. A magmatic or igneous source for Pb and S was postulated on the basis of Pb- and S-isotopes. The genetic model proposed by Glasmacher (1990) for mineralization at Prospector Mountain involves post-intrusion mixing of two fluids with different physiochemical attributes. The ore metals are thought to be derived by leaching of the surrounding Basement Metamorphic rocks, Carmacks volcanics or the Prospector Suite. Our geochemical data for the Frog prospect (Chapter 4) support this general model.

Casino

The Casino Cu-Mo-Au porphyry deposit lies approximately 50 kilometres northwest of Prospector Mountain, outside the southern Dawson Range study area, but on line with the Dawson Range mineral belt (Hart and Selby, 1998). Casino is reported to be one of the highest-grade porphyry deposits in Canada (Yukon Minfile, 1996). Mineralization is hosted by the Casino Complex, a swarm of subvolcanic intrusions and related breccia bodies, comprising an undivided volcanic unit, tuffs, tuff breccias, cobble breccias, and the Patton porphyry, surrounded by the mid-Cretaceous Dawson Range

Batholith. The volcanic unit is a pale, pervasively altered quartz- and sanidine-phyric rock that occurs as small isolated outcrops. The Casino Intrusion comprises the Patton porphyry, which contains 50 vol.% phenocrysts of plagioclase, with lesser biotite, hornblende, quartz and opaques, and encloses a central breccia pipe. The conical Casino breccia pipe is composed of fragments of flow-banded tuff, tuff breccia, and cobble breccia containing fragments of tuff breccia. The Patton porphyry has been dated at between 69 and 72 Ma, and is thus the same age as the Carmacks volcanic group (Godwin, 1975; 1976; Selby and Nesbitt, 1998).

Hypogene alteration at the Casino deposit is characterized by a nearly concentric zonation of potassic, phyllic, argillic, and propylitic alteration facies centred on the Casino Intrusion (Godwin, 1976). The potassic alteration zone is located on the northern edge of the breccia pipe, and contains biotite, quartz, K-feldspar, sericite, magnetite, tourmaline, ankerite and gypsum, with finely disseminated sulphides. The phyllic alteration zone is characterized by quartz and sericite, abundant tourmaline, and hematite and magnetite, with supergene clay minerals, and contains an internal pyrite halo. The ore zone is located within the phyllic alteration zone between the potassic core and the pyrite halo, where copper and molybdenum attain their highest values. Clay minerals, minor amounts of carbonate and chlorite, and the absence of abundant sericite and quartz define a weak outer argillic facies. Abundant chloritization and carbonitization of amphibole and biotite, minor clay minerals, albite and epidote characterize a peripheral propylitic alteration zone. A 60 metre thick supergene oxide alteration zone characterized by limonite and jarosite staining has been enriched in copper by a factor of 1.7 by the replacement of chalcopyrite and pyrite by chalcocite (Yukon Minfile, 1996; Godwin, 1976; Archer and Main, 1971).

Ore mineralization at the Casino deposit consists of primary chalcopyrite, molybdenite and gold, with minor bornite, tetrahedrite, huebnerite, galena and sphalerite, along with supergene native copper, chalcanthite, malachite, brochanite, tenorite, azurite, chalcocite, covellite, and digenite, as well as fluorite and zeolite gangue (Selby and

Nesbitt, 1998; Yukon Minfile, 1996; Archer and Main, 1971). The mineralization occurs as veins, disseminations, irregular patches, boxworks, and as coatings on pyrite grains (Selby and Nesbitt, 1998). Associated veins of sphalerite, argentiferous galena, chalcopyrite and pyrite, in quartz and barite gangue, are found in the Dawson Range Batholith country rock surrounding the Casino area (Archer and Main, 1971). The geological reserves at the Casino deposit are 675 million tonnes grading 0.25 wt.% Cu, 0.02 wt.% Mo, and 0.48 g/t Au (Selby and Nesbitt, 1998; Yukon Minfile, 1996).

Copper-molybdenum mineralization is also found in the Pattison Creek pluton, a Casino intrusion located approximately 30 kilometres south of the Casino deposit. There is some uncertainty as to the age and therefore the affinity of the Pattison Creek pluton. It has been correlated with both the mid-Cretaceous Dawson Range Batholith as well as with the Late Cretaceous Casino Intrusion (Patton porphyry) (Hart and Selby, 1998; see also Godwin, 1976). Molybdenite, chalcopyrite, and pyrite are found in narrow quartz veins cutting quartz monzonite and alaskite, which are weakly phyllically and variably argillically altered (Hart and Selby, 1998). Hart and Selby (1998) report fluid inclusion homogenization temperatures that average 240 ± 30°C, and salinities between 0.2 and 5 wt.% NaCl equivalent, an average $\delta^{18}O$ value of 6 ± 0.4‰ and a δD value of -155 ± 9‰. The low temperature, low salinity fluid characteristics are interpreted by Hart and Selby (1998) to be closer to those of the Dawson Range epithermal vein systems rather than those of porphyry systems, although this study will show that oxygen and hydrogen isotopes from Dawson Range epithermal veins, and to a lesser degree fluid inclusion characteristics, also differ from those of the Pattison Creek deposit.

The variable styles of mineralization and geological settings make it difficult to propose a universal metallogenic model for the Dawson Range. The only obvious common features of the deposits are their close geographic proximity and the presence of gold. The following chapters will concentrate on the epithermal gold-bearing veins, and will present evidence suggesting that they can be related to a common metallogenic event.

2.6 References

Archer, A. R., and Main, C. A., 1971, Casino, Yukon – A Geochemical Discovery of an Unglaciated Arizona-type Porphyry: Geochemical Exploration, Canadian Institute of Mining and Metallurgy Special Volume 11, p. 67-77.

Bostock, H. S., 1936, Carmacks District, Yukon: Geological Survey of Canada Memoir 189, 67 p.

Carlson, G. G., 1987, Geology of Mount Nansen (115-I/3) and Stoddart Creek (115-I/6) Map Areas, Dawson Range, Central Yukon: Indian and Northern Affairs Canada, Northern Affairs: Yukon Region Open File 1987-2.

Clowes, R. M. (ed.), 1997, Lithoprobe Phase V Proposal – Evolution of a Continent Revealed: Lithoprobe Secretariat, The University of British Columbia, Vancouver, B. C., 292 p.

Engebretson, D. C., Cox, A., and Gordon, R. G., 1985, Relative motions between oceanic and continental plates in the Pacific Basin: Geological Society of America Special Paper 206, 59 p.

Francis, D. and Johnston, S. T., 1998, Isotopic constraints on lithospheric melting near the Yellowstone hotspot, Carmacks volcanics, Yukon: GSA Program with Abstracts, v. x, p. A-90.

Gabrielse, H., 1985, Major dextral transcurrent displacements along the Northern Rocky Mountain Trench and related lineaments in north-central British Columbia: Geological Society of America Bulletin, v. 96, p. 1-14.

Glasmacher, U., 1990, Petrogenetische und metallogeneitsche Entwicklung ausgewahlter Gebiete im 'Yukon – Tanana Terrane' und 'Stikine Terrane', (Yukon Territorium, Kanada) wahrend der Oberkreide und des Alttertiars: Mitteilungen zur Mineralogie und Lagerstattenkunde, Nr. 38, Aachen University Ph.D. Thesis, 605 p.

Godwin, C. I., 1975, Alternative interpretations for the Casino Complex and Klotassin Batholith in the Yukon Crystalline Terrane: Canadian Journal of Earth Sciences, v. 12, p. 1910-1915.

Godwin, C. I., 1976, Casino: Paper 35, Part B - Porphyry Copper and Copper-Molybdenum deposits of the Calc-Alkaline Suite: Porphyry Deposits of the Canadian Cordillera, CIM Special Volume 15, p. 344-354.

Grond, H. C., Churchill, S. J., Armstrong, R. L., Harakal, J. E., and Nixon, G. T., 1984, Late Cretaceous age of the Hutshi, Mount Nansen, and Carmacks groups, southwestern Yukon Territory and northwestern British Columbia: Canadian Journal of Earth Sciences, v. 21, p. 554-558.

Hart, C. J. R., and Langdon, M., 1998, Geology and mineral deposits of the Mount Nansen camp, Yukon: Yukon Exploration and Geology 1997, Exploration and Geological Services Division, Yukon, Indian and Northern Affairs Canada, p. 129-138.

Hart, C. J. R., and Selby, D., 1998, The Pattison Creek pluton – a mineralized Casino Intrusion made bigger with gamma rays: Yukon Exploration and Geology 1997, Exploration and Geological Services Division, Yukon, Indian and Northern Affairs Canada, p. 89-96.

Hunt, P. A., and Roddick, J. C., 1991, A Compilation of K-Ar Ages, Report 20: Radiogenic Age and Isotopic Studies: Report 4, Geological Survey of Canada, Paper 90-2, p. 113-143.

INAC, 1990, Yukon Exploration 1989: Exploration and Geological Services Division, Yukon, Indian and Northern Affairs Canada, 182 p.

Irving, E., and Wynne, P. J., 1990, Palaeomagnetic evidence bearing on the evolution of the Canadian Cordillera: Philosophical Transactions of the Royal Society of London, A. 331, p. 487-509.

Johnston, J. R., 1937, Geology and mineral deposits of Freegold Mountain, Carmacks District, Yukon: Geological Survey of Canada, Memoir 214, 21 p.

Johnston, S. T., 1995, Geological Compilation with Interpretation from Geophysical Surveys of the Northern Dawson Range, Central Yukon (115 J/9 and 10, 115 I/12, 1:100 000 Scale Map): Exploration and Geological Services Division, Department of Indian and Northern Affairs Open File 1995-2(G).

Johnston, S. T., Wynne, P. J., Francis, D., Hart, C. J. R., Enkin, R. J., and Engebretson, D. C., 1996, Yellowstone in Yukon: The Late Cretaceous Carmacks Group: Geology, v. 26, p. 997-1000.

Journeay, J. M., and Williams, S. P., 1995, GIS Map Library: A Window on Cordilleran Geology: Geological Survey of Canada, Open File 2948 (v. 1.0).

LeBarge, W. P., 1995, Sedimentology of Placer Gravels Near Mt. Nansen, Central Yukon Territory: Bulletin 4, Exploration and Geological Services Division, Indian and Northern Affairs Canada, Yukon Region, 155 p.

Le Couteur, P. C., and Templeman-Kluit, D. J., 1976, Rb/Sr ages and a profile of initial $^{87}Sr/^{86}Sr$ ratios for plutonic rocks across the Yukon Crystalline Terrain: Canadian Journal of Earth Sciences, v. 13, p. 319-330.

Lister, D., 1989, Character of unoxidized gold-silver mineralization and its relationship to beneficiation at the Brown-McDade Zone, Mt. Nansen Property, south-central Yukon: University of British Columbia B.Sc. Thesis.

Lowey, G. W., Sinclair, W. D., and Hills, L. V., 1986, Additional K-Ar dates for the Carmacks Group (Upper Cretaceous), west central Yukon: Canadian Journal of Earth Sciences, v. 23, p. 1857-1859.

Marquis, G., and Globerman, B. R., 1988, Northward motion of the Whitehorse Trough: paleomagnetic evidence from the Upper Cretaceous Carmacks Group: Canadian Journal of Earth Science, v. 25, p. 2005-2016.

McInnes, B. I. A., 1987, Geological and precious metal evolution at Freegold Mountain, Dawson Range, Yukon: unpublished M.Sc. thesis, McMaster University, 230 p.

McInnes, B. I. A., Goodfellow, W. D., and Crocket, J. H., 1988, Role of structure in the emplacement of gold-quartz veins and rhyolite dykes at Freegold Mountain, Dawson Range, Yukon: Current Research, Part E, Geological Survey of Canada, Paper 88-1E, p. 153-157.

McInnes, B. I. A., Crocket, J. H., and Goodfellow, W. D., 1990, The Laforma deposit, an atypical epithermal-Au system at Freegold Mountain, Yukon Territory, Canada: Epithermal Gold Mineralization of the Circum-Pacific: Geology, Geochemistry, Origin

and Exploration, II, (ed.) J.W. Hedenquist, N.C. White, and G. Siddeley, Journal of Geochemical Exploration, v. 36, p. 73-102.

Morin, J. A., 1981, Element distribution in Yukon gold-silver deposits: Yukon Geology and Exploration 1979-80, Exploration and Geological Services Division, Yukon, Indian and Northern Affairs Canada, p. 68-84.

Oppliger, G. L., Murphy, J. B., and Brimhall, G. H., 1997, Is the ancestral Yellowstone hotspot responsible for the Tertiary "Carlin" mineralization in the Great Basin of Nevada?: Geology, v. 25, p. 627-630.

Payne, J. G., Gonzalez, R. A., Akhurst, K., and Sisson, W. G., 1987, Geology of Colorado Creek (115-J/10), Selwyn River (115-J/9), and Prospector Mountain (115-I/5) Map Areas, Western Dawson Range, West-Central Yukon: Indian and Northern Affairs Canada, Northern Affairs: Yukon Region Open File 1987-3.

Saager, K., and Bianconi, F., 1971, The Mount Nansen Gold-Silver Deposit, Yukon Territory, Canada: Mineralium Deposita, v. 6, p. 209-224.

Sawyer, J. P. B., and Dickinson, R. A., 1976, Mount Nansen: Paper 34, Part B - Porphyry Copper and Copper-Molybdenum deposits of the Calc-Alkaline Suite: Porphyry Deposits of the Canadian Cordillera, Canadian Institute of Mining and Metallurgy Special Volume 15, p. 336-343.

Selby, D., 1998, Geochemistry of porphyry Cu-Au-Mo potassic ore fluids: A case study from the Yukon, Canada: SEG Newsletter, no. 35 (October, '98), p. 6.

Selby, D., and Nesbitt, B. E., 1998, Biotite chemistry of the Casino porphyry Cu-Mo-Au occurrence, Dawson Range, Yukon: Yukon Exploration and Geology 1997, Exploration and Geological Services Division, Yukon, Indian and Northern Affairs Canada, p. 83-88.

Sinclair, W. D., Cathro, R. J., and Jensen, E. M., 1981, The Cash porphyry copper-molybdenum deposit, Dawson Range, Yukon Territory: Canadian Institute of Mining and Metallurgy Bulletin, v. 74, no. 833, p. 67-76.

Souther, J. G., 1991, Volcanic Regimes, Chapter 14: Geology of the Canadian Cordillera, (ed.) H. Gabrielse, C.J. Yorath, Geological Survey of Canada, Geology of Canada, No. 4, p. 457-490.

Stevens, R. D., Delabio, R. N., and Lachance, G. R., 1982, Age determinations and geological studies; K-Ar isotopic ages, Report 16: Geological Survey of Canada, Paper 82-2, 52 p.

Tempelman-Kluit, D. J., 1984, Geology of the Lebarge and Carmacks Map Sheets: Geological Survey of Canada, Open File 1101, map sheets with legends.

Tempelman-Kluit, D. J., and Wanless, R. K., 1975, Potassium-argon age determinations of metamorphic and plutonic rocks in the Yukon Crystalline Terrane: Canadian Journal of Earth Sciences, v. 12, p. 1895-1909.

Tempelman-Kluit, D. J., and Wanless, R. K., 1980, Zircon ages for the Pelly Gneiss and Klotassin granodiorite in western Yukon: Canadian Journal of Earth Sciences, v. 17, p. 297-306.

Umhoefer, P. J., 1987, Northward translation of "Baja British Columbia" along the Late Cretaceous to Paleocene margin of western North America: Tectonics, v. 6, p. 377-394.

Wynne, P. J., Enkin, R. J., Baker, J., Johnston, S. T., and Hart, C. J. R., 1998, The big flush: paleomagnetic signature of a 70 Ma regional hydrothermal event in displaced rocks of the northern Canadian Cordillera: Canadian Journal of Earth Sciences, v. 35, p. 657-671.

Yorath, C. J., 1991, Upper Jurassic to Paleogene assemblages, Chapter 9: Geology of the Cordilleran Orogen in Canada, (ed.) H. Gabrielse and C. J. Yorath, Geological Survey of Canada, Geology of Canada, No. 4, p. 329-371.

Yukon Minfile, 1996. Version 2.05, May 31, 1996: Exploration and Geological Services Division, Indian and Northern Affairs Canada.

Chapter 3

The Carmacks Hydrothermal Event: An Alteration Study in the Southern Dawson Range, Yukon

Katherine A. Smuk, A. E. Williams-Jones and Don Francis, 1997

Department of Earth and Planetary Sciences

McGill University

Published in: Yukon Exploration and Geology 1996, Exploration and Geological Services Division, Yukon, Indian and Northern Affairs Canada, p. 92-106.

Abstract

Gold-rich polymetallic vein deposits, and gold-copper porphyry deposits, occur along a northwesterly trend across the southern Dawson Range. Vein mineralization is hosted by lithologic units ranging from the Proterozoic-Paleozoic Basement Metamorphic Complex, through the mid-Cretaceous Mt. Nansen volcanics, to the Late Cretaceous Carmacks volcanics. The mineralized areas also contain numerous porphyry dykes that are spatially associated with gold veins, and historically have been thought to be genetically linked to them. Dykes belonging to both the Mt. Nansen and Carmacks Groups are present, although Mt. Nansen dykes are the more common. Dykes proximal to mineralized veins are strongly altered to sericite and clay.

Volcanic and subvolcanic rocks of the Mt. Nansen and Carmacks Groups can be distinguished chemically on the basis of their K content; the Mt. Nansen Group is a high-K calc-alkaline suite while the Carmacks Group is a shoshonitic suite. Radiometric age determinations constrain the age of the Carmacks Group to approximately 70 Ma, while the age of the Mt. Nansen Group is approximately 105 Ma. K/Ar dates for altered Mt. Nansen dykes, however, range from 94 to 61 Ma, reflecting resetting of Mt. Nansen ages by a Carmacks-age hydrothermal event. This hydrothermal event appears to have been responsible for much of the mineralization in the southern Dawson Range.

Alteration in porphyritic dykes proximal to mineralization is characterized by a strong depletion of Na, reflecting the replacement of feldspar by sericite and clay minerals. Altered dykes also display a general depletion in the ore metals Pb, Zn, and Cu, suggesting that these elements were mobilized from the host rocks during alteration and precipitated in nearby gold-rich base metal veins. As, Sb, and Au, however, appear to have been introduced directly from the hydrothermal fluid.

3.1 Introduction

Since the early twentieth century the southern Dawson Range has been extensively explored and exploited for its precious and base metal deposits. Placer gold production has spanned the last century, although the local lode sources for this gold are still poorly understood. Several deposits in the area have been exploited historically (e.g. Mount Nansen, Laforma) and, after many years, these same deposits are again being considered for their gold potential.

The majority of the known gold showings in the southern Dawson Range are associated with nearby mid- and Late Cretaceous volcanic rocks and related intrusions, which comprise the Mt. Nansen and Carmacks Group respectively. There has been considerable confusion as to the ages and the distinction between the two volcanic groups (Sawyer and Dickinson, 1976; Carlson, 1987; McInnes et al., 1988), but subvolcanic porphyry dykes and stocks associated with mineralization have generally been assigned to the Mt. Nansen Group (mid-Cretaceous). Exploration prospects in this part of the Dawson Range occur along a northwesterly trend for a distance of approximately 50 km in a common sequence of host rocks. The styles of mineralization hosted by these lithologies, however, range in character from those of porphyry copper-gold to epithermal vein deposits. Vein mineralization predominates, and varies in character from precious metal to polymetallic. There appears to be no visible pattern to the distribution of the different vein types, although all appear to be genetically related.

The important question from an exploration perspective is whether there is a genetic relationship between mineralization and magmatism. The distinction between Mt. Nansen and Carmacks porphyry dykes is essential to an understanding of the gold mineralization in the Dawson Range, as porphyry dykes have long been recognized to be spatially associated with vein mineralization (Yukon Minfile, 1996). This paper examines the relationships between the gold occurrences and igneous rocks of the Mt.

Nansen, Freegold Mtn., and Prospector Mtn. areas in terms of the alteration developed in porphyry dykes proximal to mineralization, and presents evidence that suggests the majority of lode gold mineralization is in fact related to the Late Cretaceous Carmacks magmatic event, rather than the Mt. Nansen event to which porphyry dykes associated with mineralization have traditionally been assigned.

3.2 General Geology

The rocks of the Mt. Nansen and Carmacks Groups overlap the Yukon-Tanana and Stikine Terranes in the Dawson Range of central Yukon (Fig. 3.1). The general stratigraphy of the southern Dawson Range described here differs somewhat from that in previous geological reports (Carlson, 1987; Payne et al., 1987) largely due to recent radiometric age determinations that have refined the stratigraphy of the Mt. Nansen Volcanic Group (Table 3.1) and resulted in a re-evaluation of the Klotassin Suite.

The Paleozoic-Proterozoic Basement Metamorphic Complex comprises the oldest rocks in the area and outcrops primarily around Mt. Nansen (Fig. 3.2). Its lower metasedimentary unit (Unit 1) consists of quartzites, schists and gneisses, while the upper schist and gneiss unit (Unit 2) includes foliated plutonic rocks and amphibolites. The prominent Big Creek meta-plutonic Suite (Unit 4), which occurs mainly in the Freegold Mtn. area, was emplaced at approximately 184 Ma (Tempelman-Kluit, 1984). This unit comprises the weakly foliated Big Creek syenite (actually a monzonite) as well as a hornblendite. This intrusion was followed by eruption of the Mount Nansen Group (Unit 7) at approximately 105 Ma (Tempelman-Kluit, 1984; Carlson, 1987; Hunt and Roddick, 1991). The Mt. Nansen Group consists of bimodal volcanic breccias (andesite and rhyolite fragments) now covering a relatively small area around the Mt. Nansen mining camp. Few true lava flows have been identified by the authors, although these have been reported by earlier workers (e.g. Carlson, 1987). A swarm of intermediate to felsic quartz-feldspar porphyry dykes and stocks (Unit 9) found throughout the map area is

Figure 3.1 Regional tectonic setting of south-central Yukon and location of the southern Dawson Range study area (outlined; Fig.3.2). Terrane boundaries interpreted from Journeay and Williams (1995). Y-T - Yukon-Tanana Terrane; N.A. - North America; SK - Stikine Terrane; CC - Cache Creek Terrane; CPB - Coast Plutonic Belt.

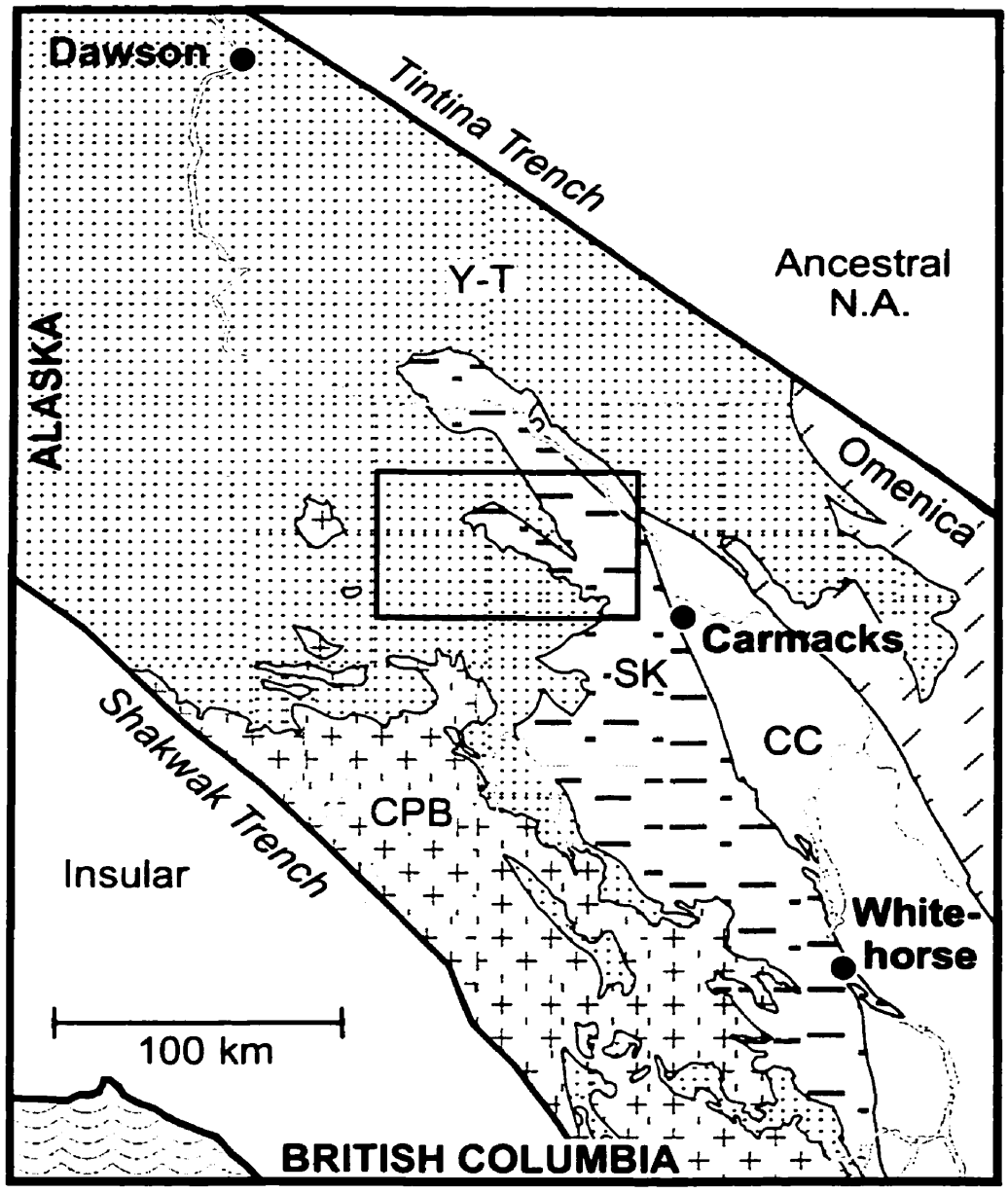
Dawson
Tintina Trench
Ancestral
N.A.
Y-T
ALASKA
Omenica
Carmacks
SK
CC
Shakwak Trench
CPB
Insular
White-
horse
100 km
BRITISH COLUMBIA

Figure 3.2 General geology of Dawson Range study area. Unit boundaries are modified from Journeay and Williams (1995). Stars indicate deposits or prospects listed in Yukon Minfile (1996).

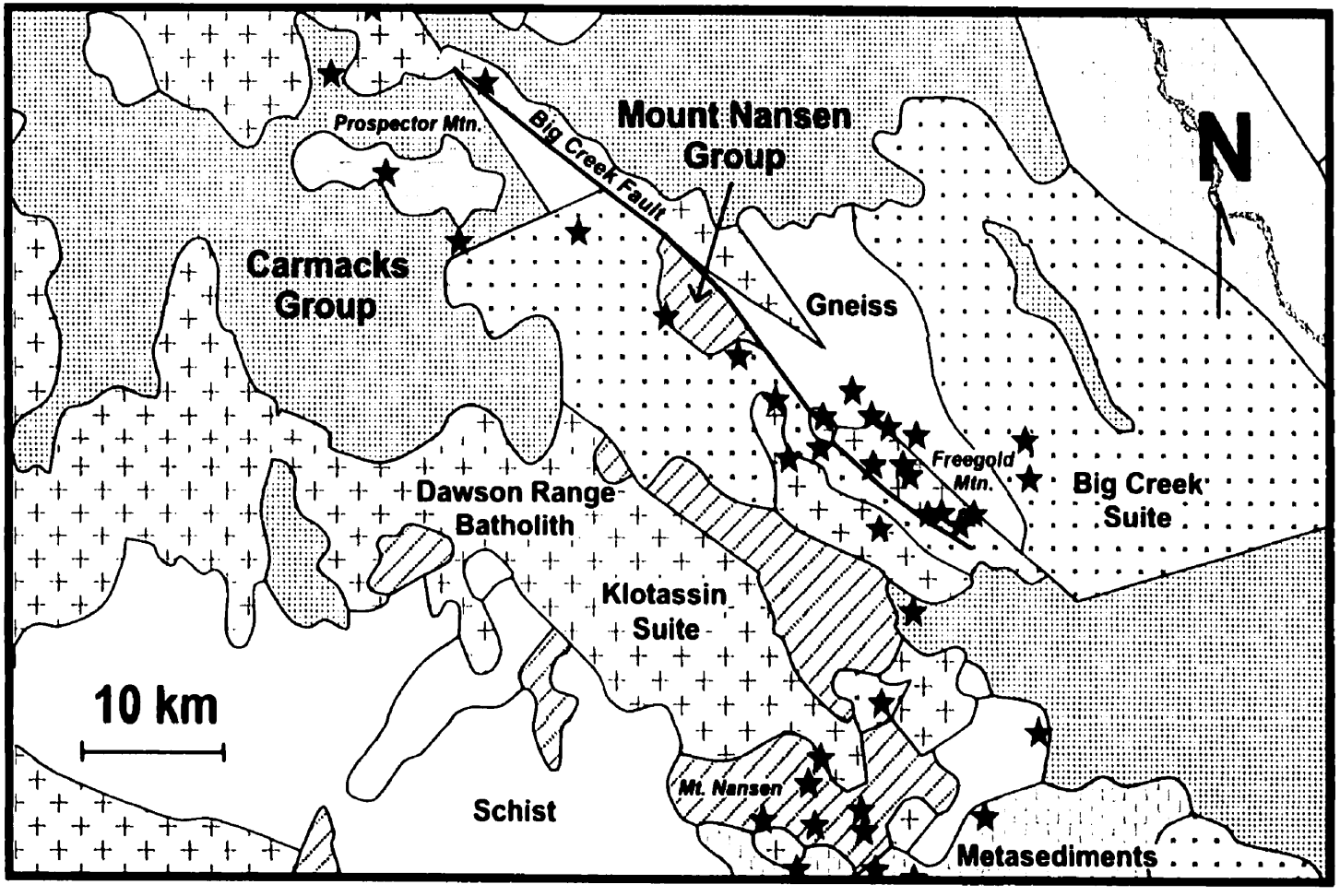
Prospector Mtn.
Big Creek Fault
Mount Nansen Group
N
Carmacks Group
Gneiss
Freegold Mtn.
Big Creek Suite
Dawson Range Batholith
Klotassin Suite
10 km
Mt. Nansen
Schist
Metasediments

Table 3.1 Volcanic and plutonic dates

Sample Number	Rock Type	Location	UTM E	UTM N	UTM Zone	Technique	Age (Ma)	Error (Ma)	Source
Carmacks Group									
SR-4	Basalt	"Smoky Ridge"	367690	6927780	8	40Ar/39Ar	71.4	1.1	*
SR-9	Ankaramitic Basalt	"Smoky Ridge"	366600	6930580	8	40Ar/39Ar	70.9	1.5	*
SR-14	Ankaramitic Basalt	"Smoky Ridge"	367160	6929850	8	40Ar/39Ar	70.5	0.5	*
AX-2	Andesite-Basalt	Apex Mtn.	652100	6930250	7	40Ar/39Ar	67.8	0.6	*
AX-22	Ankaramitic Basalt	Apex Mtn.	654160	6920000	7	40Ar/39Ar	70.9	0.6	*
ML-15	Ankaramite	Miller's Ridge	420100	6886340	8	40Ar/39Ar	68.6	1.0	*
na	Dacite Plug	Mt. Pitts	364650	6939650	8	K/Ar Biotite	71.7	1.7	Templeman-Kluit, 1984
na	Unit #13	Mt. Pitts	367500	6939450	8	K/Ar Biotite	68.0	3.4	Johnston, 1995
GSC 81-15	Basalt Plug	"Smoky Ridge"	366100	6932300	8	K/Ar Hornblende	78.4	3.2	Stevens et al., 1982
GSC 81-50	Basalt Plug	"Smoky Ridge"	366100	6932300	8	K/Ar Biotite	65.8	1.6	Stevens et al., 1982
na	Quartz Monzonite	Prospector Mtn.	355150	6926550	8	K/Ar Whole Rock	68.2	1.6	Templeman-Kluit, 1984
						AVERAGE	70.2		
Mount Nansen Group									
C-1125	Unit #9b	Mt. Nansen	na	na	8	U/Pb Zircon	105.1		Carlson, 1987
C-1083	Altered Qtz-Fp Porphyry	Mt. Nansen	na	na	8	U/Pb Zircon	101.5		Carlson, 1987
C-1115	Porphyritic Monzonite	Mt. Nansen	na	na	8	U/Pb Zircon (+64 um)	104.2		Carlson, 1987
C-1115	Porphyritic Monzonite	Mt. Nansen	na	na	8	U/Pb Zircon (-64 um)	102.8		Carlson, 1987
GSC 81-57	Felsite	Klaza Mtn.	370300	6910200	8	K/Ar Whole Rock	109	3	Templeman-Kluit, 1984
GSC 90-84	Fp-Hb Porphyry Dyke	Bow Creek	374700	6898800	8	K/Ar Whole Rock	107.9	1.6	Hunt and Roddick, 1991
						AVERAGE	105.1		
MN-24	Andesite Dyke	Mt. Nansen	381390	6886080	8	40Ar/39Ar	76.3	1.2	*
MN-30	Andesite Agglomerate	Mt. Nansen	379940	6887960	8	40Ar/39Ar	89.7	2.0	*
GSC 81-37	Bt-Fp Porphyry Dyke	Mt. Nansen	379400	6886800	8	K/Ar Biotite	70.5	2.2	Stevens et al., 1982
GSC 90-80	Altered Qtz-Fp Porphyry Dyke	Mt. Nansen	374300	6886900	8	K/Ar Whole Rock	69.7	1.4	Hunt and Roddick, 1991
GSC 90-81	Altered Bt-Fp Porphyry Dyke	Mt. Nansen	379400	6886800	8	K/Ar Whole Rock	61.2	1.2	Hunt and Roddick, 1991
GSC 90-82	Altered Qtz-Fp Porphyry Dyke	Mt. Nansen	385000	6881700	8	K/Ar Whole Rock	69	1.7	Hunt and Roddick, 1991
GSC 90-85	Trachyte Flow	Mt. Nansen	385300	6898300	8	K/Ar Whole Rock	93.7	1.5	Hunt and Roddick, 1991
F85-33B	Altered Qtz-Fp Porphyry Dyke	Laforma - Freegold Mtn.	389500	6906250	8	K/Ar Whole Rock	77.5	6.2	McInnes et al., 1985

* indicate 40Ar/39Ar age determination performed for this study by D. Lux at the University of Maine

na: not available

associated with this volcanic suite. The Dawson Range Batholith (Unit 3) includes the Klotassin Suite Granodiorite, the Casino Granodiorite and the Coffee Creek Quartz Monzonite, and ranges in age from 105 to 90 Ma (Tempelman-Kluit and Wanless, 1975; LeCouteur and Tempelman-Kluit, 1976). This unit is likely to be comagmatic with the Mt. Nansen suite.

The last unit to be emplaced was the Late Cretaceous Carmacks Group, dated at approximately 70 ± 4 Ma (Stevens et al., 1982; Tempelman-Kluit, 1984; Johnston, 1995). This suite comprises two volcanic units, a thick lower succession of andesitic tuffs and breccias (Units 12 and 13), and an upper series of extensive basaltic flows (Unit 14). The Prospector Suite (Unit 15) is represented by a contemporaneous granitic plug exposed at Prospector Mountain. Porphyritic dykes of mafic to intermediate composition of the Carmacks Group are also found throughout the map area, although they appear to be less numerous than the Mt. Nansen quartz-feldspar porphyry dykes.

Mineralization comprises a regional, trend of gold- and copper- bearing porphyry deposits, interspersed with a large number of polymetallic vein prospects, aligned along the Big Creek Fault. Locally, both polymetallic veins and porphyry dykes are also aligned in northwesterly-trending directions and probably follow small parallel structures.

Ore samples collected for this study are, for the most part, from vein deposits in the Mt. Nansen camp, the Freegold Mtn. camp and the Prospector Mtn. area. Typical ore assemblages include, in order of decreasing abundance, pyrite, galena, sphalerite, and chalcopyrite, with variable amounts of arsenopyrite, tetrahedrite-tennantite, boulangerite, jamesonite, proustite-pyrargyrite, and hematite. Gold is typically refractory in pyrite and arsenopyrite. The widespread occurrence of this assemblage suggests that many of these veins are genetically related. Local differences in mineralogy appear to reflect differences in the host rocks, which range from the Basement Metamorphic Complex through to the Lower Carmacks Group.

The porphyry deposits are characterized by disseminated and veinlet pyrite and chalcopyrite, as well as of supergene copper oxides and sulphides. Porphyry-style mineralization in the southern Dawson Range is hosted almost exclusively by Mt. Nansen quartz-feldspar porphyry stocks and granodiorites of the Dawson Range Batholith / Klotassin Suite. An important exception is the Casino porphyry deposit (northwest of the study area) which has a well-constrained age of 70 Ma (Godwin, 1976), indicating that Carmacks intrusions also host porphyry-style mineralization.

3.3 Volcanic Suites and Porphyry Dykes

It is reasonable to assume that Dawson Range gold mineralization is related spatially and temporally to either the Mt. Nansen or the Carmacks magmatic suites, as the deposits are intimately associated with porphyry dykes and because these magmatic events provided sources of heat at the time of eruption.

A compilation of available age determinations for the two magmatic suites (Table 3.1) indicates that while Carmacks volcanic and intrusive samples record a consistent Late Cretaceous age of 70 ± 4 Ma, Mt. Nansen volcanic and subvolcanic rocks show a bimodal distribution of ages. Unaltered Mt. Nansen samples taken from areas that do not host known mineralization, and altered samples that have been dated by U/Pb methods give an average age of 105 ± 3 Ma. Geological field relationships support this mid-Cretaceous age for the Mt. Nansen suite (Carlson, 1987). By contrast, altered Mt. Nansen samples, or samples found at the Mt. Nansen mining camp, yield ages ranging from 94 to 61 Ma. These Late Cretaceous dates are interpreted to indicate of partial resetting due to the alteration of these rocks, rather than the crystallization ages (Carlson, 1987; McInnes et al., 1988). The K/Ar technique used for the bulk of the samples is interpreted to date the formation of sericite during hydrothermal alteration, while the U/Pb technique dates magmatic zircons, which are resistant to alteration. The dates of the altered Mt. Nansen

dykes approach the age of the Carmacks suite. The implication of these dates is that a regional hydrothermal event of Late Cretaceous age related to Carmacks igneous activity altered the Mt. Nansen porphyritic dykes and formed precious and base metal mineralized veins in all lithologies older than the Upper Carmacks volcanic unit.

The question that arises is whether one is confident in assigning rocks with Late Cretaceous dates to the mid-Cretaceous Mt. Nansen Group rather than to the Carmacks Group. These two volcanic suites have similar calc-alkaline characteristics but can be distinguished in the Dawson Range on the basis of potassium content (Fig. 3.3). The Mt. Nansen Group is a high-K, calc-alkaline volcanic suite which trends to high silica values, while the Carmacks volcanic Group is a shoshonitic suite that does not attain the evolved compositions of the felsic members of the Mt. Nansen suite. Furthermore, the lava compositions of the Carmacks suite extend to higher Mg values than those of the Mt. Nansen suite (Fig. 3.4). It should be cautioned, however, that this distinction between the Carmacks and the Mt. Nansen suites on the basis of potassium is only applicable to Carmacks rocks in the Dawson Range. Carmacks rocks occurring in the Dawson City area to the north and the Miners Range to the south do not exhibit a shoshonitic character, and are indistinguishable from the Mt. Nansen suite on a K_2O against SiO_2 or MgO diagram.

In general, the dykes of the Mt. Nansen Group tend to be more felsic than those of the Carmacks Group, and dykes of both suites are more felsic than the lavas. As there is extensive overlap in the compositions of the subvolcanic members of the two suites (including dykes and stocks), however, this criterion cannot be used as an effective discriminant between dykes of the two groups in the field. Although Mt. Nansen dykes extend to higher silica values than Carmacks dykes, the most evolved rocks of both suites contain quartz as a major phase. In general, the porphyritic dykes or stocks of the Mt. Nansen Group contain quartz as a phenocryst phase equal in proportion to feldspar

Figure 3.3 K_2O-SiO_2 plot of fresh volcanic and plutonic rocks of the Mt. Nansen Group (black symbols) and the Carmacks Group (grey shaded symbols). Symbols: triangles - lavas; circles - dykes and intrusive rocks. Potassium field boundaries taken from Pecerillo and Taylor (1976). Additional data from Carlson (1987), McInnes et al. (1988), and Payne et al. (1987).

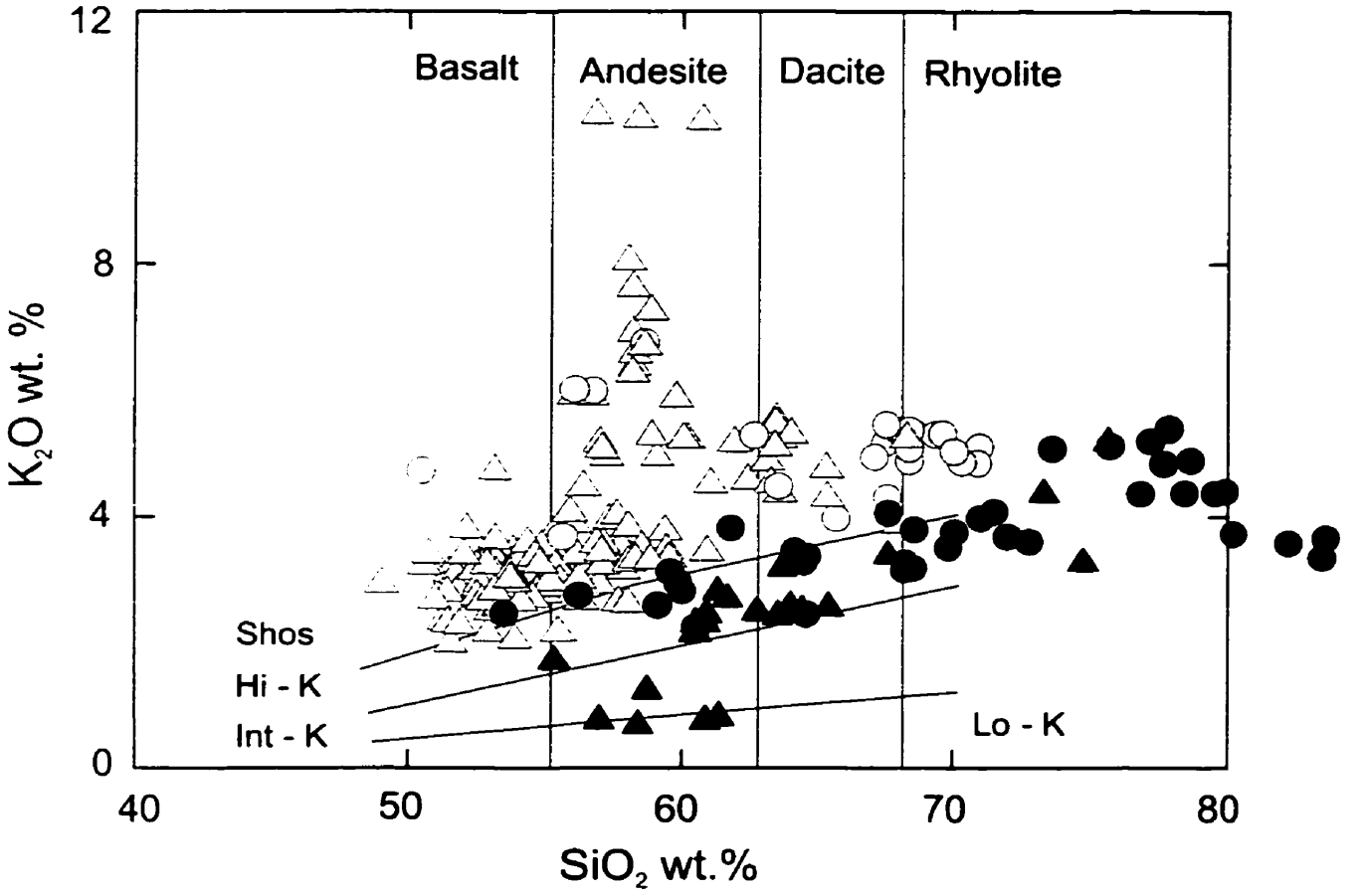
12
8
4
0
40
50
60
70
80
Basalt
Andesite
Dacite
Rhyolite
Shos
Hi - K
Int - K
Lo - K
K2O wt. %
SiO2 wt.%

Figure 3.4 K_2O-MgO plot of all volcanic and plutonic rocks of the Mt. Nansen and the Carmacks Groups. Symbols as in Figure 3.3.

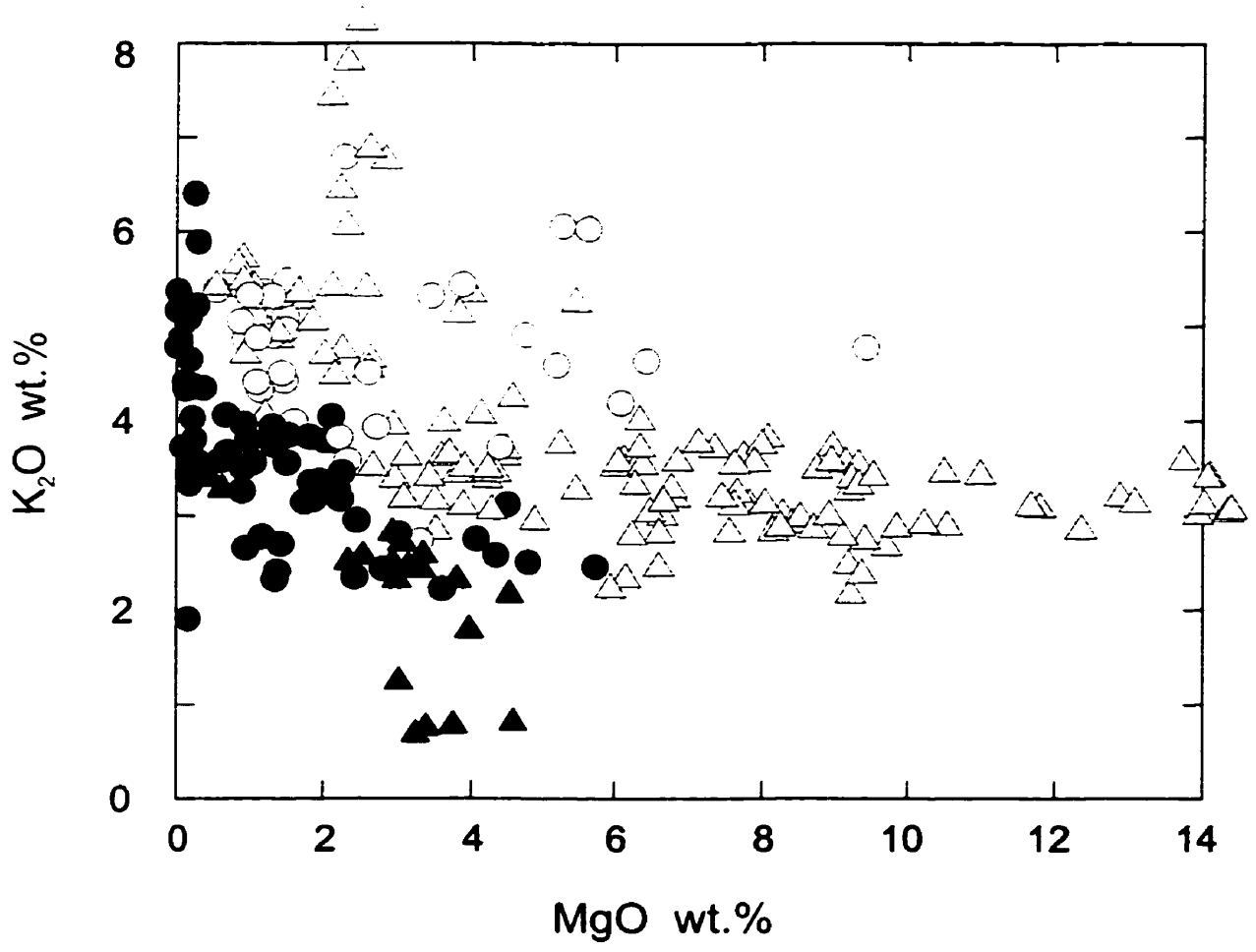
8
6
4
2
0
K_2O wt.%
0
2
4
6
8
10
12
14
MgO wt.%

(plagioclase and orthoclase), whereas the phenocrysts of the Carmacks dykes are predominantly feldspar with few or no quartz phenocrysts. Mafic phenocryst phases are more common in the Carmacks Group, although this observation may be biased by the fact that many of the samples of Mt. Nansen subvolcanic rocks were altered, and the less numerous Carmacks dykes tend to be more mafic in composition. The most striking observation is that it is difficult to distinguish the subvolcanic rocks of the Mt. Nansen suite from those of the Carmacks suite in hand sample.

The "lavas" of the Mt. Nansen suite are typically agglomerates, as is the lower unit of the Carmacks suite. The Mt. Nansen agglomerate is a well-consolidated, heterolithic rock with a bimodal population of felsic and more mafic fragments (Plate 3.1a). In contrast, the Carmacks agglomerate is a friable, monolithic rock consisting of andesitic fragments (Plate 3.1b). There are many different types of fragmental units in the lower Carmacks member, however, including agglomerates, mudflows, and water-reworked deposits. Any true mafic lava flow may be recognized almost immediately as belonging to the Carmacks Group.

3.4 Alteration

Dykes and stocks spatially associated with mineralized veins in the southern Dawson Range are invariably altered, many intensely. The main alteration minerals present in the altered dykes are sericite (here used broadly to indicate either the fine-grained K-mica muscovite or the Na-mica paragonite) and kaolinite (also possibly pyrophyllite). In addition to these ubiquitous minerals, there are variable amounts of carbonate, recrystallized quartz, and, especially in mafic dykes, clay minerals such as nontronite. Altered felsic porphyritic rocks retain quartz phenocrysts, although these are generally more rounded than in fresh dykes. In thin section, a narrow reaction rim of fine-grained recrystallized quartz typically surrounds each quartz phenocryst (Plate 3.1d). Feldspar phenocrysts turn white with alteration, reflecting their new mica, clay, and

Plate 3.1 a) Agglomerate from the lower Carmacks volcanic unit exposed at Miller's Ridge north-east of the town of Carmacks. Some fragments have been outlined for greater visibility.

b) Mt. Nansen agglomerate exposed at Mt. Nansen above Discovery Creek. Some fragments have been outlined for greater visibility.

c) Thin section of fresh Carmacks dyke (sample PR-26) under crossed polarizers. The field of view is ~5 mm. qtz - quartz; K-fp - K-feldspar; plag - plagioclase.

d) Thin section of altered Mt. Nansen dyke (sample FG-1) under crossed polarizers. The field of view is ~2 mm. fp - feldspar; ser - sericite; kaol - kaolinite.


a

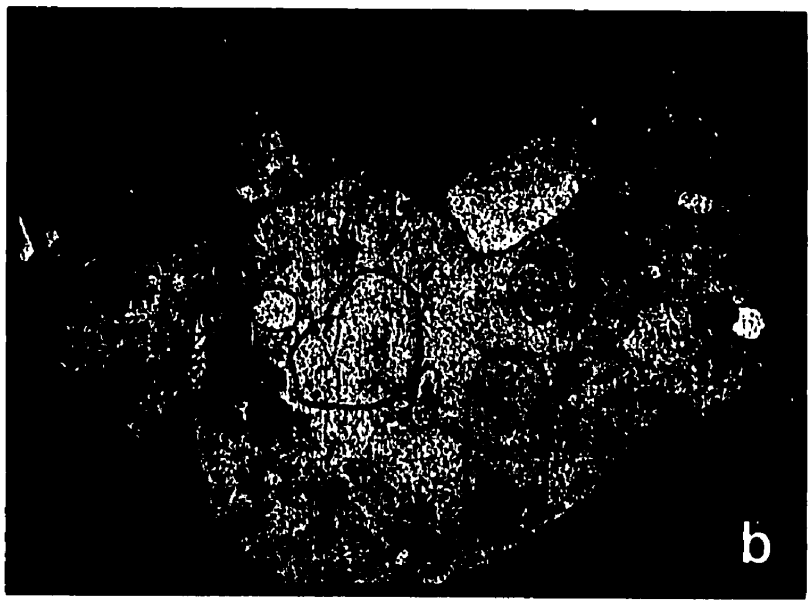
b


qtz
K-fp
plag

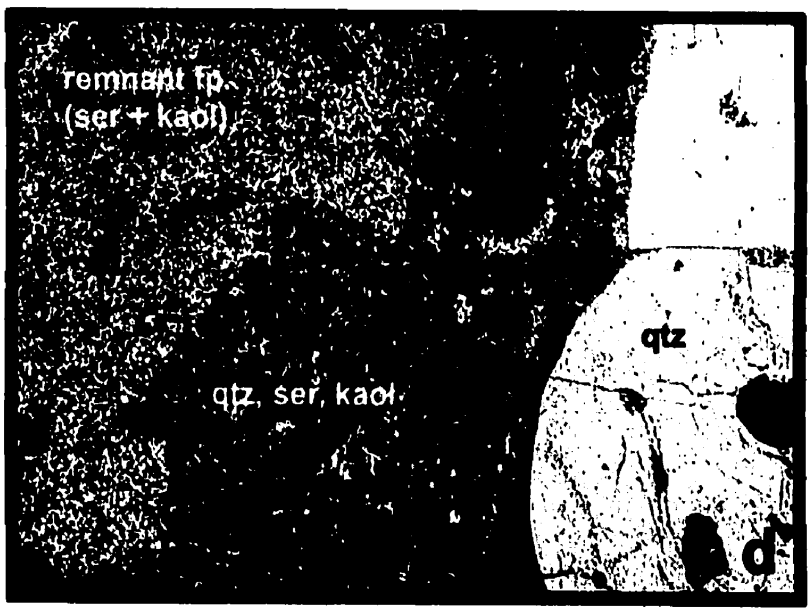
remnant fp
(ser + kaol)
qtz
qtz, ser, kaol
d

carbonate mineralogy. Altered rocks are typically white to buff and have an extremely fine-grained matrix, in contrast to fresh samples that are typically pink in colour with coarser-grained matrices. Mafic porphyritic dykes display the same general alteration characteristics, with a lightening in colour due to alteration being the most striking feature. Mafic phenocrysts (amphiboles, pyroxenes and biotite) are altered to carbonate and Mg- or Fe-bearing clay minerals.

Analysis of chemical changes due to alteration is difficult to validate because altered and fresh dykes cannot been sampled in close proximity to each other; in mineralized areas dykes are invariably altered and no fresh equivalents remain. This problem is compounded by the wide range in magmatic compositions of both fresh and altered dykes, and the uncertainty that a fresh equivalent for each altered rock has been sampled. Established methods for quantitatively estimating chemical changes due to alteration, such as Grant's (1986) isochon method or that of MacLean and Kranidiotis (1987), require the identification of a fresh precursor rock.

In order to evaluate the chemical changes, which have occurred during alteration of dykes adjacent to mineralization, it is necessary to consider the Mt. Nansen and Carmacks suites separately, because the fractionation trends for the two series are quite different (Fig. 3.5). While the Mt. Nansen suite defines a linear trend in plots of aluminum versus other immobile elements, the Carmacks data are ambiguous with respect to aluminum. In the Mt. Nansen rocks there is a continuous decrease in Al with fractionation, reflecting the fact that feldspar is a phenocryst phase even in the most mafic rocks. The behaviour of Al in the Carmacks lavas is controlled by the appearance of feldspar as a phenocryst phase, where Al rises with fractionation until the point at which feldspar begins to crystallize, after which Al decreases with continued fractionation.

Figure 3.5 TiO_2-Al_2O_3 plot showing fractionation trends for Mt. Nansen and Carmacks Groups. Symbols as in Figure 3.3.

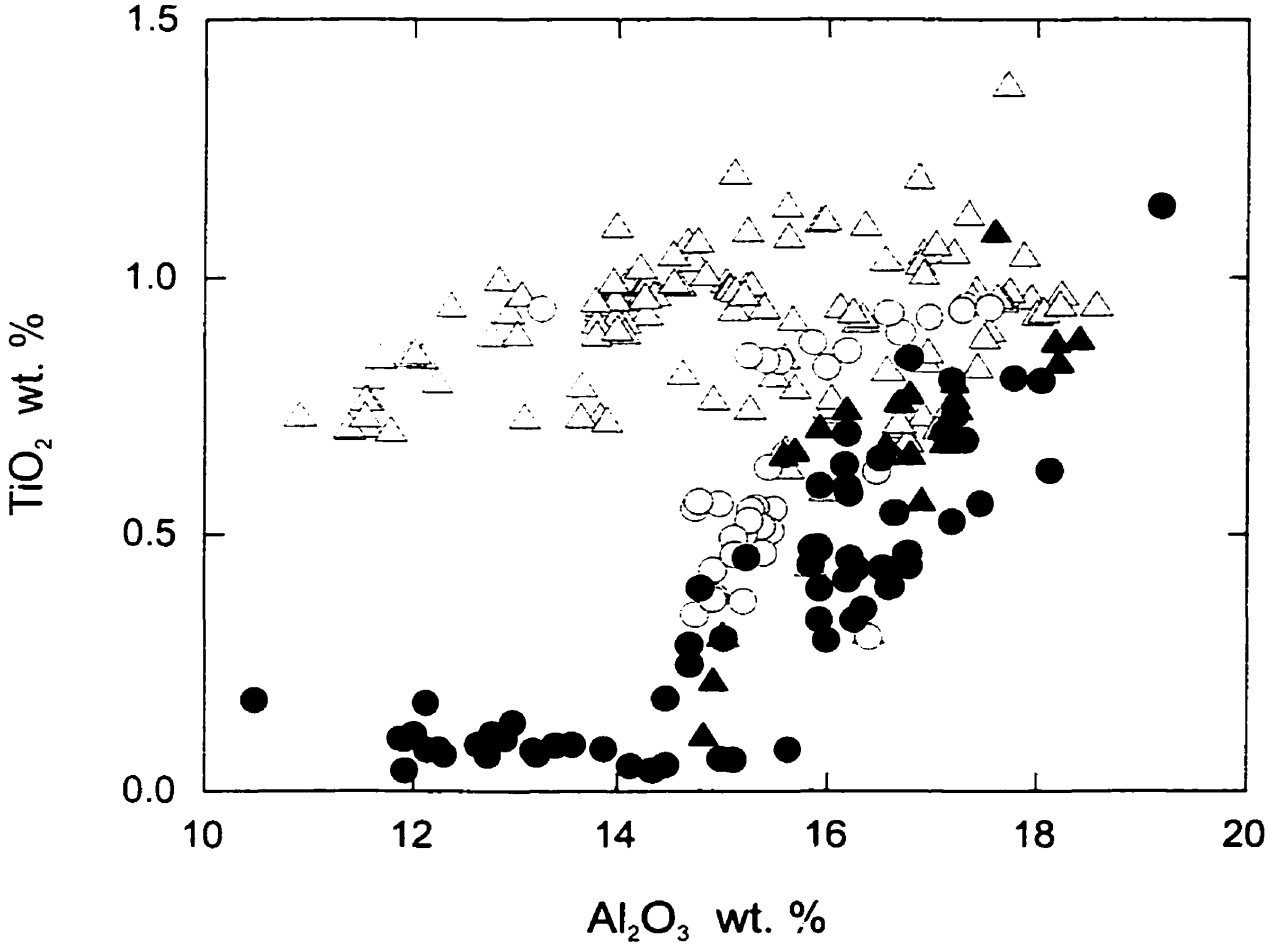
1.5
1.0
0.5
0.0
TiO2 wt. %
10
12
14
16
18
20
Al2O3 wt. %

3.4.1 Mt. Nansen Dykes

The well-behaved Al trend in the Mt. Nansen rocks allows the alteration of Mt. Nansen dyke rocks to be studied quantitatively. As seen in Figure 3.5, aluminum appears to behave as an immobile element during alteration, as well as monitors fractionation in the Mt. Nansen suite. Fresh and altered rocks fall on the same trend, indicating that Al and Ti were not affected by alteration. Implicit in this interpretation is that not only were Al and Ti immobile but also that there was no significant change in the overall mass during alteration. Plots of mobile elements against Al can therefore be used to distinguish between the effects of alteration and those due to crystal fractionation.

The largest chemical change during alteration is in sodium, which has undergone extreme depletion in the intensely altered samples (Fig. 3.6). These samples retain no textural evidence of their primary magmatic mineralogy. On the basis of this natural break in sodium values we filtered the data for Mt. Nansen dyke samples into two Na groups (Fig. 3.6): an altered group with less than 0.5 wt. % Na, and a fresh group containing over 3 wt. % Na. Grouping the data in this fashion enabled us to identify changes in other elements in the altered rocks, assuming that Al remained constant during alteration. Potassium shows a slight decrease in many altered samples, although a few appear to have undergone K addition, and the overall change is small. The parallel decrease in calcium content with aluminum concentration reflects fractionation in the Mt. Nansen suite, but the most altered samples also clearly show calcium depletion. Silicon is unambiguously added in all altered samples, reflecting the ubiquitous silicification evident in thin section.

Magnesium and iron are not consistent in their behaviour during alteration, although their relative changes are consistent with the degree of fractionation. At the mafic end of dyke compositions (i.e. those with higher aluminum contents) iron and magnesium appear slightly depleted during alteration, while in the more felsic samples these two elements are enriched. To summarize, in altered Mt. Nansen dykes proximal to

mineralization, Na is extremely depleted, Ca is depleted, K is generally somewhat depleted, Si is added, and Mg and Fe are depleted in mafic dykes and enriched in felsic dykes, relative to their fresh equivalents.

The lead, copper, and, to a lesser extent, zinc data (Fig. 3.7) for the altered Mt. Nansen dykes show considerable scatter, but suggest a slight overall depletion relative to fresh Mt. Nansen dykes. Arsenic and antimony, known to be present in appreciable concentrations in mineralized veins, display an unambiguous enrichment in all the altered dykes.

3.4.2 Carmacks Dykes

The Carmacks dyke swarm is less extensive than the Mt. Nansen dyke swarm, and relatively few Carmacks dykes have been found in mineralized areas. Most of the felsic Carmacks dykes are the intrusive rocks of the Prospector Mtn. pluton, and the few altered dykes found in mineralized areas all have basaltic to andesitic precursors. Altered dykes in the Carmacks suite are recognized petrographically by the development of sericite, clay and carbonate alteration minerals, and are characterized chemically by extreme sodium depletion.

A 7 metre-wide Carmacks basaltic dyke, sampled in DDH 95-151 on the Mount Nansen property, displays a range of alteration, thereby enabling a quantitative evaluation of the chemical changes due to alteration. The dyke is relatively fresh close to one of its margins (MN 95-33), somewhat altered (MN 95-34) in its interior, and intensely altered at the opposite margin (MN 95-35), immediately adjacent to a mineralized vein. These three samples represent a suite for which chemical changes due to alteration associated with mineralization can be confidently evaluated, because uniform initial composition and emplacement age are assured.

Figure 3.6 Major element oxides plotted against alumina to emphasize mass changes due to alteration for the Mt. Nansen suite. Symbols: open triangles - lavas; solid circles - unaltered dykes; shaded crosses - altered dykes.

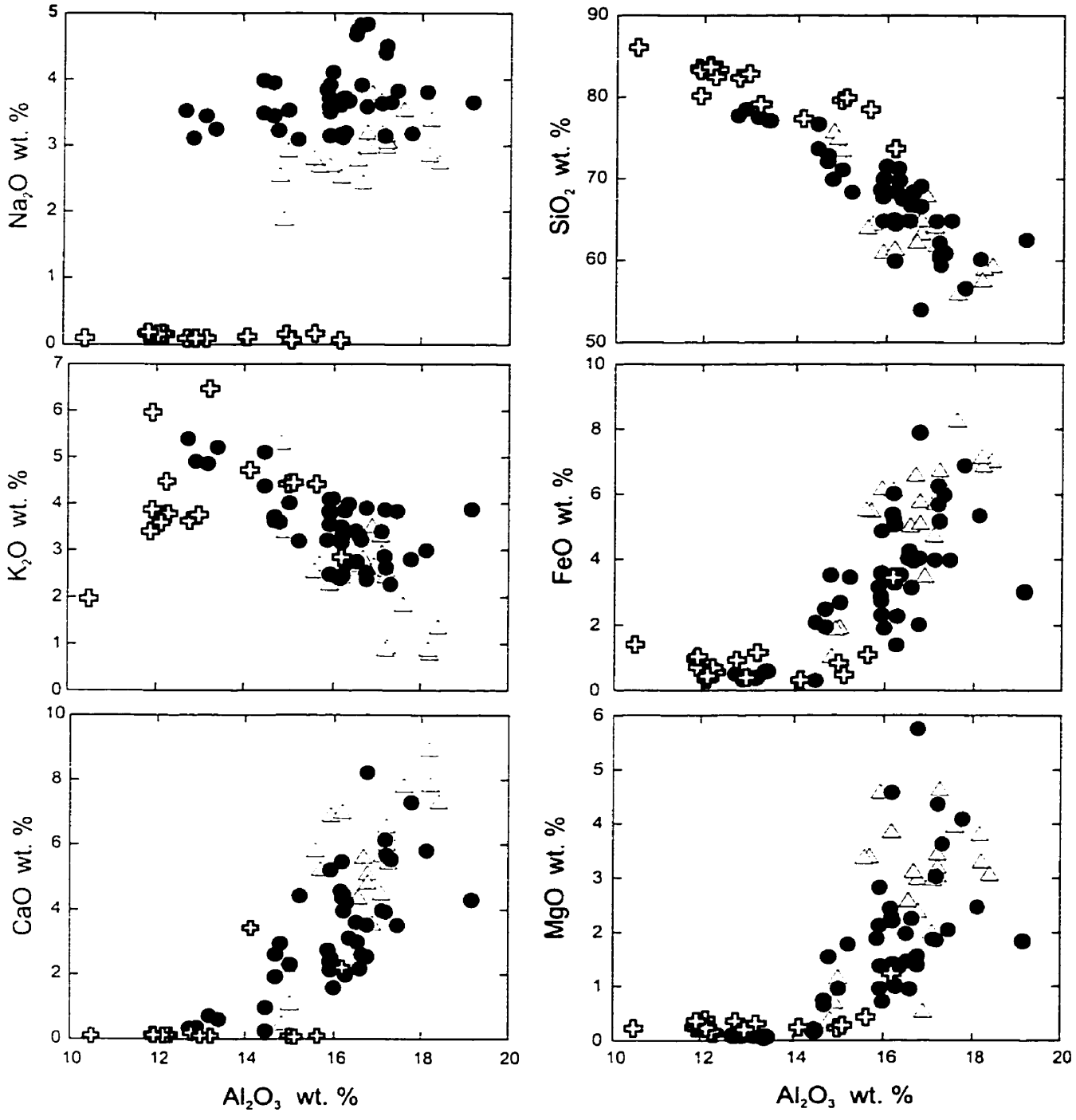
Na2O wt. %
SiO2 wt. %
K2O wt. %
FeO wt. %
CaO wt. %
MgO wt. %
Al2O3 wt. %
Al2O3 wt. %

Figure 3.7 Base metals plotted against alumina to show mass changes due to alteration for the Mt. Nansen Group. Symbols as in Figure 3.6.

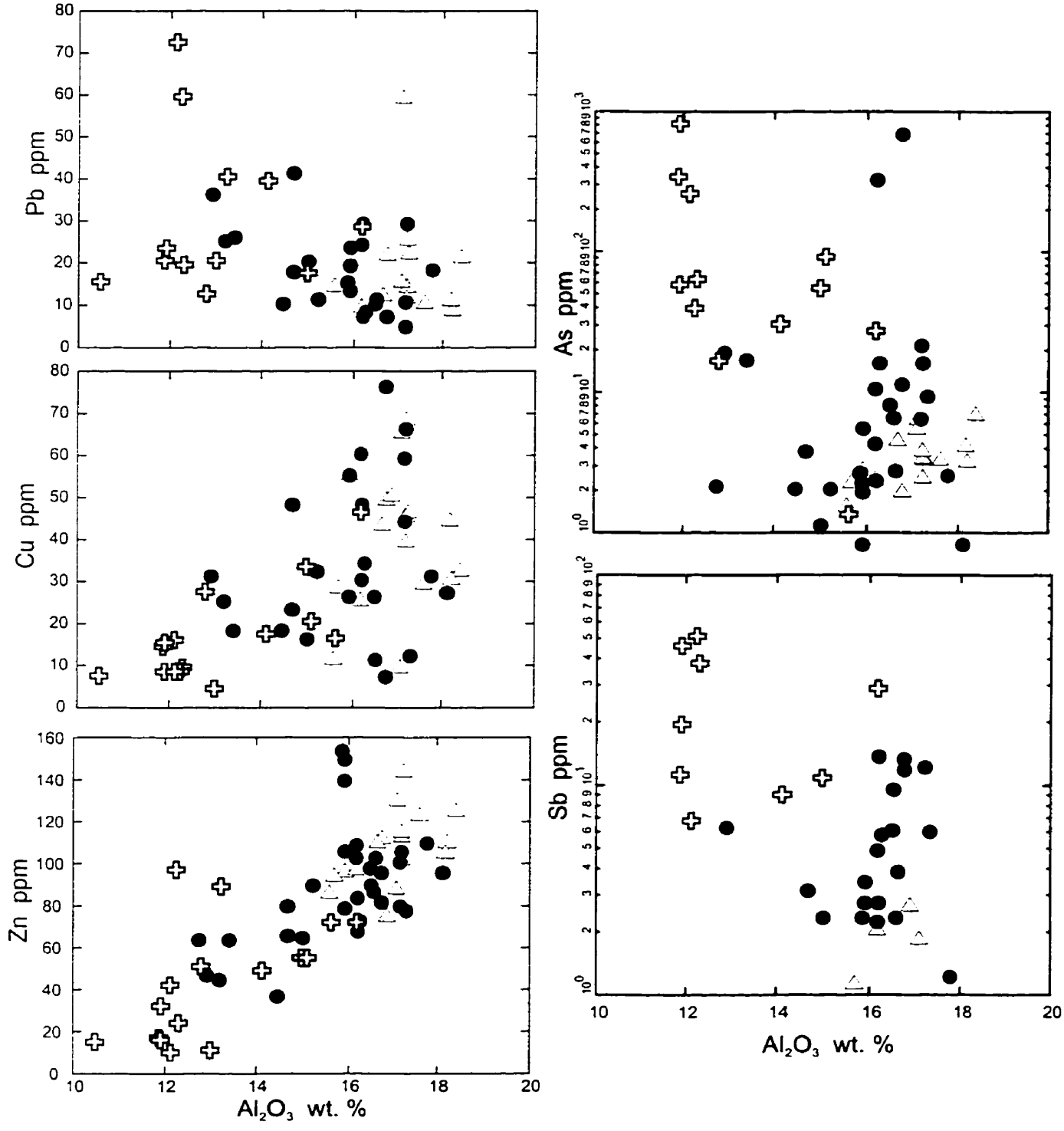
Pb ppm
Cu ppm
Zn ppm
As ppm
Sb ppm
Al_2O_3 wt. %
Al_2O_3 wt. %

For this dyke the method of mass change calculation described by MacLean and Kranidiotis (1987) and MacLean (1990) was utilized to quantify the changes in the two altered samples relative to the freshest sample (Figs. 3.8 and 3.9). In this method the masses of elements in the altered samples are recalculated to the concentration of a monitor immobile element in the fresh sample. Aluminum was chosen as the monitor because it is a major element and therefore not subject to nugget effects, because it is known to be relatively immobile during alteration (MacLean, 1990), and for consistency with the preceding approach used for Mt. Nansen samples.

The results for the Carmacks dyke are similar to those for the Mt. Nansen dykes. Na shows a strong depletion in both altered samples, as does Mg and to a lesser degree K. However, the concentration of Si is essentially constant, while Fe is enriched. Ca is depleted in the slightly altered dyke sample, but enriched in the intensely altered sample. Ore metals are consistently enriched in the intensely altered sample. In the slightly altered dyke sample, however, Pb, Cu and Zn are somewhat depleted, but As and Sb are strongly enriched.

Figure 3.8 Mass changes of major element oxides due to alteration of a Carmacks dyke following the method discussed in text. Slightly altered sample MN 95-34 (shaded) and strongly altered sample MN 95-35 (solid) are plotted with respect to unaltered sample MN 95-33 (baseline).

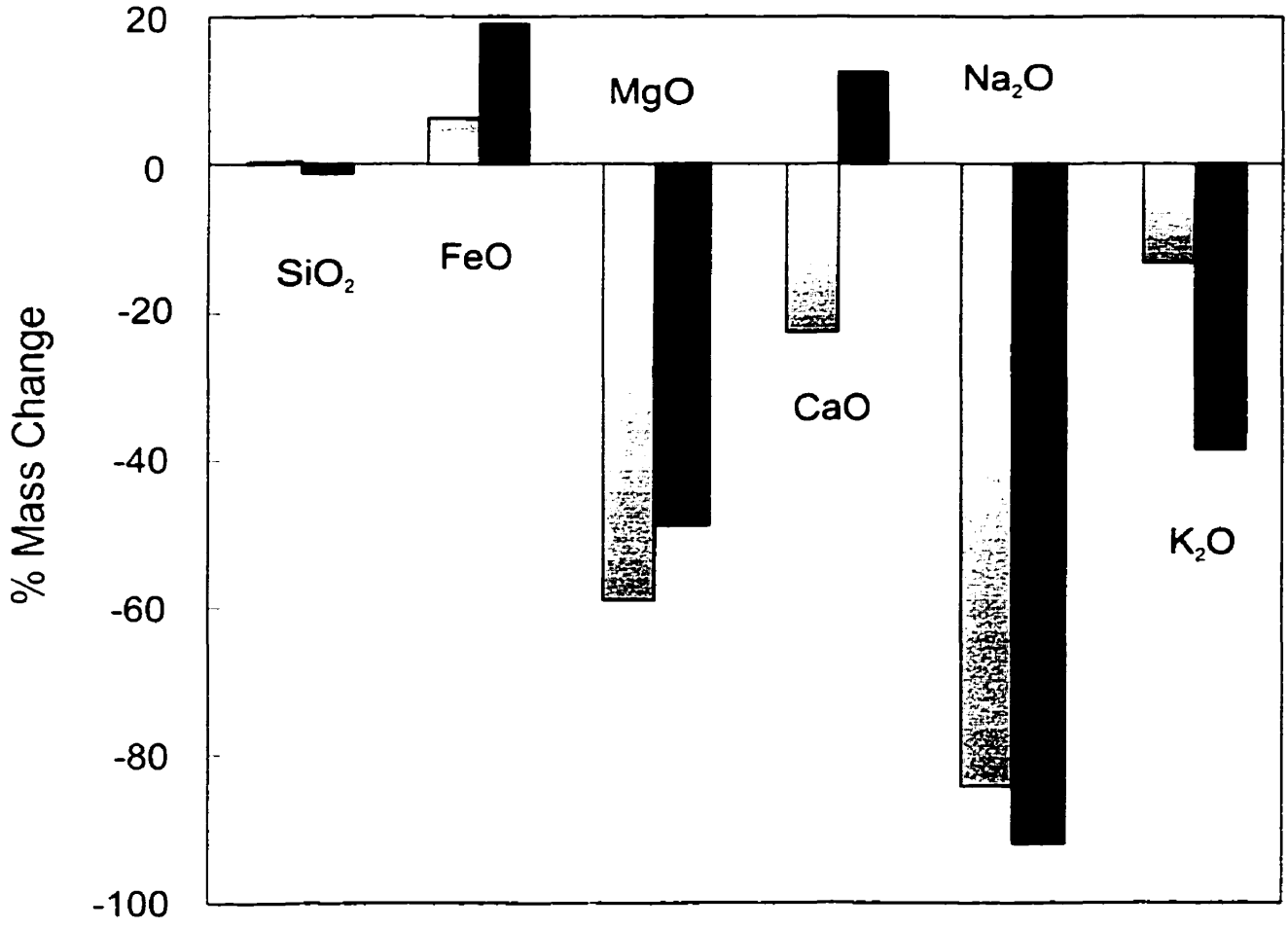
20
0
-20
-40
-60
-80
-100
% Mass Change
SiO2
FeO
MgO
CaO
Na2O
K2O

Figure 3.9 Mass changes in base metal concentrations resulting from alteration of a Carmacks dyke. Colours and technique as in Figure 3.8.

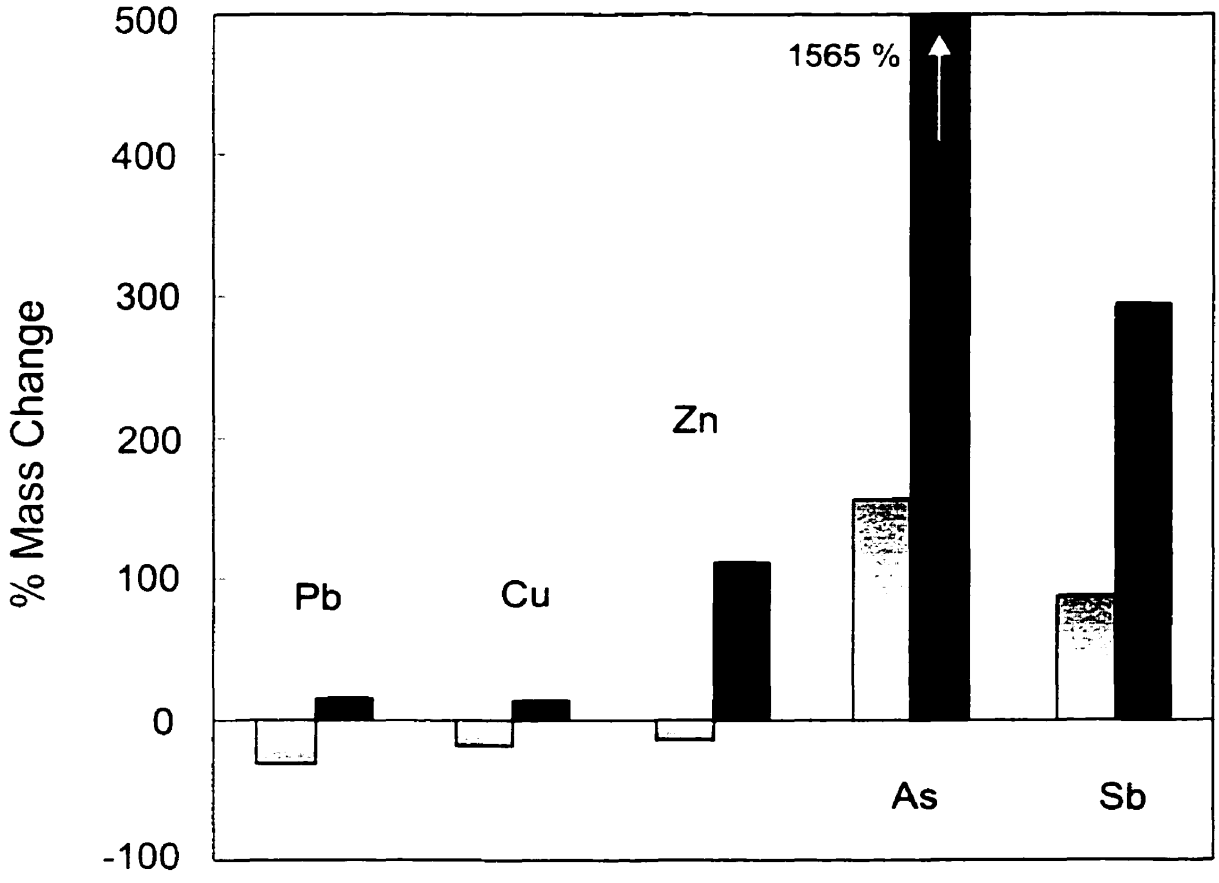
500
400
300
200
100
0
-100
% Mass Change
1565 %
Pb
Cu
Zn
As
Sb

3.5 Discussion

The most significant chemical change that accompanied alteration in both suites of altered dykes is an extreme depletion in sodium. This may be readily explained by the leaching of sodium released during feldspar breakdown by a hydrothermal fluid undersaturated with respect to sodium. Preliminary fluid inclusion data indicate a low salinity for the mineralizing fluid. Fresh dyke rocks are rich in feldspar, both as a phenocryst phase (Mt. Nansen) and as a groundmass mineral (Carmacks), and the most common alteration minerals are sericite and kaolinite. The chemical change taking place during alteration may be represented by the reactions:

$$3\ NaAlSi_3O_8 + 2\ H^+(aq.) \rightarrow NaAl_3Si_3O_{10}(OH)_2 + 6\ SiO_2 + 2\ Na^+(aq.)$$

albite paragonite quartz

$$2\ NaAl_3Si_3O_{10}(OH)_2 + 2\ H^+(aq.) + 3\ H_2O \rightarrow 3\ Al_2Si_2O_5(OH)_4 + 2\ Na^+(aq.)$$

paragonite kaolinite

Equivalent reactions involving K-feldspar and muscovite may explain the slight depletion in K observed in both suites of altered dykes because orthoclase and/or anorthoclase typically alters to muscovite and then to kaolinite under acidic conditions.

Potassium is an important element to consider in evaluating the alteration, for two important reasons. Firstly, because we have shown that alteration and mineralization were contemporaneous with shoshonitic Carmacks magmatism, the behaviour of K during alteration may provide an indication of the nature of circulating hydrothermal fluids. Magmatic water derived from a shoshonitic magma might be expected to be richer in K than typical meteoric water. As K is slightly depleted in the altered dykes of both suites, the hydrothermal fluid responsible for alteration and mineralization could have been dominantly meteoric, or undersaturated with respect to K. Secondly, because the chemical classification between the Carmacks and Mt. Nansen suites is based upon

potassium, significant K change would render this criterion useless for classifying altered rocks. Since the K change estimated for both suites of altered dykes is less than 20% for all but the most altered Carmacks sample (MN 95-35), however, by their K content Carmacks dykes can be readily distinguished from Mt. Nansen rocks.

Although the alteration of Mt. Nansen and Carmacks dykes was similar in terms of the behaviour of alkalis, other elements behaved differently in each suite. For example, Si is enriched in altered Mt. Nansen dykes, but is slightly depleted in the most altered Carmacks dyke. Conversely, Ca was depleted during alteration of Mt. Nansen dykes, but enriched in the most altered Carmacks dyke. In altered mafic Mt. Nansen dykes, Fe and Mg are depleted, while in the altered felsic Mt. Nansen dykes, these two elements are enriched. In the altered Carmacks samples (all mafic), Mg is leached, but Fe is slightly enriched.

No Mt. Nansen dykes were sampled immediately proximal to a mineralized vein, as was the case for the intensely altered Carmacks sample MN 95-35. Thus, the Mt. Nansen altered samples are better compared with the slightly altered Carmacks dyke sample MN 95-34, reflecting interaction with a mineralizing fluid distal to areas of ore deposition. The mass changes estimated for the altered Mt. Nansen samples are the same as those calculated for Carmacks sample MN 95-34, with the exception of that for Fe.

Comparison between Mt. Nansen samples and Carmacks sample MN 95-34 becomes particularly significant when assessing the changes in ore metals resulting from alteration. In the Mt. Nansen dykes, Pb, Zn, and Cu are depleted during alteration, and As and Sb are highly enriched. Except for As and Sb, ore metals in the Carmacks dyke are depleted in the slightly altered sample of the Carmacks dyke, but enriched in the most altered sample directly adjacent to the mineralized vein. It is possible that the fluid responsible for mineralization has leached Pb, Cu and Zn from the dyke and deposited them in the adjacent vein. The consistent enrichment in As and Sb with alteration,

however, indicates that these elements were introduced by the hydrothermal fluid and were not leached from the precursor dykes. The fact that Au and Sb are transportable under similar conditions by hydrothermal solutions may indicate that the Au was also introduced by the hydrothermal fluid (Williams-Jones and Normand, 1996).

3.6 Summary and Conclusions

The results of this study suggest that there is a genetic relationship between Carmacks magmatism, alteration and gold mineralization in the southern Dawson Range. Mineralization in the form of precious- and base-metal veins and gold-copper porphyries is abundant in all rock units older than the upper Carmacks in the southern Dawson Range, particularly in the areas of Mt. Nansen, Freegold Mtn. and Prospector Mtn. This area is noteworthy for its large concentration of porphyry dykes and stocks, many in areas of intense alteration. The dykes have generally been ascribed to the Mt. Nansen magmatic suite, but it is now evident that dykes of Carmacks affinity are present in the same locations, albeit in smaller numbers.

Lavas, dykes and stocks in the southern Dawson Range may be identified as belonging to either the Mt. Nansen or the Carmacks magmatic suites on the basis of their potassium content. The Carmacks Group is a shoshonitic suite while the Mt. Nansen Group is a high-K calc-alkaline suite. The Carmacks lavas extend to higher Mg contents than the Mt. Nansen suite, while the Mt. Nansen suite extends to relatively higher Si. The most mafic Mt. Nansen rocks are only andesitic in composition, while the Carmacks suite extends to primitive magnesian basalts.

The Mt. Nansen suite is well-constrained to a mid-Cretaceous age of 105 Ma, while the Carmacks suite is a 70 Ma, Late Cretaceous event. Altered Mt. Nansen dykes have been dated at between 94 and 61 Ma, and previous studies have explained these altered rocks in terms of a second Mt. Nansen event (Carlson, 1987; McInnes et al.,

1988); however we attribute these young ages to the resetting of Mt. Nansen ages by a Carmacks-age hydrothermal event that was responsible for much of the mineralization in the southern Dawson Range. The close spatial relationship between mineralized veins and Mt. Nansen dykes appears to be fortuitous because alteration of these dykes, and thus mineralization, is a Late Cretaceous, Carmacks event.

This relationship may only be true for vein mineralization, however, as it is appears that porphyry-style mineralization in Mt. Nansen stocks is a Mt. Nansen event (Sawyer and Dickinson, 1976; fluid inclusion study in progress). Carmacks intrusions also host porphyry-style mineralization, and because Mt. Nansen porphyry stocks appear to have been altered by the Carmacks hydrothermal event, the exact relationship between vein and porphyry mineralization must be examined in more detail. The strong Na and slight K depletion of altered Mt. Nansen and Carmacks dykes contrasts with the typical K-rich alteration associated with porphyry copper mineralization (Beane and Titley, 1981), and may provide a basis for evaluating the Dawson Range mineralization as representing a possible "porphyry copper to epithermal transition" type system (Cyr et al., 1984; Panteleyev, 1986; Schroeter and Panteleyev, 1986).

The most significant change due to alteration in the dykes of both suites is an extreme loss of sodium, mineralogically represented by the replacement of feldspar by sericite and clay minerals. This Na depletion is an effective guide to identifying areas of intense alteration and therefore proximal mineralization. Other common changes include addition of Si and a variably small depletion of K. Altered dykes display general depletion in Pb, Zn and Cu, suggesting that these elements were mobilized during alteration for subsequent deposition in base metal veins. As and Sb are greatly enriched in all altered dykes, and are likely to have been introduced together with gold by hydrothermal solutions responsible for the mineralization.

3.7 Acknowledgements

We are indebted to many individuals who have facilitated field work and provided valuable resources or discussion during this study: Steve Johnston and Craig Hart from the Yukon Geoscience Office, Mike Burke and Bill LeBarge from DIAND, Dave Melling and Bill Mann from B.Y.G. Natural Resources, Doug Eaton from Archer, Cathro and Associates, Ltd., Ted Tullis, and Mr. and Mrs. John Gow.

3.8 References

Beane, R.E. and Titley, S.R., 1981. Porphyry copper deposits, Part II. Hydrothermal Alteration and Mineralization. Economic Geology, 75th Anniversary Volume, p. 235-269.

Carlson, G.G., 1987. Geology of Mount Nansen (115-I/3) and Stoddart Creek (115-I/6) Map Areas, Dawson Range, Central Yukon. Indian and Northern Affairs Canada, Northern Affairs: Yukon Region Open File 1987-2.

Cyr, J.B., Pease, R.P. and Schroeter, T.G., 1984. Geology and Mineralization at Equity Silver Mine. Economic Geology, v. 79, p. 947-968.

Journeay, J.M. and Williams, S.P., 1995. GIS Map Library: A Window on Cordilleran Geology. Geological Survey of Canada, Open File 2948 (v. 1.0).

Godwin, C.I., 1976. Casino. Paper 35, Part B - Porphyry Copper and Copper-Molybdenum deposits of the Calc-Alkaline Suite; in Porphyry Deposits of the Canadian Cordillera, CIM Special Volume 15, p. 344-354.

Grant, J.A., 1986. The Isochon Diagram - A Simple Solution to Gresens' Equation for Metasomatic Alteration. Economic Geology, v. 81, p.1976-1982.

Hunt, P.A. and Roddick, J.C., 1991. A Compilation of K-Ar Ages, Report 20; in Radiogenic Age and Isotopic Studies: Report 4. Geological Survey of Canada, Paper 90-2, p. 113-143.

Johnston, S.T., 1995. Geological Compilation with Interpretation from Geophysical Surveys of the Northern Dawson Range, Central Yukon (115 J/9 and 10, 115 I/12, 1:100 000 Scale Map). Exploration and Geological Services Division, Department of Indian and Northern Affairs Open File 1995-2(G).

Le Couteur, P.C. and Tempelman-Kluit, D.J., 1976. Rb/Sr ages and a profile of initial $^{87}Sr/^{86}Sr$ ratios for plutonic rocks across the Yukon Crystalline Terrain. Canadian Journal of Earth Sciences, v. 13, p. 319-330.

MacLean, W.H., 1990. Mass change calculations in altered rock series. Mineralium Deposita, v. 25, p. 44-49.

MacLean, W.H. and Kranidiotis, P., 1987. Immobile Elements as Monitors of Mass Transfer in Hydrothermal Alteration: Phelps-Dodge Massive Sulfide Deposit, Matagami, Quebec. Economic Geology, v. 82, p. 951-962.

McInnes, B.I.A., Goodfellow, W.D., Crocket, J.H., and McNutt, R.H., 1988. Geology, geochemistry and geochronology of subvolcanic intrusions associated with gold deposits at Freegold Mountain, Dawson Range, Yukon; in Current Research, Part E, Geological Survey of Canada, Paper 88-1E, p. 137-151.

Panteleyev, A., 1986. Ore Deposits #10. A Canadian Cordilleran Model for Epithermal Gold-Silver Deposits. Geoscience Canada, v. 13, p. 101-111.

Payne, J.G., Gonzalez, R.A., Akhurst, K. and Sisson, W.G., 1987. Geology of Colorado Creek (115-J/10), Selwyn River (115-J/9), and Prospector Mountain (115-I/5) Map Areas, Western Dawson Range, West-Central Yukon. Indian and Northern Affairs Canada, Northern Affairs: Yukon Region Open File 1987-3.

Pecerillo, A. and Taylor, S.R., 1976. Geochemistry of some calc-alkaline volcanic rocks from the Kastamonu area, northern Turkey. Contributions to Mineralogy and Petrology, v. 58, p. 63-81.

Sawyer, J.P.B. and Dickinson, R.A., 1976. Mount Nansen. Paper 34, Part B - Porphyry Copper and Copper-Molybdenum deposits of the Calc-Alkaline Suite; in Porphyry Deposits of the Canadian Cordillera, CIM Special Volume 15, p. 336-343.

Schroeter, T.G. and Panteleyev, A., 1986. Lode gold-silver deposits in northwestern British Columbia; in Mineral Deposits of Northern Cordillera, CIM Special Volume 37, p. 178-190.

Stevens, R.D., Delabio, R.N., and Lachance, G.R., 1982. Age determinations and geological studies; K-Ar isotopic ages, Report 16. Geological Survey of Canada, Paper 82-2, 52 p.

Tempelman-Kluit, D.J., 1984. Geology of the Lebarge and Carmacks Map Sheets, Geological Survey of Canada, Open File 1101.

Tempelman-Kluit, D.J. and Wanless, R.K., 1975. Potassium-argon age determinations of metamorphic and plutonic rocks in the Yukon Crystalline Terrane. Canadian Journal of Earth Sciences, v. 12, p. 1895-1909.

Williams-Jones, A.E. and Normand, C., 1996. Physiochemical Controls on the Mineralogy of Hypogene Antimony Deposits in the System Fe-Sb-S-O. GAC-MAC Programs with Abstracts, v. 21, p. A102.

Yukon Minfile, 1996. Version 2.05, May 31, 1996. Exploration and Geological Services Division, Indian and Northern Affairs Canada.

Appendix 3.1 Representative chemical analyses of the Mount Nansen group

Mt. Nansen Group						
Sample No.	**MN-21**	**KZ-7**	**MN-52**	**SR-1**	**FG-1**	**MN 95-31**
Description	Lava	Lava	Fresh Dyke	Fresh Dyke	Altered Dyke	Altered Dyke
Location	Mt. Nansen	Klaza Mtn.	Mt. Nansen	"Smoky Ridge"	Freegold Mtn.	(DDH 95-151)
X	382730	370260	386840	367140	388610	387455
Y	6887950	6906150	6886675	6926410	6908600	6881700
UTM Zone	8	8	8	8	8	8
Major Elements in wt. % (XRF - McGill University)						
SiO2	55.54	63.52	63.71	77.32	77.70	68.07
TiO2	1.08	0.65	0.64	0.08	0.06	0.38
Al2O3	17.57	15.54	16.27	13.19	14.73	15.01
FeO	8.14	5.34	3.91	0.33	0.39	3.11
MnO	0.17	0.09	0.07	0.01	0.01	0.07
MgO	3.89	3.31	1.92	0.05	0.22	1.10
CaO	7.69	5.08	3.51	0.66	0.01	2.00
Na2O	3.48	2.62	4.59	3.42	0.02	0.02
K2O	1.76	2.60	3.32	4.82	4.28	2.58
P2O5	0.21	0.12	0.29	0.02	0.02	0.11
LOI	0.27	0.85	1.24	0.40	2.11	6.54
Total	99.80	99.71	99.47	100.30	99.55	99.00
Trace Elements in ppm (Ba, Rb, Sr, Y, Zr, Nb, Cr, Ni by XRF McGill, others by ICP-MS)						
Ba	1146.0	1108.0	1834.0	437.0	1171.0	1831.0
Rb	42.6	81.1	100.8	233.8	154.0	80.5
Sr	677.0	319.5	733.1	62.3	17.3	41.3
Sc	26.0	19.0	9.0	0.0	3.0	4.0
Y	23.2	24.5	14.7	24.4	11.7	17.5
Zr	112.1	173.9	194.3	57.6	46.8	193.5
Nb	6.5	9.8	12.4	21.6	12.3	9.7
V	223.0	116.0	67.0	7.0	0.0	37.0
Ta	0.0	0.0	0.9	0.0	0.0	0.6
Hf	3.6	0.0	4.8	3.3	4.3	5.2
Th	0.0	0.0	12.0	22.2	8.3	32.0
U	0.0	0.0	3.1	2.4	3.5	4.1
Pb	10.0	0.0	10.0	24.9	0.0	28.0
Cu	29.0	28.0	26.0	25.0	20.0	46.0
Zn	122.0	93.0	97.0	44.0	54.0	71.0
Cr	17.1	89.6	44.5	0.0	0.0	4.8
Co	21.0	10.0	10.0	0.0	5.0	10.0
As	3.2	2.2	7.9	0.0	88.2	26.3
Sb	0.0	1.1	6.0	0.0	0.0	28.1
Rare Earth Elements in ppm (ICP-MS - Activation Laboratories Ltd.)						
La	0.00	0.00	42.07	10.18	10.96	67.63
Pr	0.00	0.00	7.21	2.00	1.84	9.66
Ce	53.00	0.00	75.14	19.59	20.12	108.10
Nd	0.00	0.00	32.95	7.90	7.29	37.00
Sm	0.00	0.00	5.28	1.52	1.30	4.62
Eu	0.00	0.00	1.49	0.48	0.38	1.12
Gd	0.00	0.00	3.81	1.65	1.22	3.95
Tb	0.00	0.00	0.52	0.33	0.22	0.50
Dy	0.00	0.00	2.50	1.95	1.02	2.55
Ho	0.00	0.00	0.41	0.57	0.22	0.52
Er	0.00	0.00	1.14	1.43	0.57	1.50
Tm	0.00	0.00	0.15	0.29	0.10	0.26
Yb	0.00	0.00	1.02	1.64	0.56	1.53
Lu	0.00	0.00	0.15	0.24	0.08	0.29

Appendix 3.2 Representative chemical analyses of the Carmacks group

Carmacks Group						
Sample No.	**PR-23**	**ML-21**	**PR-26**	**MN95-33**	**MN 95-34**	**MN 95-35**
Description	Lava	Lava	Fresh Dyke	Fresh Dyke	Altered Dyke	Altered Dyke
Location	Prospector Mtn.	Miller's Ridge	Prospector Mtn.	(DDH 95-151)	(DDH 95-151)	(DDH 95-151)
X	355380	427950	354125	387455	387455	387455
Y	6927510	6883410	6926375	6881700	6881700	6881700
UTM Zone	8	8	8	8	8	8
Major Elements in wt. % (XRF - McGill University)						
SiO2	60.35	50.55	64.78	51.62	52.73	48.20
TiO2	0.84	0.71	0.61	0.78	0.83	0.77
Al2O3	16.81	10.70	16.22	15.04	15.32	14.24
FeO	4.99	7.80	3.88	7.27	7.86	8.19
MnO	0.25	0.15	0.08	0.16	0.17	0.28
MgO	1.43	15.85	1.58	5.71	2.39	2.77
CaO	1.93	6.42	3.13	5.92	4.66	6.30
Na2O	1.53	2.05	3.72	2.72	0.44	0.21
K2O	10.34	2.88	3.94	3.95	3.49	2.30
P2O5	0.34	0.45	0.26	0.36	0.38	0.35
LOI	0.31	1.96	1.31	5.59	10.99	14.95
Total	99.13	99.52	99.50	99.12	99.26	98.56
Trace Elements in ppm (Ba, Rb, Sr, Y, Zr, Nb, Cr, Ni by XRF McGill, others by ICP-MS)						
Ba	1959.0	1493.0	1609.0	3359.0	2021.0	1878.0
Rb	366.7	74.1	163.0	109.8	97.7	69.1
Sr	321.2	527.4	540.6	768.2	166.8	155.9
Sc	0.0	19.0	0.0	17.0	26.0	20.0
Y	21.5	17.3	17.7	23.3	25.4	24.1
Zr	247.3	105.4	209.6	145.1	135.9	125.3
Nb	24.1	7.9	14.9	6.7	8.5	8.2
V	93.0	144.0	64.0	141.0	172.0	149.0
Ta	2.0	0.0	1.3	0.4	0.6	0.3
Hf	6.1	2.0	5.7	3.4	3.4	3.2
Th	24.9	0.0	18.8	8.2	7.4	6.8
U	9.2	0.0	7.7	2.5	2.0	2.2
Pb	254.0	7.4	51.0	23.0	16.0	25.0
Cu	61.0	82.0	50.0	63.0	52.0	68.0
Zn	150.0	110.0	126.0	154.0	135.0	309.0
Cr	14.4	1092.0	13.7	190.9	242.9	238.8
Co	6.0	48.0	5.0	22.0	11.0	32.0
As	7.3	3.5	12.3	1.3	3.4	20.5
Sb	6.4	0.0	8.1	8.8	17.9	36.7
Rare Earth Elements in ppm (ICP-MS - Activation Laboratories Ltd.)						
La	40.88	0.00	37.39	27.38	28.04	26.33
Pr	6.44	0.00	6.29	5.83	6.06	5.52
Ce	70.78	48.00	66.47	52.72	54.43	50.08
Nd	27.46	0.00	28.24	27.38	29.18	26.65
Sm	4.72	0.00	4.61	5.48	5.61	5.29
Eu	1.19	0.00	1.28	1.71	1.61	1.53
Gd	3.77	0.00	3.87	4.65	4.81	4.60
Tb	0.57	0.00	0.56	0.73	0.74	0.70
Dy	3.12	0.00	2.83	3.80	4.20	3.84
Ho	0.60	0.00	0.52	0.73	0.78	0.74
Er	1.81	0.00	1.51	2.08	2.25	2.12
Tm	0.28	0.00	0.23	0.30	0.33	0.30
Yb	1.74	0.00	1.40	1.99	2.05	1.95
Lu	0.29	0.00	0.23	0.31	0.34	0.31

Bridge to Chapter 4

In the previous chapter, the Mount Nansen and the Carmacks volcanic groups were distinguished on the basis of petrography, major and trace element geochemistry, and ages. The alteration of country rocks in the vicinity of gold mineralization was shown to be characterized by an extreme depletion of Na^+, which could be a useful exploration guide in this area. Ar dating showed that the ages of the Mount Nansen rocks in the vicinity of gold mineralization were thermally reset to that of the Carmacks group.

Chapter 4 pursues the possible role of the Carmacks magmatic event in the regional gold metallogeny of the Dawson Range with a study of epithermal gold veins themselves. Fluid inclusion microthermometry, decrepitate analyses, gas chromatography, and stable isotope data are presented, along with sulphur and lead isotopic analyses of base metal sulphides. These data are brought together in the formulation of a cohesive Au metallogenic model for the Dawson Range.

Chapter 4

Late Cretaceous Epithermal Metallogeny of the Southern Dawson Range, Yukon: Fluid Inclusion and Isotopic Evidence

K. A. Smuk, A. E. Williams-Jones and D. Francis
Department of Earth and Planetary Sciences
McGill University

Abstract

The southern Dawson Range of the south central Yukon contains a series of structurally controlled epithermal veins hosted by lithologies ranging from Proterozoic metasedimentary assemblages to Late Cretaceous volcanic rocks. Two volcanic suites are present in the area: the 105 Ma Mount Nansen group and the 70 Ma Carmacks group, both of which also host small Au-Cu(±Mo) porphyry deposits.

The epithermal veins are dominated by base metal sulphides in the paragenetic sequence: pyrite, arsenopyrite, sphalerite, chalcopyrite, galena, enargite, (sulphosalts), and tetrahedrite. Gold occurs predominantly as submicroscopic inclusions within a variety of sulphide minerals. Fluid inclusion microthermometry, decrepitate analyses, and gas chromatography indicate that the mineralizing hydrothermal fluid had an average salinity of 5.8 wt.% NaCl equiv. (2-16 wt.%), was Na^+-dominated with lesser K^+ and Ca^{2+}, had Cl^- and S^{2-} concentrations of approximately 0.99 *m* and 0.20 *m*, respectively, and was moderately CO_2-rich (0.6-1.4 mol.%), and that the deposition of ore minerals occurred at a temperature of approximately 300°C (210-380°C). The oxygen and hydrogen isotopic composition of inclusion fluids indicate that the fluid was dominantly meteoric, and evolved through interaction with country rocks ($\delta^{18}O$ = -15.0 to –5.0‰; δD = -85 to –108‰). A small magmatic fluid contribution is suggested by a small proportion of samples with heavier $\delta^{18}O$, and the relatively high temperature, salinities, ΣS, and CO_2. The fluids from inclusions in vein ore have significantly heavier δD than present-day meteoric water in the Dawson Range, suggesting the possibility of significant northward motion since their formation. Sulphur isotopic values ($\delta^{34}S$ = -2.4 to +0.2 ‰) suggest an igneous or magmatic sulphur source, and the isotopic composition of Pb in galenas is similar to the initial whole rock values of the Carmacks volcanic group. The log fO_2 and pH conditions of mineralization are interpreted to have been between -34 and -36, and <5, respectively. The fluids are thought to be part of a regional hydrothermal event related to the Late Cretaceous Carmacks volcanic group.

The Dawson Range veins differ from typical low sulphidation epithermal deposits in the presence of high sulphidation ore minerals such as enargite, tennantite, and barite, alteration minerals such as sericite and clay with little to no adularia, and fluids with low pH, high ΣS, and moderately high CO_2, characteristics which may be attributed to the contribution of fluids from the shoshonitic Carmacks volcanic group. A model is proposed whereby acid hydrothermal fluids driven by the emplacement of the Carmacks group resulted in sericitic and argillic alteration, triggering the deposition of numerous gold- and base metal-rich epithermal veins that are transitional between classic low and high sulphidation types. The deposition of base metal sulphides is interpreted to have been caused by an increase in pH due to the consumption of H^+ during sericitic and argillic alteration of the host rocks. This deposition of base metal minerals reduced the ΣS, which destabilized gold bisulphide complexes (the dominant form of soluble Au), thereby causing the precipitation of native gold.

4.1 Introduction

The Dawson Range gold belt is a northwest-trending series of gold-rich epithermal vein deposits, copper-gold porphyry deposits, minor skarns, and extensive in-situ (LeBarge, 1995) placer deposits, that stretch for approximately 100 kilometres parallel to the Big Creek fault, northwest of Carmacks, in the south-central Yukon (Fig. 4.1). Important epithermal vein deposits in this belt have been exploited by the Mount Nansen and the Laforma gold mines. Other significant epithermal deposits include the Tawa, Tinta Hill, Emmons Hill and Frog prospects. These deposits share a common geological setting, and are mineralogically similar, suggesting that they represent a single metallogenic event. Although uneconomic, porphyry Cu-Au deposits such as Revenue, Nucleus, and Cash, along the southwest side of the Big Creek fault, and Cyprus at the Mount Nansen camp, are noteworthy in their close association with, but uncertain relationship to the epithermal deposits. Recent exploration has focussed mostly on the

Figure 4.1 Geological setting and gold prospects of the southern Dawson Range, Yukon, simplified from Carlson (1987) and Payne et al. (1987). Indicated are the three exploration camps, Mount Nansen, Freegold Mountain, and Prospector Mountain, and all vein and porphyry deposits or prospects in the area (Yukon Minfile, 1996).

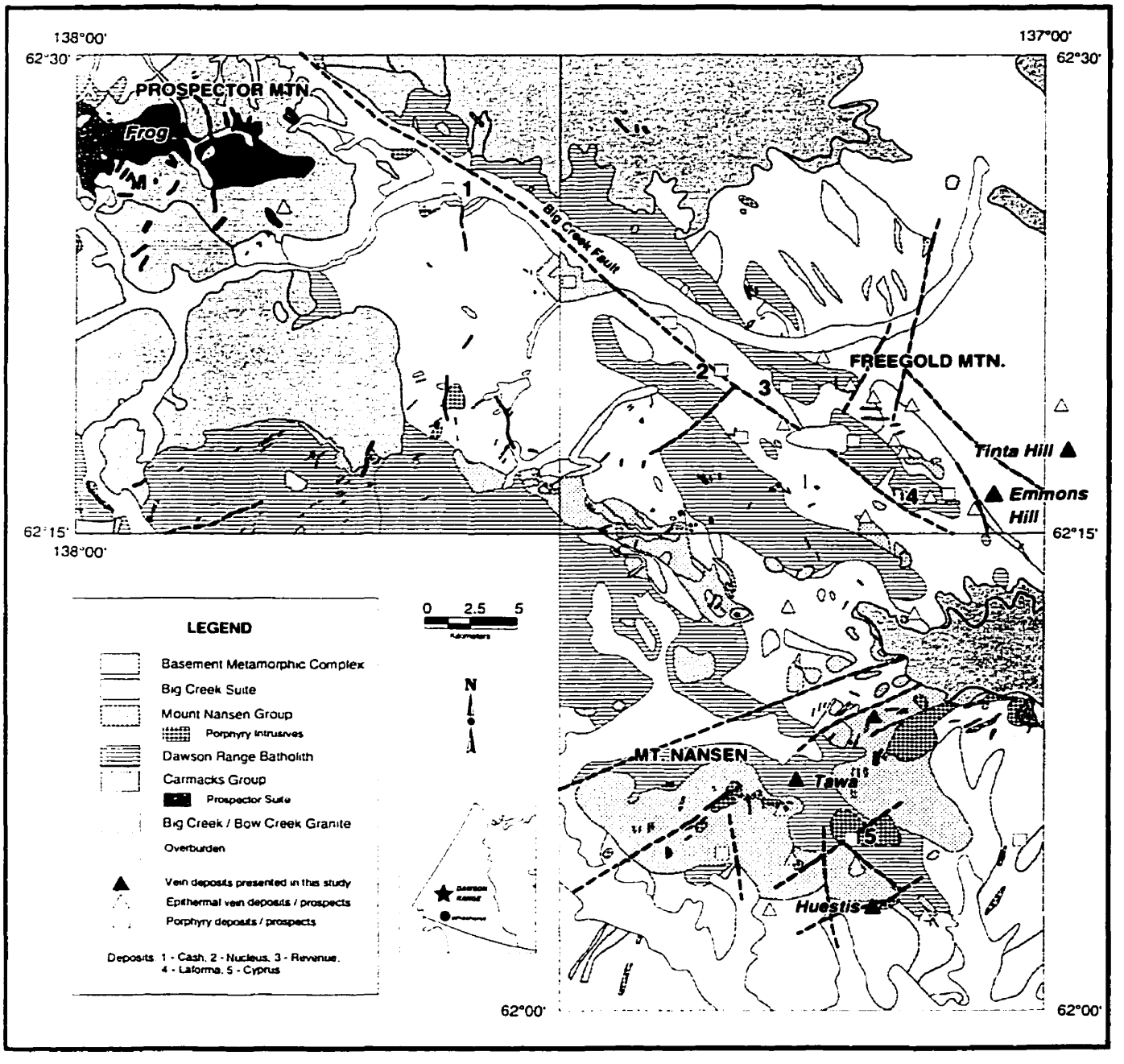
138°00'
137°00'
62°30'
62°15'
62°00'
PROSPECTOR MTN
Frog
Big Creek Fault
FREEGOLD MTN.
Tinta Hill
Emmons Hill
MT. NANSEN
Tawa
Huestis
1
2
3
4
5
LEGEND
Basement Metamorphic Complex
Big Creek Suite
Mount Nansen Group
Porphyry intrusives
Dawson Range Batholith
Carmacks Group
Prospector Suite
Big Creek / Bow Creek Granite
Overburden
Vein deposits presented in this study
Epithermal vein deposits / prospects
Porphyry deposits / prospects
Deposits 1 - Cash, 2 - Nucleus, 3 - Revenue,
4 - Laforma, 5 - Cyprus
0 2.5 5
N

northernmost Casino Cu-Mo-Au porphyry deposit, outside the present southern Dawson range study area.

Although most of the deposits of the Dawson Range have been described in some detail, and some have been studied geochemically, there has been no previous attempt to develop a comprehensive metallogenic model. Some of the prerequisites to understanding Au metallogenesis in the Dawson Range are establishing the relationships, if any, among the various vein deposits, between the epithermal deposits and the porphyry deposits, and between mineralization and volcanism. The purpose of this study is to characterize the nature of the epithermal vein deposits of the southern Dawson Range, and to establish their origin, using the following as representative examples: from south to north, the Huestis and Tawa deposits of the Mount Nansen camp, the Tinta Hill and Emmons Hill deposits of the Freegold Mountain camp, and the Frog deposit at the Prospector Mountain camp.

The epithermal veins of the southern Dawson Range have mineralogical and alteration characteristics most similar to the adularia-sericite (Hedenquist et al., 1996; Hayba et al., 1985; Heald et al, 1989), or low-sulphidation, type of epithermal deposit. Certain ore, alteration, and fluid characteristics of the deposits, however, suggest that they may be transitional between low-sulphidation and high-sulphidation types. The epithermal veins of the southern Dawson Range differ as a group from typical adularia-sericite deposits in that adularia is generally absent, while argillic and sericitic alteration is well-developed, and in the occurrence of some high-sulphidation state minerals, the sulphide-rich character of the veins, as well as in the chemistry of the ore-forming fluid. The sulphide minerals comprise, in general order of abundance, pyrite, galena, sphalerite, and chalcopyrite, and varying proportions of arsenopyrite and sulphosalt minerals (mainly Sb-bearing). Gold is reported to occur most commonly as submicroscopic inclusions in several of the sulphide minerals (Saager and Bianconi, 1971; McInnes et al., 1990; Glasmacher, 1990; Hart and Langdon, 1998). The deposits are hosted by a wide variety of host rocks, including Proterozoic-Paleozoic metasedimentary rocks, Jurassic to

Cretaceous plutons, and Late Cretaceous andesitic to basaltic tuffs and flows. Sericitic, silicic, argillic and rare potassic alteration has been noted surrounding the vein mineralization.

Previous researchers have investigated some of the epithermal deposits. McInnes (1987) and McInnes et al. (1990) described the geology and geochemistry of the Laforma deposit of the Freegold Mountain camp (Fig. 4.1) and concluded that gold and minor base metal mineralization in quartz veins was emplaced in a boiling system genetically related to subvolcanic porphyry dykes of the Mount Nansen volcanic group. Glasmacher (1990) modelled the Frog deposit at the Prospector Mountain camp as the product of a meteoric-magmatic fluid system derived from and caused by the extrusion of the Carmacks volcanic group. Hart and Langdon (1998) described the geology of the Mount Nansen vein-porphyry system and attributed both styles of mineralization to the intrusion of Mount Nansen porphyry stocks. Most workers in the Dawson Range have attributed both porphyry-style and epithermal vein mineralization outside of Carmacks group lithologies to the Mount Nansen volcanic event (Carlson, 1987; McInnes, 1987; Yukon Minfile, 1996; Hart and Langdon, 1998). Johnston et al. (1996), Smuk et al. (1997), and Hart et al. (1998), however, have suggested that the epithermal mineralization may be related to the Carmacks volcanic event based on evidence from hydrothermal alteration and paleomagnetic data. In this study we present fluid inclusion and isotopic data that characterize the geochemistry of the sulphide and gold rich epithermal system in the southern Dawson Range, and suggest that a Late Cretaceous metallogenic event was responsible for epithermal mineralization that was superimposed on earlier mid-Cretaceous porphyry-style mineralization.

4.2 Geological Setting

The Dawson Range straddles the Yukon-Tanana and the Stikinia Cordilleran terranes. The Yukon-Tanana terrane comprises the pericratonic Kootenay terrane and the Proterozoic to Paleozoic Nisling terrane, a metamorphosed passive continental margin

sedimentary sequence. The Stikinia terrane consists of Devonian to Lower Jurassic platform carbonate rocks, island arc volcanic and volcaniclastic rocks, and comagmatic plutons (Clowes, 1997). Paleomagnetic evidence consistently suggests that the Canadian Cordilleran terranes originated at considerable distances south of their present latitudes. Umhoefer (1987), Wynne et al. (1998), Irving and Wynne (1990), and Engebretson et al. (1985) have suggested that the northern Cordillera was at the latitude of southern California at 100-90 Ma, and has dislocated northwards a distance of some 2000 km by about 55 Ma with respect to the North American continent.

The oldest rocks in the southern Dawson Range study area comprise the Paleozoic to Proterozoic Basement Metamorphic Complex, a series of metasedimentary units overlain by schists and gneisses (Tempelman-Kluit and Wanless, 1980; Carlson, 1987; Payne et al., 1987). This package has been metamorphosed from greenschist to the lower amphibolite facies, and comprises part of the Yukon-Tanana terrane. These rocks have been intruded by the 192 Ma Granite Batholith (Tempelman-Kluit, 1984), a foliated diorite to granodiorite, and the 184 Ma Big Creek Syenite (Tempelman-Kluit, 1984; Carlson, 1987), a plagioclase-hornblende-quartz (± potassium feldspar megacrysts) monzonite, which together comprise the Big Creek Meta-Plutonic Suite of the Stikinia terrane.

The earliest volcanic unit, which outcrops in the southern part of the field area, is the mid-Cretaceous Mount Nansen group with high-potassium, calc-alkaline affinities. This 105 Ma (Tempelman-Kluit, 1984; Carlson, 1987; Hunt and Roddick, 1991; Smuk et al., 1997) unit consists of a coarse, well-consolidated, bimodal volcanic breccia, with fragments of variably altered andesite and rhyolite in a fine-grained andesitic matrix. The Mount Nansen group is metamorphosed to the greenschist facies, and Carlson (1987) interprets the exposure as the roots of the volcanic system, implying a large degree of erosion since mid-Cretaceous time. A coeval swarm of quartz- and feldspar-phyric rhyolitic dykes are found throughout the study area (Smuk et al., 1997), and have been considered to be genetically related to epithermal and porphyry-style mineralization

(Carlson, 1987; McInnes, 1987; Yukon Minfile, 1996; Hart and Langdon, 1998). The comagmatic Dawson Range Batholith ranges in age from 106 to 90 Ma (Tempelman-Kluit and Wanless, 1975; LeCouteur and Tempelman-Kluit, 1976), and comprises at least two distinct units, the prominent biotite-hornblende Casino Granodiorite, and the granitic to quartz monzonitic Coffee Creek Granite.

The Carmacks group is an extensive sequence of shoshonitic volcanics that has been dated at 70 Ma (Stevens et al., 1982; Grond et al., 1984; Tempelman-Kluit, 1984; Johnston, 1995; Smuk et al., 1997). The Lower Carmacks unit is divided into a >500 metre-thick lowermost succession of andesitic volcanic breccias, tuffs, and minor thin flows, and also includes minor mudflows and water-reworked deposits. This lowermost unit grades upward into a 500 metre-thick suite of interbedded andesitic to basaltic tuffs and flows. The Upper Carmacks unit comprises a nearly flat-lying series of thick, olivine- and clinopyroxene-phyric ankaramite to basalt flows (Johnston et al., 1996; Smuk et al., 1997). A small volume of coeval intrusive rocks is represented by the Prospector Suite, a granite plug exposed at Prospector Mountain, and the Casino Intrusion, which hosts the Casino Cu-Mo-Au porphyry deposit (Godwin, 1976; Tempelman-Kluit, 1984; Selby and Nesbitt, 1998) northwest of the study area. A swarm of feldspar-phyric mafic to intermediate dykes also occurs throughout the study area, albeit less frequently than the more felsic dykes associated with the Mount Nansen group (Smuk et al., 1997). Based on its geochemical and paleomagnetic signatures, Johnston et al. (1996) interpret the Carmacks group as the product of shallow lithospheric melting caused by the Late Cretaceous Yellowstone hotspot. The small Bow Creek Granite, a biotite quartz monzonite to granite pluton, outcrops just north of Mount Nansen, and has been tentatively correlated with the Carmacks group based on dates of 60 Ma (Carlson, 1987) and 85 Ma (Tempelman-Kluit, 1984).

The general structural fabric of the Dawson Range runs northwest by southeast, paralleling the Tintina fault to the east and the Shakwak-Denali Trench to the southwest. The Big Creek fault is the largest structure in the Dawson Range, and has been interpreted

as a normal fault with the southwest side down (Carlson, 1987) that has also experienced a dextral displacement of some 14 kilometres (McInnes, 1987). Numerous smaller faults trending 130° to 160°, also displaying both normal and dextral strike-slip motion (McInnes et al., 1988; Hart and Langdon, 1998) are prominent throughout the southern Dawson Range, and host the majority of porphyry dykes of both volcanic groups as well as mineralized veins. Two other sets of northeast-trending (20° and 50°-80°), sinistrally-displaced faults are also developed in the area and are also commonly associated with dykes and veins. There is also some evidence of northeast-trending (40°), post-mineralization faulting (Anderson and Stroshein, 1998). The numerous mineral deposits of the Dawson Range follow a northwest linear trend along the southwest of the Big Creek fault, and are offset slightly further to the southwest in the Mount Nansen camp.

4.3 Mineral Deposit Geology

Five epithermal vein deposits were sampled from three large exploration camps in the southern Dawson Range. They are found in a wide range of host rocks, and represent a small range in mineralization styles. These veins are the Huestis and Tawa deposits of the Mount Nansen camp, the Tinta Hill and the Emmons Hill deposits of the Freegold Mountain camp, and the Frog deposit of the Prospector Mountain camp (Fig. 4.1). Observations of the geology of the mineral deposits were restricted to those that could be made on samples collected from muck piles at the deposits, as underground workings were inaccessible. It was therefore necessary to depend on reports of earlier researchers for descriptions of the immediate geological setting to the deposits and host rock alteration.

4.3.1 Mount Nansen Camp

Huestis

The Huestis deposit forms part of the interconnected vein system of the Mount Nansen trend (Hart and Langdon, 1998) that extends for approximately 12 kilometres in a

northwest trending horst occupied by granodiorite of the Dawson Range Batholith and schists and gneisses of the Basement Metamorphic Complex. Andesites of the Mount Nansen group host a small proportion of the vein prospects. Hart and Langdon (1998) document extensive argillic (kaolinite, illite, and montmorillonite) and common phyllic (sericite, quartz, disseminated pyrite) alteration in up to 10 m wide envelopes surrounding epithermal veins of the Mount Nansen trend. The degree of alteration around veins was found to reflect the host rock composition; granodiorite host rocks are the most extensively altered, followed by andesites, and then the basement metamorphic rocks (Hart and Langdon, 1998).

The base metal- and gold-rich Huestis quartz vein strikes 320° and dips at 80° to the northeast, and has been traced for approximately 550 metres along strike and 400 metres down dip. Underground reserves have been calculated at 123, 800 tonnes grading 14.1 g/t Au and 291 g/t Ag (Hart and Langdon, 1998), although anomalous grades of up to 246 g/t Au and 2226 g/t Ag have been reported (Morin, 1981). The plagioclase-hornblende to amphibolite gneiss and feldspar mica schist hosting the Huestis deposit (Anderson and Stroshein, 1998) are altered from 1.5 to 15 metres (5-50 feet) away from the vein (Saager and Bianconi, 1971), but lack a consistent alteration zonation. This alteration is dominantly sericitic and is characterized by sericite, quartz, pyrite, chlorite, and carbonate. Argillic alteration is locally evident by the kaolinization of feldspars and the bleaching of the host rocks. Silicification occurs immediately adjacent to the vein, and sporadic zones of carbonate and epidote, while minor quartz, pyrite, and chlorite, replace host gneisses distally.

The Huestis vein is a sulphide-rich, finely laminated to massive structure that is locally brecciated. Three textural types of polymetallic sulphide ore have been identified; massive, laminated, and breccia, all displaying the same mineral paragenesis (Fig. 4.2). The massive ore is characterized by a ratio of sulphides to quartz of approximately 3:1, and is dominated by early euhedral arsenopyrite and sphalerite surrounded by grains of later euhedral quartz. The sulphide-dominant laminated type is characterized by zones of

Figure 4.2 Generalized paragenetic sequence of mineralization at the Huestis, Tawa, Tinta Hill, Emmons Hill, and Frog deposits. Dashed lines represent variable or minor occurrence. Specific paragenetic sequences for each deposit are described in the text.

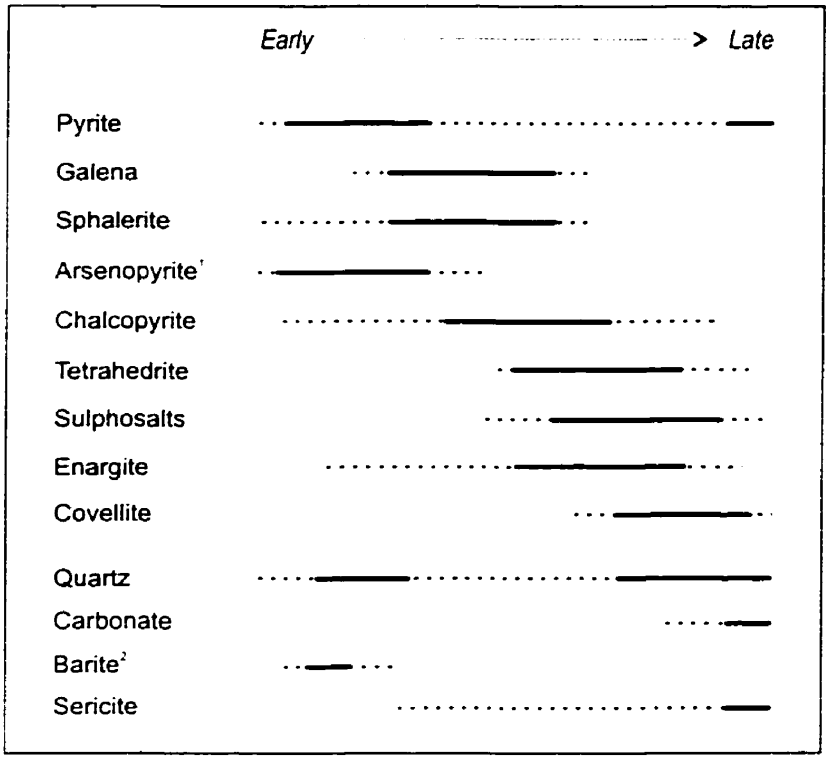

[1] Arsenopyrite does not occur at Tinta Hill

[2] Barite occurs only at Emmons Hill

alternating arsenopyrite-rich, sphalerite-rich, and tetrahedrite-rich ore on a mm- to cm-scale. The brecciated type ore is cemented and veined by quartz and pyrite, with open spaces being filled by late carbonate. Other phases within the Huestis vein include minor interstitial galena partially replaced by tetrahedrite, boulangerite, jamesonite, zinkenite, and chalcostibite. The Huestis vein also contains an unidentified euhedral bladed to fibrous Pb(±Fe, Ag)-Sb-sulphosalt possibly replacing the earliest phase enclosed in arsenopyrite and sphalerite. Semi-quantitative electron microprobe EDS analyses also indicate the presence of several unknown Pb-(Cu)-Sb-(As)-sulphosalt species in Huestis ore samples. Sb typically predominates over As, although As occasionally equals or exceeds Sb. Sphalerite displays fine oscillatory zoning from a deep red to amber colour, corresponding to a compositional range from 17.0 to 6.5 mol.% FeS.

Hart and Langdon (1998) found that between 10% and 25% of the Mount Nansen gold occurs as free gold or electrum, mostly as grains within quartz as well as associated with pyrite, chalcopyrite and arsenopyrite. Anomalous concentrations of gold were detected by electron microprobe WDS analyses of pyrite, while silver was found to be concentrated within sulphosalts (up to 10 mol.%). Saager and Bianconi (1971) report a gold fineness of approximately 800 for the Mount Nansen deposit. Ag is reported to occur in freibergite, galena and jamesonite, and Au to form small interstitial particles of the native metal between or occurring as inclusions within galena, freibergite, jamesonite, bournonite, sphalerite, pyrite, arsenopyrite, and gangue minerals (Saager and Bianconi, 1971). Total silver to gold ratios average 20:1 but range from 10:1 to 200:1 from vein to vein (Hart and Langdon, 1998). Saager and Bianconi (1971) have also documented the presence of freibergite, bournonite and stibnite in the Huestis veins.

Tawa

The Tawa deposit lies on the eastern flanks of Mount Nansen, and is the inferred northwesternmost extension of the Mount Nansen vein system that includes the Huestis vein to the southeast (Hart and Langdon, 1998). The Tawa veins are hosted by the Coffee

Creek Granite and the Casino Granodiorite of the Dawson Range Batholith within fault zones trending 110° to 140°. Saunders (1980) reports that the vein-fault zones dip steeply to the northeast, while the Yukon Minfile (1996) reports a steep dip to the southwest, indicating that the zones are nearly vertical. Assays have been highly variable along the length of the vein system, but the best assays include 5.62 g/t Au and 31.5 g/t Ag over 2.5 metres, and 15.1 g/t Au and 483.6 g/t Ag over 1.8 metres (Yukon Minfile, 1996). The host rocks have been subjected to strong argillic alteration (pervasive kaolinization of feldspars (Saunders, 1980)) and minor phyllic alteration (sericite and pyrite). It is, however, not known whether the argillic alteration is of hypogene or supergene origin.

Three ore types have been identified at the Tawa deposit: pyrite-rich quartz veins, massive arsenopyrite-pyrite veins, and laminated polymetallic sulphide-rich veins. Pyrite-rich ore consists of >50% early euhedral pyrite, followed by large, euhedral quartz grains, and later interstitial chalcopyrite which was replaced by enargite (famatinite) and tetrahedrite, with minor covellite replacing all three. The massive ore consists primarily of arsenopyrite and pyrite, followed by minor quartz, sphalerite with well-developed chalcopyrite disease, galena, and chalcopyrite, and later tetrahedrite and enargite which replace chalcopyrite. The banded ore is characterized by three concentric 5 cm-wide zones that contain the same mineral species in the same paragenetic order, but in different proportions (Fig 4.2). The outer zone consists primarily of large, euhedral crystals of arsenopyrite and pyrite, which grades into a finer-grained zone dominated by arsenopyrite and pyrite, and then into a core zone dominated by sphalerite and galena. Quartz forms large euhedral crystals that deposited temporally between pyrite and galena, as well as later, small crystals and veinlets enclosing minor pods of sericite. Sulphosalts are generally absent in this deposit, although very minor concentrations of late-stage jamesonite may be present locally. Sphalerite contains coarse, irregular, red to amber concentric zones, similarly to the sphalerite of the Huestis deposit. Gold was detected by semi-quantitative electron microprobe EDS analyses in tetrahedrite, although it probably also occurs as inclusions in other sulphide minerals, as documented for the Huestis deposit.

4.3.2 Freegold Mountain Camp

Tinta Hill

The Tinta Hill deposit lies several kilometres east of Freegold Mountain, within foliated and locally gneissic granodiorite or quartz diorite of the Granite Batholith of the Big Creek Meta-Plutonic Suite. The deposit comprises a series of quartz-sulphide veins that occur in a near-vertical, northwest-trending (300°) shear zone that is at least 3500 metres long (INAC, 1990) and up to 30.5 metres wide (Yukon Minfile, 1996). The main vein is 0.9 to 1.8 metres wide. Reserves have been estimated at over 500,000 tonnes grading 222.9 g/t Ag, 4.1 g/t Au, 7.2 wt.% Pb, 2.6 wt.% Zn, and 0.4 wt.% Cu (Carlson, 1987; Yukon Minfile, 1996). According to Morin (1981), the host rock is argillically and propylitically altered, whereas the Yukon Minfile (1996) reports weak potassic and phyllic alteration envelopes around the veins. Tough (1981) describes intense alteration in the vicinity of the main shear zone consisting of pink K-feldspar, clay minerals, sericite, chlorite, silica, and epidote. Based on samples collected from muck piles, the dominant alteration minerals are sericite in the host rock groundmass and kaolinite after feldspar.

Mineralized veins from the Tinta Hill deposit comprise banded and sugary massive textural types. Banded veins are by far the most common, and are characterized by coarse ore minerals, crack and seal veinlets, and cockscomb-textured quartz. Pyrite and minor chalcopyrite deposited first in a band near the vein margins, followed by quartz, which forms large euhedral crystals. Chalcopyrite was then partially replaced by enargite, galena precipitated after enargite, and both minerals were in turn replaced partially by tetrahedrite (Fig 4.2). The outer band grades inward into one in which quartz is the first phase precipitated, and yellow, anhedral, unzoned sphalerite and then galena follows chalcopyrite, and pyrite almost disappears. Chalcopyrite was replaced by enargite, galena by tetrahedrite, and rare pyrargyrite (with 1:6 As:Sb) replaced pyrite. The centres of the veins are dominated by quartz and coeval sphalerite and galena, while

chalcopyrite occurs only as a minor interstitial phase, and carbonate rarely occurs as open-space fill. Discrete stringer veinlets with core zone mineralogy can also be seen in quartz veins, at least some of which are paragenetically late.

The sugary massive veins differ only in texture from the banded veins. They are dominated by small rounded crystals of quartz, yellow sphalerite, and galena, and have numerous vugs lined with drusy quartz. Sphalerite compositions in both vein types only range from 1.7 to 3.6 mol.% FeS, and there is no evident systematic zoning. Late-stage stringer veinlets tend to contain more Fe-rich sphalerite (3.5 to 9.1 mol.%). Covellite and anglesite were the only supergene minerals observed in the two ore types, although Tough (1981) also reports cerrusite, smithsonite, azurite and malachite. Gold was detected by electron microprobe EDS analyses in chalcopyrite and galena.

Emmons Hill

The Emmons Hill deposit is hosted by an inlier of the Basement Metamorphic Complex in the Big Creek Meta-Plutonic Suite. The host rock is a north-striking biotite-quartz-feldspar gneiss intercalated with amphibolite and minor feldspathic quartzite, cut by grey-green, feldspar-hornblende-phyric and pale white-green quartz-phyric dykes (Morin, 1981). The Yukon Minfile (1996) reports quartz-feldspar porphyry dykes that sporadically follow the vein-fault zone. The Emmons Hill vein is at least 120 metres long and 10 metres wide, strikes north-northeast and dips steeply to the east (Morin, 1981; Yukon Minfile, 1981). Morin (1981) and McInnes (1987) report intense, pale green argillic alteration in the wallrock schist. Specimens from this deposit grade up to 24.0 g/t Au, 5.5 g/t Ag and 3.6 wt.% Sb (Yukon Minfile, 1996).

Samples collected for this study from the Emmons Hill deposit comprise mineralized and unmineralized barite-carbonate veins and some minor barite-carbonate-quartz breccias. Morin (1981) describes four different types of breccia ore from the deposit characterized by: 1) grey rounded quartz clasts in a coarse-grained stibnite and

galena matrix, 2) white angular quartz clasts in a black, fine-grained, sulphide-rich, siliceous "sinter", 3) dark brown siderite clasts in a grey ankerite ± barite matrix, and 4) minor clasts of black sinter in a quartz matrix. The "sinter" ore type was not represented among the samples collected for this study. McInnes (1987) reports the occurrence of stibnite-supported breccia samples with clasts of rhyolite, metasediments and strongly banded silica.

Where present, ore minerals constitute less than 50 vol.% of the vein material, and are dominated by early, euhedral to rounded sphalerite, which is irregularly zoned from yellow to orange corresponding to 0.01 to 1.48 mol.% FeS. Sphalerite precipitation was followed closely by barite, as well as by dendritic aggregates of arsenopyrite laths encrusted onto pyrite. McInnes (1987) identified this combination as marcasite, but electron microprobe EDS analyses confirm the presence of FeAsS with micron-sized FeS_2 centres. These centres may be marcasite but are more likely to be pyrite, given that discrete pyrite crystals occur in the veins. Later small, subhedral quartz masses and pods of sericite surround the earlier phases, which were followed closely by galena and minor chalcopyrite. Enargite (luzonite (?), and possibly also famatinite) occurs as minor, late discrete aggregates and replacements, and galena and chalcopyrite are replaced by an unidentified Pb-As-sulphosalt (Fig 4.2). This assemblage is cemented by up to 50 vol.% brown, concentrically zoned to unzoned carbonate. McInnes (1987) and Morin (1981) report the presence of stibnite, cinnabar, and orpiment, although these phases were not observed by the authors. Sporadic concentrations of gold were detected in pyrite, sphalerite, and galena by microprobe EDS analysis. The Emmons Hill ore differs from other examined Dawson Range deposits in that As dominates over Sb in sulphosalts and pseudo-sulphosalts.

4.3.3 Prospector Mountain Camp

Frog

The Frog or Lilypad deposit occurs on the western flank of Prospector Mountain within andesitic flows, tuffs, and volcanic breccias of the lower Carmacks group, which have been intruded by the granitic Prospector Suite. The volcanic succession overlies the Basement Metamorphic Complex. Veins strike north-northeast, dip steeply to the east, and range up to several metres in width and several hundred metres in length (Payne et al., 1987; Yukon Minfile, 1996). Payne et al. (1987) mapped sericitic and silicic alteration of the quartz monzonite in the vicinity of the Frog deposit, and found argillic envelopes surrounding mineralized veins, as was observed by the authors. Glasmacher (1990), however, divided alteration envelopes around the veins into an inner quartz-muscovite zone, an intermediate quartz-adularia zone, and an outer propylitic zone. The veins have been leached by weathering to a depth of at least 150 metres (Payne et al., 1987; Yukon Minfile, 1996).

The mineralized veins observed at the Frog deposit differ from the polymetallic veins encountered elsewhere in the southern Dawson Range in that there are five spatially separate types of vein, each of which is characterized by its dominant minerals: 1) galena, 2) chalcopyrite-galena, 3) sphalerite-quartz, 4) specular hematite, and 5) tourmaline veins. All the sulphide veins, however, display a similar paragenesis, and differ only in the proportions of mineral phases (Fig. 4.2). The sulphide veins are located on the order of tens of metres apart.

The galena veins are almost monominerallic, but contain minor chalcopyrite and quartz filling the void spaces between galena grains, which are coated with anglesite. The chalcopyrite-galena veins contain early quartz followed by pyrite; later galena and chalcopyrite occur as large crystals replaced by an unidentified Pb-Cu-Sb sulphosalt (possibly bournonite) and a small proportion of jamesonite and boulangerite. All are

corroded by later quartz and supergene covellite. Late-stage quartz, minor sericite, hematite, goethite, and malachite veinlets dominate the groundmass and replace the original sulphides. Sphalerite-quartz veins are dominated by multi-phase quartz. Arsenopyrite is a minor early phase, and was followed by precipitation of large euhedral quartz crystals with interstitial chalcopyrite and deep orange sphalerite with chalcopyrite disease. The sphalerite has been replaced almost completely by covellite. Late fine-grained quartz is accompanied by small sericite pods and minor bladed hematite. Relics of unaltered sphalerite were analyzed by electron microprobe and were found to contain 3.6 to 11.6 mol.% FeS. Gold was detected in arsenopyrite, and silver was detected in galena. Glasmacher (1990) also reports the presence of molybdenite, native gold, boulangerite, tennantite-tetrahedrite, bornite, digenite, and cubanite from unknown locations in the Frog deposit.

4.4 Regional Alteration

Altered porphyritic dykes occur in close proximity to the mineralized veins, and have been traditionally related to ore formation (e.g. Yukon Minfile, 1996). Although dykes in the southern Dawson Range have been historically assigned to the Mount Nansen group, our work has shown that dykes belonging to both the Mount Nansen and the Carmacks groups occur in mineralized areas (Smuk et al., 1997). Two average ages are prominent within the dyke suites (see compilation in Smuk et al., 1997); Carmacks porphyry dykes and plugs with an average age of 70 Ma, and fresh Mount Nansen dykes with an average age of 105 Ma. Altered Mount Nansen dykes yield ages between 77 and 61 Ma, i.e., similar to those of the Carmacks group. Alteration is ubiquitous and intense in dykes proximal to the mineralized camps, and McInnes (1987) has reported that andesite dykes (Carmacks group) are less altered than felsic dykes (Mount Nansen group) around the Laforma gold deposit in the Freegold Mountain camp.

The main alteration mineral is sericite (muscovite and/or paragonite), although kaolinite, pyrophyllite, and variable proportions of carbonate and fine-grained quartz are

also present (Smuk et al., 1997). Alteration of the felsic dykes of the Mount Nansen group resulted in recrystallized quartz rims around rounded quartz phenocrysts, the bleaching of feldspar phenocrysts, and an overall change in colour of the rock from the original pink to white or buff. The mafic phenocrysts of Carmacks porphyritic dykes are altered to carbonate and (Mg,Fe)-bearing clay minerals. In both suites, alteration is characterized by extreme depletion in sodium, a slight depletion in potassium, and the addition of silicon (Smuk et al., 1997). Altered dykes are also depleted in lead, zinc, and copper, implying that the dykes, and possibly other country rocks, contributed a small proportion of the base metals in the mineralized veins. Altered dykes are, however, enriched in base metals immediately adjacent to mineralized veins, implying that there was also an important contribution of base metals from the alteration fluid. Altered dykes are ubiquitously strongly enriched in arsenic and antimony, suggesting that these elements, and by inference gold (Williams-Jones and Normand, 1997), were derived entirely from the hydrothermal fluid responsible for alteration and mineralization.

4.5 Fluid Inclusions

A fluid inclusion study was undertaken on the five vein deposits of the southern Dawson Range, in order to make comparisons among the fluids responsible for ore deposition in the various mineralized camps. Where possible, fluid inclusions were studied in sphalerite in preference to those in gangue minerals, on the assumption that the former were more likely to represent the ore-forming fluid. In the case of the Emmons Hill deposit, data for a small population of fluid inclusions in sphalerite was supplemented by fluid inclusions in paragenetically early barite. Similarly, for the Frog deposit, the small amount of sphalerite and the paucity of visible fluid inclusions therein necessitated the study of inclusions in paragenetically earlier quartz (the early, large, euhedral quartz crystals in sphalerite-quartz veins discussed in Section 4.3.3).

4.5.1 Petrography

Primary fluid inclusions in sphalerite from the southern Dawson Range consistently contain liquid and vapour, with the vapour bubble occupying 15 to 20% of the inclusion volume. They differ among deposits in their clarity, which is a function of sphalerite colour, and their abundance. Liquid-vapour ratios are consistent both within and between sphalerite grains, regardless of compositional zoning. Primary inclusions in sphalerite are isolated and randomly oriented, but occur rarely in small clusters or planes parallel to growth surfaces. Their diameters range from 5 to 30 μm, and their shapes range from ovoid to negative crystals. Commonly these inclusions are very dark due to internal light refraction, and have thick black rims on their interior circumferences, which in some cases makes microthermometric measurements difficult.

Primary fluid inclusions in sphalerite from the Huestis deposit occur as rare isolated ovoids, 10 to 15 μm-long, and appear to be trapped preferentially in deep red, Fe-rich zones. As a result, they are commonly very dark. In the Tawa deposit, primary fluid inclusions range in diameter from 5 to 15 μm, although the majority are approximately 5 μm long. They occur as trains and clusters of dark grey to black inclusions in amber to deep red sphalerite. They are commonly obscured by numerous solid inclusions, primarily of chalcopyrite, and did not yield reliable cryogenic data due to their dark colour and small size. Primary fluid inclusions in sphalerite from the Tinta Hill deposit are relatively large (10 to 30 μm) and clear owing to the light yellow colour of the host, and yielded reliable microthermometric data. Emmons Hill fluid inclusions are typically <10 μm-long, isolated, rare, and occur in yellow to orange sphalerite amongst numerous unidentified solid inclusions.

Trapped solids are rarely observed in primary fluid inclusions in sphalerite from the Tinta Hill and the Tawa deposits. Trapped solids observed in ten primary fluid inclusions from Tinta Hill range from 1 to 5 μm in length, and include a small triangular opaque mineral that is probably chalcopyrite, and a prismatic to anhedral, anisotropic

mineral. These two trapped minerals rarely occur together. Approximately 5% of primary inclusions at the Tawa deposit contain a <2 μm long trapped solid similar to the anisotropic solid described above for Tinta Hill.

Primary liquid-vapour fluid inclusions in barite from the Emmons Hill deposit are dark grey in colour, generally rounded, and up to 20 μm in diameter. They occur as isolated inclusions or in small clusters with no obvious relationship to crystal form. Primary, liquid-vapour fluid inclusions in quartz from the Frog deposit occur in clusters and along planes subparallel to grain boundaries. In contrast to inclusions in sphalerite, primary inclusions in quartz are irregularly shaped and relatively transparent, with diameters ranging from approximately 5 to 20 μm.

Secondary liquid-vapour fluid inclusions comprise less than 10% of the fluid inclusion populations of sphalerite, quartz, and barite. They are elongated to irregularly shaped, shallow, more transparent compared to primary fluid inclusions, and lie along oriented planar trains within and across mineral grains. Secondary inclusions have variable sizes, ranging from 1 to over 200 μm in length, and the vapour bubble typically constitutes from 5 to 10% of the inclusion volume.

4.5.2 Microthermometry

Microthermometric analyses were undertaken on primary fluid inclusions in sphalerite from the Huestis, Tawa, Tinta Hill, and Emmons Hill deposits, in barite from the Emmons Hill deposit, and in quartz from the Frog deposit. Analyses were performed on a Fluid Inc.-modified U.S.G.S. gas-flow heating-freezing stage (Reynolds, 1992), and calibrated using synthetic CO_2 and H_2O inclusions. Measurement accuracies are ± 0.2°C for subzero temperatures and ± 2.0°C for higher temperatures.

Microthermometric and inferred salinity data for the five deposits are presented in Table 4.1 and Figures 4.3 and 4.4, respectively. All primary fluid inclusions

Table 4.1 Fluid inclusion microthermometric data

Deposit	Sample	Mineral	Number of Inclusions	Range of T_h (°C)	Mode (°C)	Number of Inclusions	Range of T_m (-°C)	Mean (-°C)
Mount Nansen Camp								
Huestis	MN-9D	sphalerite	21	260.1-300.5	285.9	16	5.8-1.4	3.8
	MN 95-5	sphalerite	17	235.9-272.6	253.6*	14	11.9-1.9	6.1
Tawa	MN 95-10	sphalerite	33	262.3-350.2	333.7	4	6.0-3.9	5.0
Freegold Mountain Camp								
Tinta Hill	FG TH-2A1	sphalerite	36	264.7-310.0	294.1	27	6.6-2.1	4.2
	FG TH-B	sphalerite	53	250.7-320.6	295.0	25	11.8-1.0	3.4
	FG TH-2C	sphalerite	11	115.0-232.3	116.0	10	2.0-1.0	1.3
	FG 95-15	sphalerite	42	241.6-303.3	246.5, 291.0	27	7.2-2.7	5.0
Emmons Hill	FG 95-7	sphalerite	9	209.1-308.1	244.0*	1	2.1	2.1
	FG 95-7	barite	17	228.8-344.6	312.0	6	4.9-0.0	2.4
Prospector Mountain Camp								
Frog	PR 95-18	quartz	25	243.5-384.1	303.5	18	4.3-0.3	3.2
Frog[1]	LP-4	quartz	14	281.0-331.0	312.2	14	3.6-2.0	2.8

* indicates average value where no distinct mode exists

[1] unpublished data from Hart and Selby

homogenized to liquid. Upon cooling, inclusions froze at temperatures ranging from -35° to -50°C. First ice melting was rarely observed, and eutectic temperatures were routinely overestimated as the temperature of first movement of the vapour bubble. Where liquid could be distinguished from ice, first ice melting temperatures were no lower than -24°C, suggesting that the fluid is dominated by NaCl + KCl (Roedder, 1984). Final ice melting occurred when the movement of the vapour bubble ceased. Secondary fluid inclusions all had final ice melting temperatures ranging from -1.0° to 0.0°C, and homogenized to liquid at temperatures ranging from approximately 100° to 200°C.

Mount Nansen Camp

Homogenization temperatures (T_h) for primary fluid inclusions in sphalerite from the Huestis deposit ranged from 236° to 301°C, but exhibited narrower ranges for each ore type. Those in polymetallic ore (MN 95-5) yielded T_h values ranging from 236° to 273°C, with no distinct modal temperature. In massive ore (MN-9D), the fluid inclusions gave higher T_h values ranging from 260° to 300°C with a mode at 286°C. Fluid inclusions in sphalerite from the nearby Tawa deposit displayed a slightly wider range of T_h, from 262° to 350°, with a significant mode at 334°C (Fig. 4.3).

Final ice melting temperatures (T_m) for fluid inclusions in polymetallic ore ranged between -11.9° and -1.9°C, with an average of -6.1°C, while those of massive ore ranged between -5.8° and -2.0°C, with an average of -3.8°C. These data correspond to average salinities of 8.0 and 6.4 wt.% NaCl equiv., respectively (Potter et al., 1978) (Fig. 4.4). The few fluid inclusions in sphalerite from the Tawa deposit that yielded reliable cryogenic data yielded final ice melting temperatures from -6.0°C to -3.9°C, with an average of -5.0°C corresponding to a salinity of 5.0 wt.% NaCl equiv.

Figure 4.3 Stacked histograms of fluid inclusion homogenization data for the a) Mount Nansen camp, b) Freegold Mountain camp, and c) Prospector Mountain camp (* indicates unpublished data from Hart and Selby).

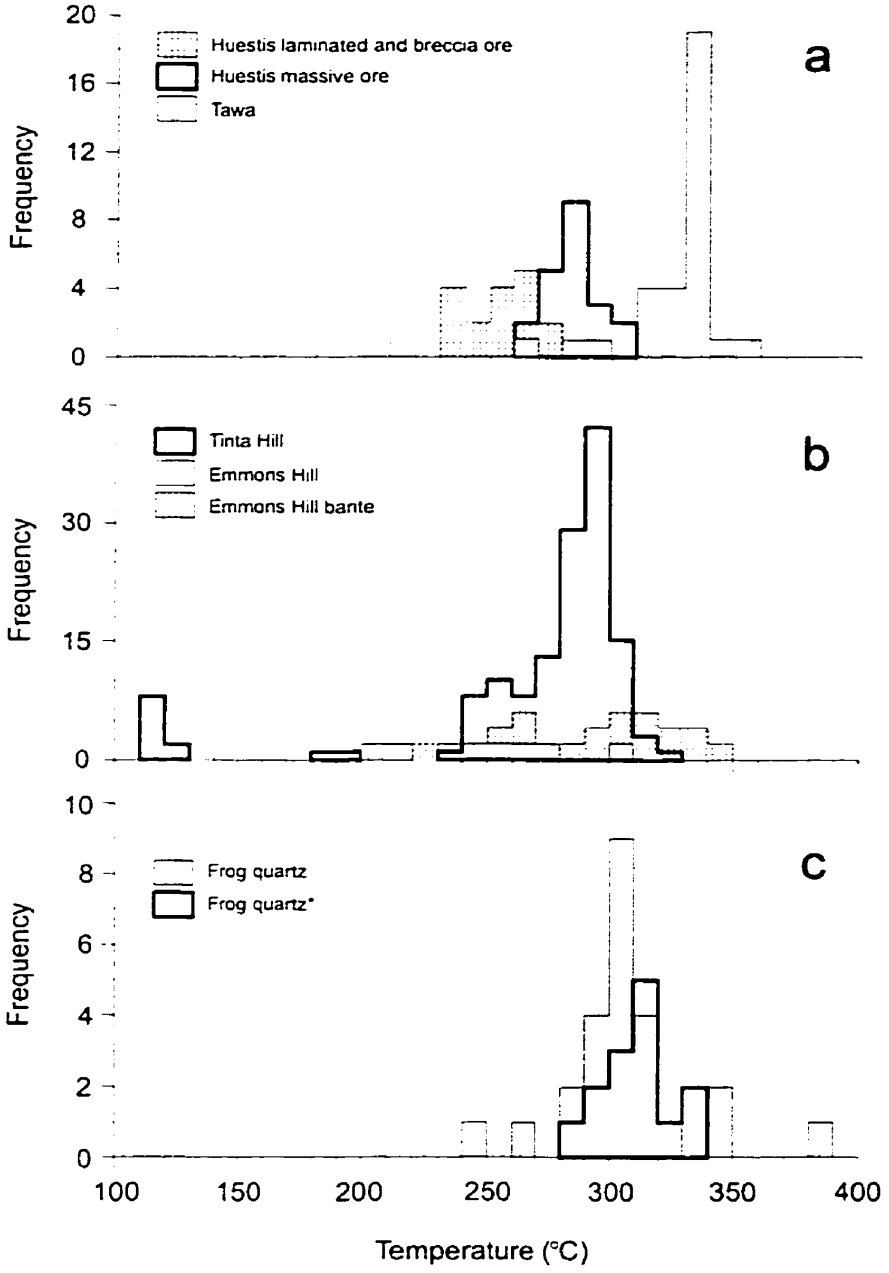
a
Huestis laminated and breccia ore
Huestis massive ore
Tawa
Frequency
20
16
12
8
4
0
b
Tinta Hill
Emmons Hill
Emmons Hill barite
Frequency
45
30
15
0
c
Frog quartz
Frog quartz*
Frequency
10
8
6
4
2
0
100
150
200
250
300
350
400
Temperature (°C)

Figure 4.4 Stacked histograms of calculated fluid inclusion salinity data for the a) Mount Nansen camp, b) Freegold Mountain camp, and c) Prospector Mountain camp (* indicates unpublished data from Hart and Selby).

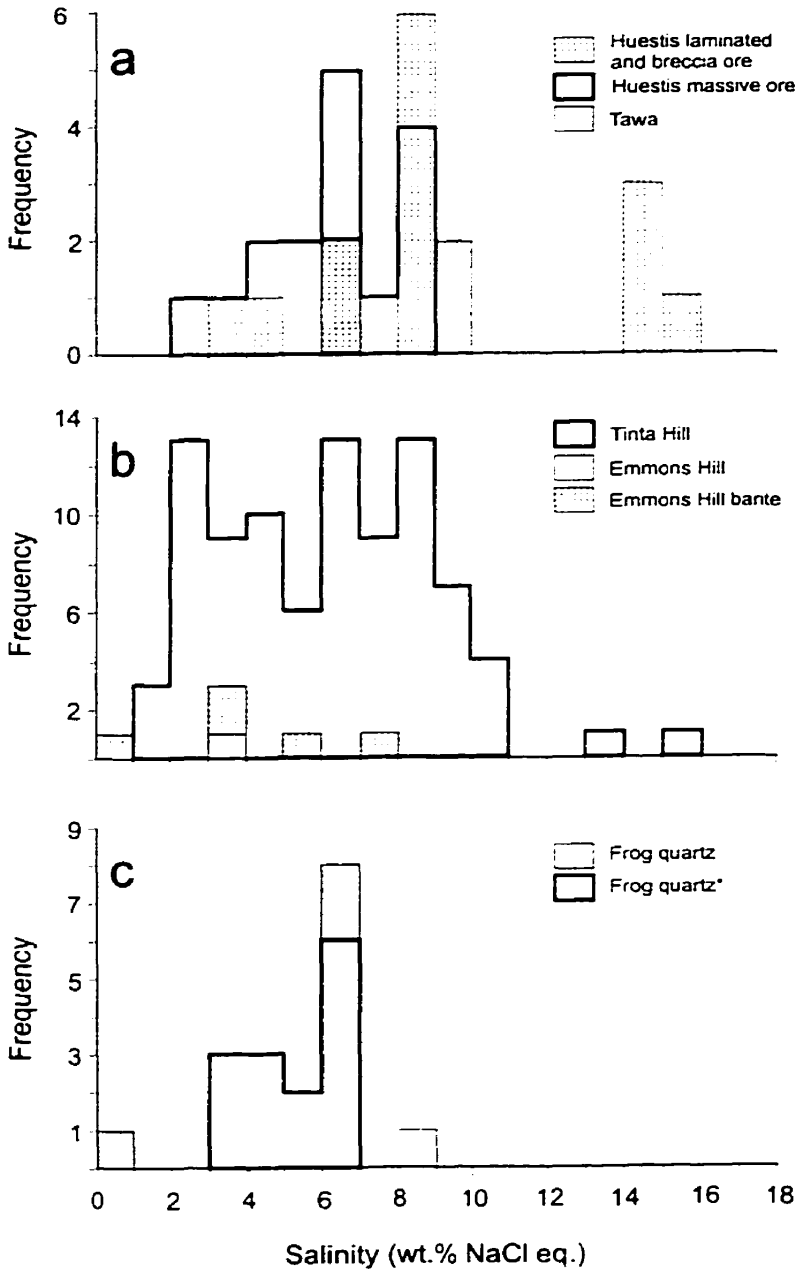
a
Huestis laminated and breccia ore
Huestis massive ore
Tawa
Frequency
b
Tinta Hill
Emmons Hill
Emmons Hill bante
Frequency
c
Frog quartz
Frog quartz*
Frequency
Salinity (wt.% NaCl eq.)

Freegold Mountain Camp

Homogenization temperatures for fluid inclusions in sphalerite from the Tinta Hill deposit ranged between 242° and 321°C with a large distinct mode at approximately 293°C for three samples. Sample FG TH-2C was exceptional, with T_h ranging from 115° to 232°C, with a mode at 116°C, reflecting lower temperature sphalerite deposition in a late stringer veinlet. Fluid inclusions in sphalerite from the Emmons Hill deposit yielded homogenization temperatures ranging from 209° to 308°C, with an average of 244° and slightly higher temperatures for barite, ranging from 229° to 345°C with a mode at 312°C (Fig. 4.3).

Tinta Hill fluid inclusions yielded a wide range of ice melting temperatures from -1.0° to -11.8°C, corresponding to salinities of 1.7 to 10.7 wt.% NaCl equivalent. Fluid inclusions from late veinlet sphalerite (FG TH-2C) displayed the highest T_m, ranging from -2.0° to -1.0°C. Only one fluid inclusion from sphalerite from the Emmons Hill deposit yielded a reliable T_m: -2.1°C, corresponding to a salinity of 3.5 wt.% NaCl equiv. Barite from the Emmons Hill deposit yielded T_m ice temperatures from -4.9° to 0.0°C, with an average of -2.4°C and a salinity of 3.8 wt.% NaCl equiv. (Fig. 4.4).

Prospector Mountain Camp

Primary fluid inclusions in pre-ore quartz (PR 95-18) from the Frog deposit yielded homogenization temperatures in the range of 244° to 384°C, with a distinct mode at 304°C. Unpublished data from Hart and Selby (LP-4) on post-ore quartz veinlets yielded similar temperatures, in the range of 281° to 331°C, with a mode at 312°C (Fig. 4.3). Cryogenic data for the two quartz populations are similar, with a range in final ice melting temperatures for the pre-ore quartz of -4.3° to -0.3°C with an average of -3.2°C, and for post-ore quartz of -3.6° to -2.0°C with an average of -2.8°C, corresponding to average salinities of 6.4 and 6.2 wt.% NaCl equiv., respectively (Fig. 4.4).

4.5.3 Decrepitate Analyses

Semiquantitative SEM-EDS analyses were performed on precipitates from decrepitated fluid inclusions in doubly-polished chips of sphalerite and small cubes of galena from the Huestis, Tinta Hill and Frog deposits. Samples were cleaned repeatedly in nanopure water, mounted on silica plates, rapidly oven-heated to 600°C, and immediately carbon-coated and analyzed. The high temperature of 600°C necessary to decrepitate sphalerite-hosted fluid inclusions was determined by stepwise heating, and the same temperature was applied to galena samples. Volatility of solutes is known to be significant at temperatures above 400°C (Alderton et al., 1982; Roedder, 1984; Haynes et al., 1988), and is likely to be a problem at the high temperatures required for the decrepitation of fluid inclusions in sphalerite. Chlorine was at least partially conserved in precipitates from galena, but was not retained in precipitates from sphalerite, and thus the results for sphalerite samples were discarded. The precipitates analyzed were mainly from the liquid released by inclusions onto the silica substrate. In some cases precipitates on the galena surfaces were analyzed but these were corrected for sulphur.

Decrepitate residues from fluid inclusions in galena contain Na, K, Ca, Cl and S in the approximate atomic percent proportions of 25:14:13:39:9 for the Huestis deposit, 23:11:43:17:6 for the Tinta Hill deposit, and 21:5:27:32:15 for the Frog deposit (Table 4.2). Charge balance is approximately conserved in the galena precipitates for the Huestis and Frog deposits, but for the Tinta Hill galena precipitates cation charge greatly exceeds the anionic charge, which may be due either to undetected carbonic species, volatile loss, or analysis of trapped solids. It should also be noted that the large proportion of Ca estimated for the Tinta Hill deposit is not supported by eutectic ice melting temperatures (Roedder, 1984). The mineralizing fluids are in the NaCl-KCl-$CaCl_2$-H_2O system, but results are interpreted based on the NaCl-H_2O system.

Table 4.2 Decrepitate data for fluid inclusions in galena (wt.%)

Deposit	Sample		Na	K	Ca	Cl	S
Huestis	MN 95-5		23.36	17.57	6.72	45.99	6.37
			28.00	1.60	21.21	40.51	8.68
			32.60	0.00	16.72	30.21	20.48
			16.99	39.14	9.51	30.50	3.86
		Avg.	*25.15*	*13.78*	*13.33*	*38.71*	*9.02*
Tinta Hill	FG TH-B		65.00	12.91	2.75	10.05	9.29
			4.72	14.79	65.56	7.10	7.83
			11.78	0.00	77.61	10.60	0.00
			31.59	16.13	8.07	34.82	9.39
		Avg.	*22.46*	*11.05*	*43.20*	*16.86*	*6.42*
Frog	PR 95-7		40.20	0.00	0.00	14.72	45.09
			20.79	2.66	43.86	32.69	0.00
			21.09	5.00	30.91	28.80	14.20
			0.00	18.40	4.31	77.30	0.00
			19.21	2.21	46.94	20.95	10.69
		Avg.	*21.67*	*4.79*	*26.52*	*32.03*	*14.99*

4.5.4 Gas Chromatography

No evidence of significant dissolved CO_2 or CH_4 was observed in fluid inclusions, however, small concentrations of CO_2 and CH_4 were detected by gas chromatographic analysis of fluids released from bulk samples of sphalerite and galena from the Huestis, Tinta Hill, and Frog deposits (Table 4.3). Since secondary fluid inclusions make up less than 10% of the fluid inclusion population in sphalerite and galena co-precipitated with sphalerite, these results are taken to largely reflect the composition of primary fluid inclusions investigated microthermometrically. We cannot exclude, however, the possibility that the proportion of secondary inclusions is larger in galena than in sphalerite. Sufficient pure mineral separates for gas chromatography could not be obtained from the Tawa or the Emmons Hill deposits.

The analyses were performed with an HP®-5890 Series-II gas chromatograph equipped with a wide bore capillary column, a micro-thermal conductivity detector (TCD), and a photoionization detector (PID). A detailed description of the analytical system is provided by Salvi (1994) and Salvi and Williams-Jones (1997). Galena samples were reduced to fragments less than 2 mm in diameter, hand-picked to ensure purity, washed repeatedly in doubly-distilled water, and dried under a fumehood (see Bray et al., 1991). Between 0.5 and 2 g of material were crushed and the released gases were introduced into the gas chromatograph with an argon carrier gas. The absolute concentrations of the gas species are a function of the volume of water released from the fluid inclusions.

The fO_2 of the fluids was calculated from the measured CO_2/CH_4 ratio using the equilibrium constant for the reaction:

$$CO_2 + 2H_2O = CH_4 + 2O_2$$

Log K values were calculated using the average homogenization temperatures for each sample and 300 bar pressure using the program SUPCRT92 (Johnson et al., 1991; Shock, 1998). Correction factors for the ratio CH_4/CO_2 between entrapment and analysis

Table 4.3 Gas chromatographic fluid inclusion data

Deposit	Sample	Mineral	T (°C)	N_2		CH_4		CO_2		H_2O		CH_4/CO_2	log K^1	log fO_2
				(nmol)	(mole %)	(nmol)	(mole %)	(nmol)	(mole %)	(nmol)	(mole %)			
Huestis	MN 95-5	sphalerite	250	0.48	0.0036	4.67	0.0350	114.95	0.8607	13235	99.10	0.04	-76.73	-37.67
Tinta Hill	FG TH-2C	sphalerite	120	0.15	0.0079	0.18	0.0095	15.98	0.8426	1880	99.12	0.01	-107.16	-52.61
	FG 95-17	galena	290	2.00	0.0284	0.61	0.0086	41.98	0.5955	7005	99.37	0.01	-70.58	-34.37
Frog	PR 95-7	galena	300	0.36	0.0290	-	-	16.81	1.3553	1223	98.60	-	-	-
	PR 95-11	galena	300	5.15	0.0802	-	-	76.03	1.1841	6340	98.74	-	-	-

[1] calculated using SUPCRT92 (Johnson et al., 1992; Shock, 1998)

Analyses reproducible to better than ±15% (Salvi and Williams-Jones, 1997)

temperatures were close to unity (Dubessy, 1984). The highest concentration of CH_4 was measured in the sample from the Huestis deposit ($CH_4/CO_2 = 0.04$), followed by the two samples from the Tinta Hill deposit ($CH_4/CO_2 = 0.01$). In contrast to these deposits, no CH_4 was detected in the two samples from the Frog deposit. The absence of CH_4 may reflect a shorter fluid residence time and consequent lack of equilibration in the system C-O-H (Giggenbach, 1997). The data for one of the Tinta Hill samples and the Huestis sample yield similar values of calculated log fO_2 of -37.7 and -34.4, whereas the log fO_2 of the paragenetically late sample FG TH-2C from Tinta Hill is much lower at -52.6. The activities of CO_2 in fluid inclusions in galena determined by gas chromatography are not sufficiently high to significantly affect the salinities estimated from freezing point depression temperatures (Hedenquist and Henley, 1985).

4.6 Oxygen and Hydrogen Isotopes

Analyses of the hydrogen and oxygen isotopic compositions of fluid inclusions in six hand-picked samples of sphalerite and galena from the Huestis, Tinta Hill, and Frog deposits were performed at the Stable Isotope Laboratory at Queen's University, following the method described in Koehler et al. (1991) (Fig. 4.5). Errors using this technique are ±5 ‰ for δD_{H_2O} and ±1 for $\delta^{18}O_{H_2O}$ for alkali brine solutions.

The δD values obtained from fluid inclusions in sphalerite ranged from -108 to -85 ‰, while the $\delta^{18}O$ values range from -15.0 to -5.0 ‰. (Table 4.4). Within this range, oxygen is isotopically lightest at Tinta Hill, plotting on the meteoric water line, and is progressively heavier at Huestis and Frog. These data are consistent with a dominantly meteoric ore fluid. The shift in $\delta^{18}O$ may indicate either progressive water-rock interaction, describing a horizontal line through the data, and/or some degree of progressive mixing with magmatic water/vapour.

Table 4.4 Oxygen and hydrogen isotope data from fluid inclusions

Deposit	Sample	Mineral	$\delta^{18}O$ (per mil)	δD (per mil)
Huestis	MN 95-5	sphalerite	-9.6	-85
Huestis	MN 9A	sphalerite	-12.4	-102
Tinta Hill	FG 95-17	sphalerite	-15.0	-104
Frog	PR 95-7	galena	-9.9	-108
Frog	PR 95-9	galena	-6.8	-85
Frog	PR 95-11	galena	-5.0	-100

Figure 4.5 Oxygen and hydrogen isotope data for sphalerite- and galena-hosted inclusion fluids. Open symbols indicate galena data from McInnes et al. (1990). Fields of representative geothermal waters from the Yellowstone area are shown by shaded (Parry and Bowman, 1990), open (Parry and Bowman, 1990), stippled (Thordsen et al., 1992), and dashed open (Mariner et al., 1992) fields. The composition of Dawson Range rainwater is from McInnes et al. (1990). Average magmatic water and igneous rock fields were taken from Taylor (1974).

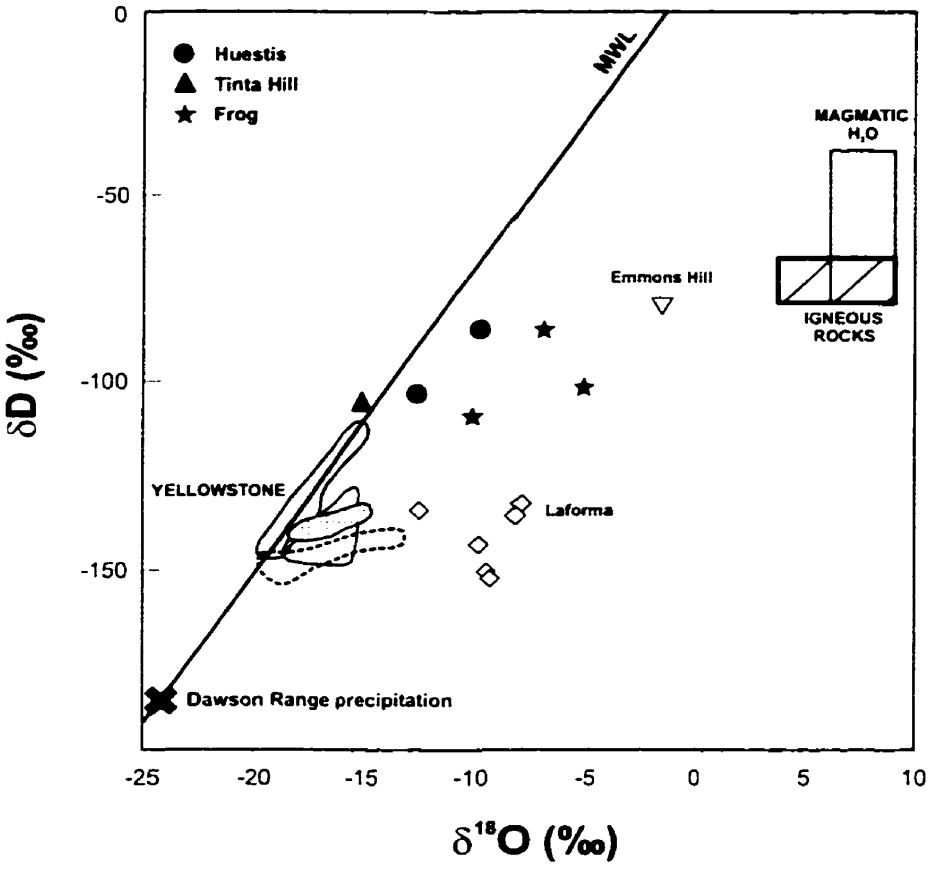
0
-50
-100
-150
δD (‰)
-25
-20
-15
-10
-5
0
5
10
δ18O (‰)
Huestis
Tinta Hill
Frog
MWL
MAGMATIC H2O
IGNEOUS ROCKS
Emmons Hill
YELLOWSTONE
Laforma
Dawson Range precipitation

4.7 Sulphur Isotopes

Samples of galena, sphalerite, and barite from the five deposits were analyzed for their sulphur isotopic composition at the Ottawa-Carlton Geoscience Centre Stable Isotope Facility using a VG SIRA12 mass spectrometer and the method described in Fritz et al. (1974). Analytical errors associated with this method are estimated to be ±0.2 ‰.

The $\delta^{34}S$ values obtained on galena ranged from -9.1 to -0.8 ‰. The lowest value is from an anomalously low-temperature sample (FG TH-2C) from Tinta Hill, and the highest value is from the Frog deposit. Sphalerite $\delta^{34}S$ values ranged from -5.9 ‰. (Tinta Hill FG TH-2C), to +0.2 ‰ at Emmons Hill. The single analysis of barite, however, from Emmons Hill gave a value of +15.3 ‰. $\delta^{34}S_{H_2S}$ values were calculated for a hydrothermal fluid in equilibrium with each mineral at T_h, using the fractionation factors of Ohmoto and Rye (1979) (Table 4.5). These values show a narrow range from -1.6 to +1.6 ‰ for both galena and sphalerite, with the exception of the low-temperature sample FG TH-2C from Tinta Hill (-6.6 to -4.9 ‰) and barite from Emmons Hill (+13.5 ‰).

4.8 Lead Isotopes

Lead isotopic analyses were conducted on six galena separates representing the five mineral deposits investigated, four whole rock samples of Mount Nansen volcanic rocks, and nineteen representative whole rock samples (part of a larger data set from Francis and Johnston (1998)) of the Carmacks Group (Table 4.6). Samples were analyzed at the GEOTOP laboratory of the Université du Québec à Montréal using anion-exchange chromatography (Manhès et al., 1980) for lead separation and a single collector VG SECTOR thermal ionization mass spectrometer for isotope analysis. The 2σ uncertainties for the lead isotope ratios are 0.1%/amu.

Table 4.5 Sulphur isotope data

Deposit	Sample	Mineral	Temperature (°C)	$\delta^{34}S$ (per mil)	Enrichment Factor	$\delta^{34}S_{H,S}$[2] (per mil)	Mineral Pairs	Calculated[1] Temp. (°C)
Huestis	MN 95-5	galena	253	-2.4	-2.3	-0.1	sphal-gal	250
	MN 95-5	sphalerite	253	-1.2	0.4	-1.6		
Tawa	MN 95-10	galena	333	-2.4	-1.7	-0.7	sphal-gal	330
	MN 95-10	sphalerite	333	-0.4	0.3	-0.7		
Tinta Hill	FG TH-2C	galena	116	-9.1	-4.2	-4.9	sphal-gal	114
	FG TH-2C	sphalerite	116	-5.9	0.7	-6.6		
Emmons Hill	FG 95-7	galena	244	-0.8	-2.4	1.6	sphal-gal	241
	FG 95-7	sphalerite	244	+0.2	0.4	-0.2	bar-gal	492
	FG 95-7	barite	312	+15.3	1.8	13.5	bar-sphal	480
Frog	PR 95-7	galena	303	-1.9	-1.9	0.0	-	-

[1] Temperatures from fluid inclusion homogenization temperatures, inferred for galena from sphalerite

[2] Equations from Ohmoto and Rye, 1979, based on data from Czamanske and Rye, 1974

Table 4.6 Lead isotope data

Location	Sample	Type	$^{206}Pb/^{204}Pb$	$^{207}Pb/^{204}Pb$	$^{208}Pb/^{204}Pb$
Mineral Deposits					
Huestis	MN 95-05	galena	19.146	15.621	38.759
Tawa	MN 95-10	galena	19.101	15.611	38.690
Tinta Hill	FG TH-2C	galena	19.165	15.636	38.802
Emmons Hill	FG 95-41	galena	19.192	15.649	38.857
Frog	PR 95-7	galena	19.139	15.625	38.758
	PR 95-11	galena	19.168	15.653	38.862
Mount Nansen Volcanics					
Klaza Mtn.	KZ-4	rhyolitic fp ppy dyke	19.475	15.688	39.250
	KZ-6	andesite	19.508	15.694	39.444
	KZ-11	andesite	19.572	15.700	39.445
	KZ-12	dacite	19.557	15.706	39.435
Carmacks Volcanics					
Fire Lookout	FL-1	basalt	19.342	15.605	38.778
	FL-4	basalt	19.312	15.628	38.874
	FL-7	basalt	19.320	15.627	38.906
	FL-10	ankaramite	19.330	15.627	38.966
	FL-12	andesite	19.304	15.620	38.873
	FL-16	ankaramite	19.301	15.621	38.878
Miller' s Ridge	ML-7	high-Mg andesite	19.328	15.627	38.912
	ML-20	ankaramite	19.317	15.635	38.874
	ML-21	ankaramite	19.326	15.635	38.942
	ML-28	andesite	19.361	15.555	39.405
	ML-41	basalt	19.326	15.619	38.882
	ML-50	basalt	19.238	15.621	38.836
Prospector Mtn.	PR-10	andesite	19.300	15.645	38.918
	PR-11	rhyolitic qtz-fp ppy dyke	19.469	15.638	38.971
	PR-12	andesite	19.220	15.625	38.820
	PR-13	dacitic qtz-fp ppy dyke	19.462	15.667	39.193
"Smoky Ridge"	SR-4	high-Mg andesite	19.359	15.627	38.913
(N. Big Creek)	SR-8	andesite	19.358	15.598	38.913
	SR-11	ankaramite	19.320	15.596	38.775

Lead isotope data for galenas from the southern Dawson Range cluster at compositions more radiogenic than would be expected for a single-stage evolution (Doe and Stacey, 1974; Cumming and Richards, 1975; Stacey and Kramers, 1975). The galena lead isotopic data coincides mainly with those for the Carmacks group at 70 Ma, but define a linear trend towards the Pb isotopic composition of the Mount Nansen group at 70 Ma (Fig. 4.6).

4.9 Discussion

4.9.1 P-T Conditions

All deposits presently exposed in the southern Dawson Range were covered by the extensive flat-lying volcanic flows of the Carmacks group during Late Cretaceous time. However, evidence presented by Souther (1991) indicates that the Carmacks group was deposited on a surface with significant relief, implying a large variation in the thickness of volcanic cover. Ignoring any significant erosion between mid-Cretaceous and Late Cretaceous time, the present maximum thickness (1200 m) of the Carmacks volcanics would indicate a maximum lithostatic pressure of approximately 360 bars. The corresponding hydrostatic pressure would be 120 bars, whereas the minimum trapping pressure given by the intersection of the isochore with the boiling curve would be ~80 bars. Corrections for fluid inclusion homogenization temperatures at a pressure of 360 bars are approximately 20°C (Potter, 1977). Emmons Hill is the lowest-lying deposit in the study area at approximately 1100 metres above sea level, while Frog at Prospector Mountain is at an elevation of just over 1500 metres. The difference in elevation of 400 metres, or 120 bars (lithostatic), is equivalent to a correction of the homogenization temperatures to trapping temperatures of approximately 5°C, which is far less than the observed spread in the temperature data.

Isotopic fractionation of sulphur between coexisting sphalerite and galena reflects temperatures ranging from 241 to 330°C, with the exception of sample FG TH-2C which implies a temperature of 114°C (Table 4.5). Sulphide isotopic temperatures are

Figure 4.6 Lead isotope data for the Mount Nansen and Carmacks volcanic groups and galenas of the Dawson Range. The solid symbols represent new data from this study, while the open symbols are data from Godwin et al. (1988). Whole-rock Pb-isotopic values from the Carmacks group have been corrected to their formation age of 70 Ma (see Smuk et al., 1997). In order to evaluate the source relationship between galena Pb-isotopes and the two volcanic groups, the whole-rock Pb-isotopic values for the Mount Nansen samples have been corrected to 70 Ma, the age of Carmacks extrusion, as well as to 105 Ma, the average age of the Mount Nansen group (dates from Smuk et al., 1997). The galena evolution curve (crosses with dates) (data from Cumming and Richards, 1975, and Stacey and Kramers, 1975), the Shale Curve of Godwin and Sinclair (1982), analogous to Zartman and Haines' (1988) Upper Crustal Curve, the Bluebell Curve of Andrew et al, (1984), and the Mantle Evolution Curve of Doe and Zartman (1979) modified by Zartman and Haines (1988) are shown for comparison.

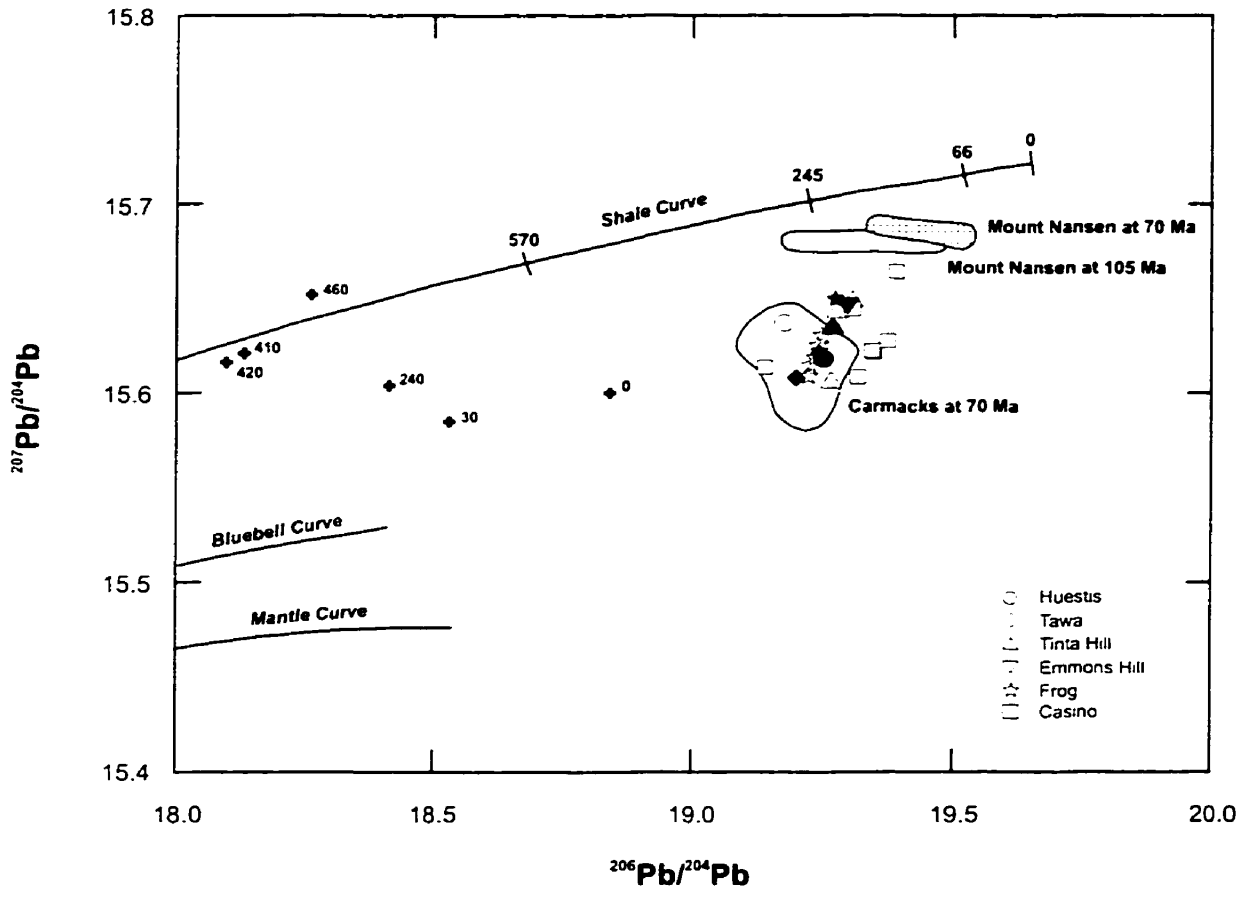
15.8
15.7
15.6
15.5
15.4
18.0
18.5
19.0
19.5
20.0
$^{207}Pb/^{204}Pb$
$^{206}Pb/^{204}Pb$
Shale Curve
0
66
245
570
460
410
420
240
30
0
Mount Nansen at 70 Ma
Mount Nansen at 105 Ma
Carmacks at 70 Ma
Bluebell Curve
Mantle Curve
Huestis
Tawa
Tinta Hill
Emmons Hill
Frog
Casino

very similar to the fluid inclusion homogenization temperatures, implying that pressures were equal to or less than those estimated above. Barite-sulphide pairs from Emmons Hill yield anomalously high temperatures (480° and 492°C), suggesting that these minerals were deposited under disequilibium conditions, with barite predating the sulphide minerals.

Although sulphur isotope temperatures were not obtained for the Frog deposit, a low pressure of formation may be inferred geologically. Glasmacher (1990) estimated a maximum pressure of 400 bars based on the discrepancy of 20-30°C between fluid inclusion homogenization temperatures and those determined from arsenopyrite, sphalerite-pyrrhotite, and chlorite geothermometers. In summary, we estimate that the deposits investigated in this study formed at temperatures of approximately 300°C (285 ± 45°C) and a pressure of ~ 300 bars.

4.9.2 Fluid Origin

As discussed earlier, the δD and $\delta^{18}O$ values analyzed in this study reflect a dominance by meteoric water, but indicate some modification by water-rock interaction and/or some degree of progressive mixing with magmatic fluid. Support for a possible small magmatic contribution for all Dawson Range veins is the relatively high CO_2 content of fluid inclusions (1.4-0.6 mol.%) (Table 4.2), comparable to values of ≤3.0 mol.% for high sulphidation deposits as opposed to typical low sulphidation deposit values of ≤0.4 mol.% (Graney and Kesler, 1995). The presence of CO_2-bearing fluids is also suggested by the carbonate alteration of mafic phenocrysts in Carmacks dykes (Smuk et al., 1997). The shifts of the Huestis and Frog fluids from the meteoric water line (and Tinta Hill fluid) towards heavier $\delta^{18}O$ correlate with increasing temperature and CO_2 content. The Tinta Hill fluids have a meteoric water signature, with a T_h of ~250-290°C, and the lowest CO_2 concentration (0.6 mol.%), while the Frog fluids have higher homogenization temperatures (T_h = ~300-315°C) as well as the highest CO_2 contents (1.4 mol.%).

There is a large difference between the δD value (-184 ‰) of present-day Dawson Range rainwater (summer 1986) as measured by McInnes et al. (1990) and the δD values of Dawson Range vein ore (-85 to −108 ‰), implying some degree of latitude change, or a difference in elevation. If the δD shift is taken solely as an indication of latitude, data from the southern Dawson Range suggest that the veins were deposited at latitudes south of present-day Yellowstone (or possibly at the same latitude as Yellowstone but in a coastal environment and/or at a lower elevation).

δD values reported by McInnes et al. (1990) from fluid inclusions in quartz from deep ore from the Laforma deposit at the Freegold Mountain camp are considerably lower than those obtained in this study. The shift in $\delta^{18}O$ (calculated from $\delta^{18}O_{qtz}$) from the meteoric water line suggests similar fluid-rock interaction (± fluid mixing) to our Dawson Range data, but the position of Laforma data with respect to δD could indicate that this deposit formed more recently and thus further north than the other Dawson Range deposits. The idea that the Laforma deposit may be metallogenically separate from the other southern Dawson Range gold deposits is supported by the lower temperatures and salinities of the Laforma ore fluids, the paucity of base metals in the deposit, and the indication of fluid boiling (McInnes et al., 1990).

The values of $\delta^{18}O$ calculated from calcite and δD values from fluid inclusions in coexisting barite from the Emmons Hill deposit are higher than those determined for the other deposits in this study, and were tentatively interpreted by McInnes et al. (1990) as an isotopic shift due to possible boiling. These higher values may simply reflect a greater degree of water-rock interaction or fluid mixing, or alternately reflect a different source for the oxidized sulphur in barite that would also account for the lack of S-isotopic equilibrium between coexisting barite and sulphides. For example, the proximity of the barite from Emmons Hill to the magmatic water field (Fig. 4.5) could suggest a magmatic SO_2 input.

Glasmacher (1990) proposed, on the basis of fluid inclusion microthermometry, that the formation of the Frog deposit involved the mixing between meteoric and magmatic fluids. However, this is not supported by fluid inclusion homogenization temperature and salinity relationships from the present study, i.e. there is no trend of decreasing salinity with decreasing temperature (Fig. 4.7).

The oxygen and hydrogen isotopic composition of fluid inclusions in the ore minerals of the five vein deposits of the southern Dawson Range indicate that the fluid is dominantly of meteoric origin, and most likely evolved through interaction with country rocks. The data are also consistent with a small input of magmatic water, an interpretation that is supported by the correlation of heavier isotopic compositions with high fluid inclusion temperatures, salinities, and mole fractions of CO_2.

4.9.3 Sources of Ore Components

Values of $\delta^{34}S$ of H_2S calculated from the equilibria of dissolved H_2S in the ore fluids with galena and sphalerite range from 1.6 to +1.6 ‰, indicating that the source of the sulphur was primarily igneous (Ohmoto and Goldhaber, 1997). These values are similar to those calculated from pyrite from the Laforma deposit (-0.05 to +0.95 ‰) (McInnes et al., 1990), whereas those determined by Glasmacher (1990) from pyrite, galena and sphalerite in the Frog deposit are systematically higher ($\delta^{34}S_{H_2S}$ = -1.3 to +4.5 ‰), with only one out of nine values being negative. The reason for the higher $\delta^{34}S$ values reported for the Frog ores is unknown.

The lead isotopic compositions of galenas from several vein deposits from the southern Dawson Range are similar to lead isotopic values from the Carmacks volcanic group after correction of the latter to 70 Ma. The trend of data towards the Mount Nansen volcanic group may imply some degree of mixing with lead from these older volcanics. However, in the absence of Pb-isotopic data from other country rocks in the area, especially the Basement Metamorphic Complex, the possibility of an enriched source

Figure 4.7 Salinity (wt.% NaCl equiv.) versus homogenization temperature for fluid inclusions from the southern Dawson Range.

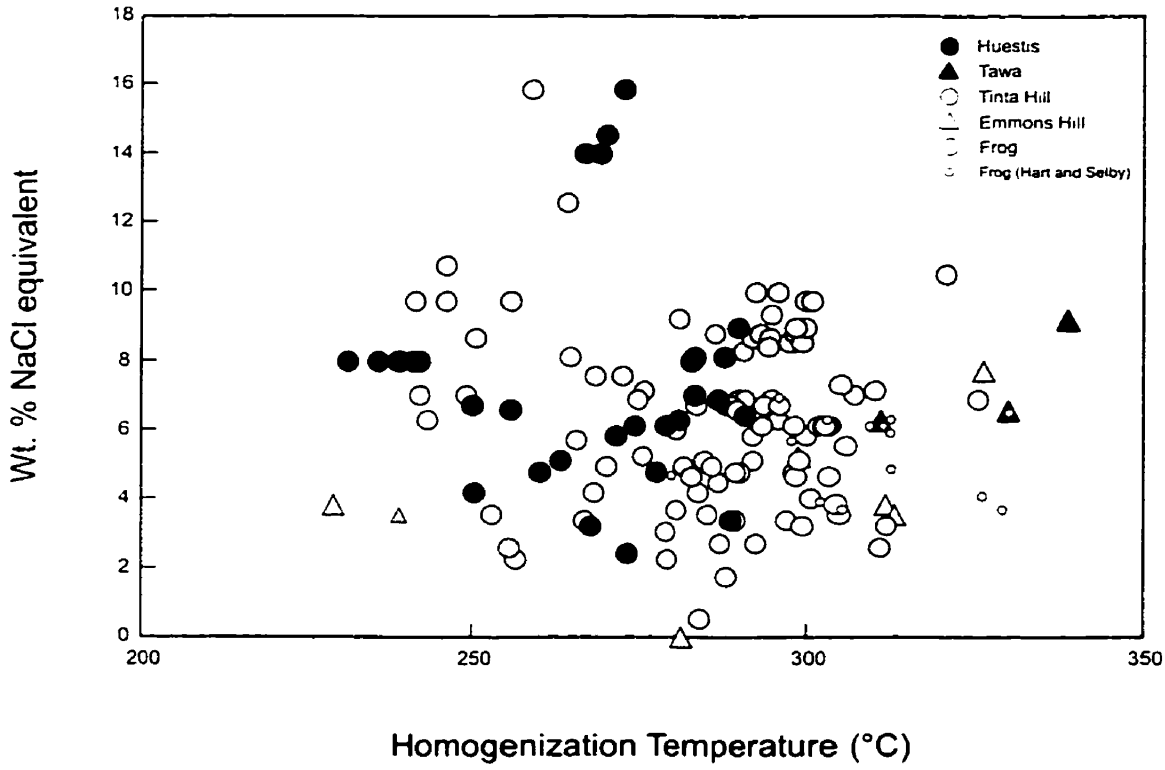
Wt. % NaCl equivalent
Homogenization Temperature (°C)
Huestis
Tawa
Tinta Hill
Emmons Hill
Frog
Frog (Hart and Selby)
0
2
4
6
8
10
12
14
16
18
200
250
300
350

other than the Mount Nansen volcanics cannot be ruled out. The metasedimentary rocks of the Basement Metamorphic Complex may be tentatively correlated with the North American pericratonic sediments used to construct Godwin and Sinclair's (1982) Shale Curve, and thus the trend in the galena lead data may reflect mixing with lead from these older rocks.

A depletion in base metals in altered Mount Nansen and Carmacks porphyry dykes has been taken as an indication that the dykes were a possible source of ore metals (Smuk et al., 1997), and is supported by the trend of the galena Pb-isotopic data towards the Pb-isotopic composition of the Mount Nansen volcanic rocks. Significant additions of As and Sb to the altered dykes, however, indicate that these metals, and by inference gold (Oppliger et al., 1997; Williams-Jones and Normand, 1997), were introduced from a larger reservoir by the hydrothermal fluid. Regardless of some possible mixing with more radiogenic Pb, the bulk of the lead and presumably other metals in epithermal veins of the southern Dawson Range and in the Carmacks-hosted Casino porphyry deposit appears to be derived from the Carmacks volcanics.

4.9.4 fO_2 – pH Conditions

Log fO_2 - pH conditions during the formation of mineralized veins are reasonably well-constrained by mineral assemblages in the veins and in alteration zones, as well as by direct measurement of mineral and fluid compositions. Log fO_2 - pH diagrams were constructed at a temperature of 300°C and a pressure of 300 bars, the homogenization temperature of fluid inclusions and the estimated lithostatic load, and at two different total sulphur activities (Fig. 4.8a, b). The activities of most fluid components were estimated from their concentration ratios in fluid inclusion decrepitate results for the Huestis deposit, the Debye-Hückel relationship, and the microthermometrically determined salinity. The activities of Na^+, K^+, Ca^{2+}, Cl^-, and S^{2-} so estimated are 0.48 *m*, 0.16 *m*, 0.14 *m*, 0.99 *m*, and 0.20 *m*, respectively. The measured sulphur concentration is surprisingly

high, but is consistent in all three deposits. However, such a high sulphur concentration would imply a large field of stability for sulphur that is not supported by field observation. In view of this, a maximum activity of 0.1 *m* was assumed (Fig. 4.8a). The effect of lowering ΣS is illustrated for a ΣS concentration of 0.01 *m* in Figure 4.8b.

The calcite solubility curve was constructed using CO_2, CH_4 and H_2O concentrations of 115 *ηm*, 4.7 *ηm* and 13235 *ηm*, respectively, values measured by gas chromatography on Huestis ore. The Huestis results were used for consistency with decrepitate results, and are representative of the data for the other deposits, except Frog, as discussed earlier. The CO_2 concentration as a function of H_2O is high at 0.48 *m* (X_{CO_2}=0.009) but is consistent with the absence of clathrate in frozen fluid inclusions.

Log *K* values for reactions describing the predominance fields for sulphur species, phase boundaries among K-feldspar, muscovite and kaolinite, the stability fields for Fe- and Cu-sulphide and oxide minerals, and the calcite saturation curve, were calculated using the SUPCRT92 software package (Johnson et al., 1991) and the complementary thermodynamic database of Shock (1998). Activity coefficient parameters for the above calculations were taken from Helgeson et al. (1981). Zinc and lead solubility curves, at aqueous concentrations of 1 and 100 ppm (Anderson, 1973), were calculated at 300°C assuming the dominant Zn complex is $ZnCl^{\circ}_2$ (Ruaya and Seward, 1986), and the Pb complex is $PbCl^{-}_3$ (Seward, 1984). Activity coefficient data for these zinc and lead complexes were taken from Barrett and Anderson (1988). Lines showing the variation of X_{Fes} in sphalerite were calculated using the procedure described in Barton & Skinner (1979).

Gold solubility curves were calculated for $Au(HS)^{-}_2$ (Shenberger and Barnes, 1989), $AuCl^{-}_2$ (Gammons and Williams-Jones, 1995a; 1995b), and $AuHS^{\circ}$ complexes (Benning and Seward, 1996), using the thermodynamic parameters provided by these authors. The gold species $AuHS^{\circ}$ and $AuCl^{-}_2$ may become important in high temperature, low pH systems (Benning and Seward, 1996; Gammons and Williams-Jones, 1995a;

Figure 4.8 Log fO_2-pH stability fields of Fe-S-O minerals, K-feldspar, muscovite, kaolinite, calcite, anglesite, galena, chalcopyrite, bornite + pyrite, and predominance fields for the aqueous sulphur species at 300°C, 300 bars. Figures a) and b) are for ΣS of 0.1 *m* and 0.01 *m*, respectively, for activities of Cl^-, K^+, and Ca^{2+} of 1, 0.16, and 0.14, respectively. X_{FeS} in sphalerite in the H_2S field is contoured as a dashed-dot line. Solubilities of Zn and Pb are contoured as dotted lines, and the solubilities of $Au(HS)^-_2$, $AuHS^\circ$, and $AuCl^-_2$ as thin solid lines. The probable initial and depositional conditions of the ore fluid are shown by the shaded areas.

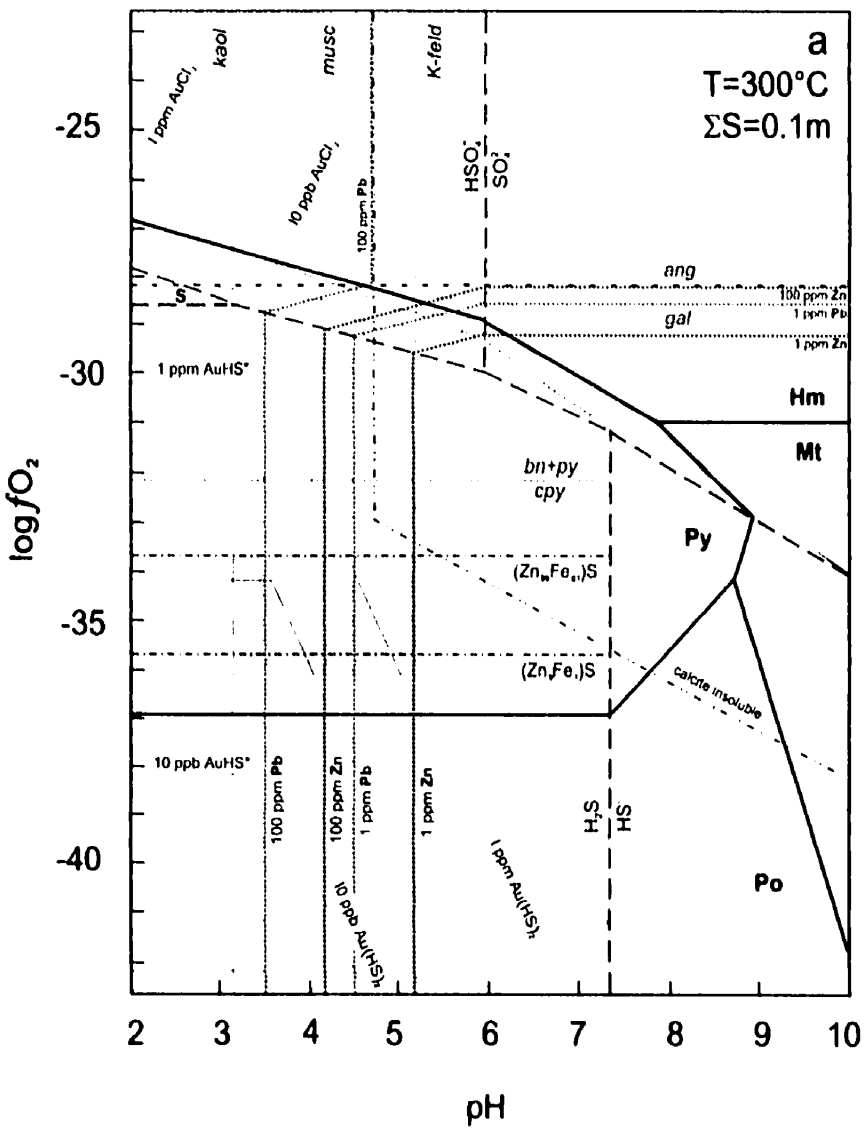
a
T=300°C
ΣS=0.1m
kaol
musc
K-feld
1 ppm AuCl,
10 ppb AuCl,
100 ppm Pb
HSO4-
SO4--
ang
gal
100 ppm Zn
1 ppm Pb
1 ppm Zn
1 ppm AuHS°
Hm
Mt
bn+py
cpy
Py
(Zn,Fe)S
calcite insoluble
10 ppb AuHS°
100 ppm Pb
100 ppm Zn
1 ppm Pb
1 ppm Zn
10 ppb Au(HS)2-
1 ppm Au(HS)2-
H2S
HS-
Po
-25
-30
-35
-40
2
3
4
5
6
7
8
9
10
log fO2
pH

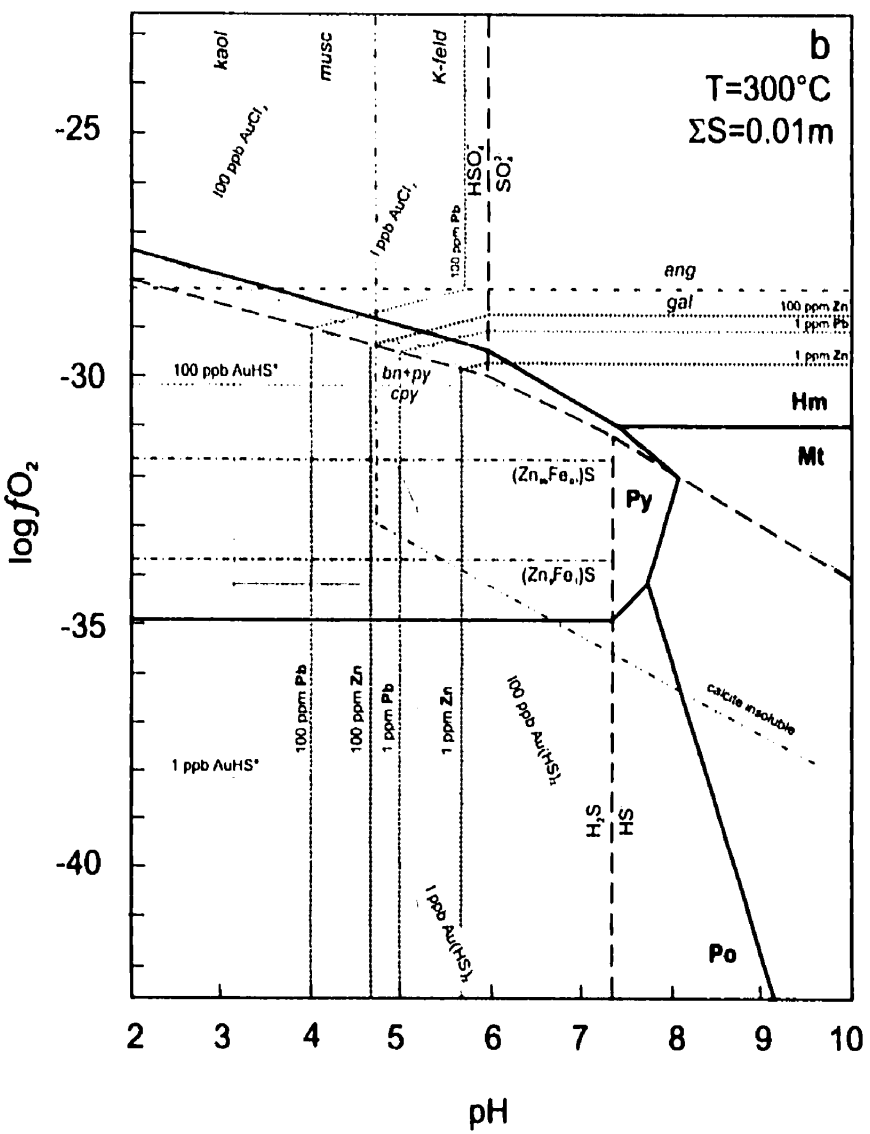
b
T=300°C
ΣS=0.01m
kaol
musc
K-feld
100 ppb AuCl,
1 ppb AuCl,
100 ppm Pb
HSO4-
SO4--
ang
gal
100 ppm Zn
1 ppm Pb
1 ppm Zn
100 ppb AuHS°
bn+py
cpy
Hm
Mt
(Zn,Fe)S
Py
calcite insoluble
1 ppb AuHS°
100 ppm Pb
100 ppm Zn
1 ppm Pb
1 ppm Zn
100 ppb Au(HS)2-
1 ppb Au(HS)2-
H2S
HS-
Po
-25
-30
-35
-40
2
3
4
5
6
7
8
9
10
log fO2
pH

1995b), although Mikucki (1998) recently demonstrated that $Au(HS)^-_2$ is likely the dominant species for the temperature, pH, and ΣS conditions of Dawson Range epithermal fluids.

The constraints on initial log fO_2 - pH conditions for ΣS = 0.1 *m* are shown by the shaded box in Figure 8a. pH is constrained to values between approximately 3 and 5 by the common host rock alteration of K-feldspar to sericite (and to a smaller extent to kaolinite), as well as by the general absence of calcite, except as late-stage infilling, in the mineralized veins. Limits on log fO_2 are constrained by the pyrite stability field, the absence of bornite, and the FeS content (<1-17 mol.%) of sphalerite (approximately between -36 and –34), and gas chromatographic results for CO_2-CH_4 equilibria indicating log fO_2 values of -37.7 and -34.4 bars for the Huestis and Tinta Hill deposits, respectively. At these estimated initial conditions, the concentration of Zn in solution would have been from ~1-1000 ppm, and that of Pb would have been ≤1-100 ppm. Gold would have been predominantly in the form of $Au(HS)^-_2$ and would have had a concentration of 100 ppb-1 ppm.

4.9.5 Fluid Evolution and Depositional Controls

The Dawson Range epithermal system is initially best described by the behaviour of its base metal components, since the ratio of base metals to reported precious metal concentrations is on the order of at least 10:1. In addition, although the exact location and paragenesis of gold in the epithermal veins is unknown, anomalous concentrations have been found in various base metal sulphides, most notably in sphalerite and arsenopyrite.

Although the hydrothermal fluid that was responsible for the alteration of feldspar to mica and clay must initially have been acidic, the consumption of H^+ during alteration caused the fluid pH to increase:

$$3\ KAlSi_3O_8 + 2\ H^+ = KAl_3Si_3O_{10}(OH)_2 + 6\ SiO_2 + 2\ K^+.$$

An increase in pH greatly decreases the solubility of Zn and Pb as chloride complexes (Fig. 4.8a):

$$ZnCl_2^\circ + H_2S = ZnS + 2\ Cl^- + 2\ H^+.$$

The resultant precipitation of these metals as sulphide minerals would have been facilitated by the high concentration of sulphur in the fluid. The solubility of base metals is also strongly dependant on temperature (Anderson, 1973), and the precipitation of sphalerite and galena would have been enhanced by cooling of the hydrothermal fluid as it came into contact with the relatively cold host rocks. A shift to higher pH, across the calcite solubility line, is suggested by the presence of late calcite in several of the veins.

If the gold in the hydrothermal fluid was predominantly complexed as $Au(HS)^-_2$, as predicted by Figure 4.8a, a simple increase in pH would have increased its solubility. However, the precipitation of sphalerite and galena (as well as other sulphide minerals) would have served to reduce the concentration of ΣS in the fluid, and thus reduce the stability of $Au(HS)^-_2$ as shown by the shift of the solubility lines to higher log fO_2, thereby promoting the deposition of Au metal (Fig. 4.8b).

4.9.6 Metallogenic Model

It is reasonable to assume that epithermal veins formed during or closely following one of the two volcanic events in the southern Dawson Range. Paleomagnetic evidence suggests that the voluminous extrusion of the Carmacks volcanic group caused a large-scale regional hydrothermal event (Johnston et al., 1996; Wynne et al., 1998), a model supported by the thermal resetting of 105 Ma Mount Nansen porphyry dykes to a Carmacks alteration age of 70 Ma (Smuk et al., 1997). Sulphur isotopic data suggest that the hydrothermal fluid had an igneous or magmatic source, and the galena lead isotopic compositions are similar to the age-corrected whole rock Pb-isotopes of the Carmacks volcanic group, implicating that this group was a major source of metals. The depletion of base metals in altered dykes of both volcanic groups suggests that a small component of the metals was likely derived locally from the other lithological units that host the

deposits. The large additions of As and Sb in the altered dykes, however, suggest an external source for these, and probably other, metals. Fluid inclusion microthermometric data and oxygen and hydrogen isotopic data require a meteoric water dominated system, but are consistent with some degree of water-rock interaction, or small degrees of mixing with magmatic water. In view of these data, it is likely that the hydrothermal fluid responsible for epithermal mineralization was predominantly meteoric in origin, but was driven by the heat of the Carmacks igneous event and scavenged metals from the Carmacks volcanic pile, as well as the underlying country rocks.

The relatively high chlorinity estimated for the hydrothermal fluid permitted the transport of significant concentrations of base metals as chloride complexes, and the accompanying high sulphur activity facilitated the deposition of these metals as sulphide minerals. The deposition of base metals from solution was likely caused by an increase in fluid pH due to the consumption of H^+ during sericitic and argillic alteration of the host rocks. The pH increase promoted the solubility of gold that was present predominantly as $Au(HS)^-_2$, but this effect was small relative to the destabilization of the gold-bisulphide complexes due to the reduction in ΣS caused by the deposition of base metal sulphides.

Although the epithermal veins of the southern Dawson Range may be best described as low sulphidation deposits, several characteristics of the mineralization suggest that the deposits may be transitional between low and high sulphidation types. Characteristics that differ from typical (Hedenquist et al., 1996; Arribas, 1995; Heald et al., 1987; Hayba et al., 1985) low sulphidation epithermal deposits include the presence of ore minerals such as enargite, (tennantite and barite), alteration minerals such as sericite and kaolinite with little to no adularia, and fluids with low pH, high ΣS, and moderately high CO_2, as well as slightly high temperatures and salinities. This characterization is perhaps best demonstrated by the Emmons Hill deposit, which contains barite, fluids with isotopically heavy oxygen (McInnes, 1987), and As-rich sulphides and sulphosalts. The Dawson Range veins have many similarities to the Kelian low sulphidation Au deposit of Indonesia, for which relatively hot, saline, and CO_2-rich

hydrothermal fluids, and depth of formation (~1500 m), have been cited as evidence of a transitional setting between epithermal and porphyry styles of mineralization (Van Leeuwan et al., 1990; Hedenquist et al., 1996). The transitional nature of the epithermal veins could be explained in part by their close association with the shoshonitic Carmacks volcanics. In alkalic-type low sulphidation epithermal gold deposits, such as the well-known Cripple Creek, Black Hills, Porgera, Ladolam, and Emperor districts, evidence of a magmatic fluid or vapour contribution is supported by high temperatures (≤350°C), high salinities (≤10 wt.% NaCl equiv.), variable CO_2 contents, As and Sb enrichments, and heavy $\delta^{18}O$ values (Richards, 1995; 1992; Paterson et al., 1989; Mutschler and Mooney, 1993). Au-telluride mineralization typical of alkalic-type epithermal veins is not, however, present in the Dawson Range. Spatial and genetic associations between gold-copper mineral deposits and potassic igneous suites have been noted around the Circum-Pacific (Müller and Groves, 1997).

The paleomagnetic (Johnston et al., 1996; Wynne et al., 1998) and alteration (Smuk et al., 1997) evidence that the Carmacks magmatic event was responsible for a widespread hydrothermal event throughout the Dawson Range is further evidence that the genesis of the gold-bearing, base metal-rich, epithermal veins of the southern Dawson Range was associated with Carmacks magmatism. In the Mount Nansen area, this mineralizing event was likely superimposed on a mid-Cretaceous Cu-Au porphyry system hosted by Mount Nansen intrusions. If the epithermal veins were higher-level counterparts to a porphyry system (Hayba et al., 1985; Panteleyev, 1986; Heald et al., 1987), they would correlate with the 70 Ma Casino Cu-Mo-Au deposit, and could have been located below a high-level vein system typical of low sulphidation hot spring deposits. Considering the amount of weathering and glacial erosion that has taken place since the Late Cretaceous (LeBarge, 1995; Carlson, 1987), as well as the abundance of proximal placer gold deposits, it is likely that such high-level lode veins are absent in this area. However, additional deposits of the Carmacks polymetallic vein-type may be discovered in areas proximal to and in Carmacks group successions in outlying areas.

4.10 Conclusions

The results of this study provide evidence for a regional metallogenic event related to Late Cretaceous shoshonitic volcanism, which resulted in the development of epithermal gold- and base metal-rich veins transitional between low and high sulphidation types. The intense alteration (Smuk et al., 1997) and paleomagnetic resetting (Johnston et al., 1997; Wynne et al., 1998) of pre-existing country rocks provide evidence for a large-scale hydrothermal system through the southern Dawson Range driven by the Carmacks magmatic event. The hydrothermal fluid and resultant mineralized veins were focussed in fault systems. The Au-Cu porphyry deposits hosted by mid-Cretaceous Mount Nansen group intrusions, however, are likely unrelated to the epithermal veins.

The hydrothermal fluid was dominantly of meteoric origin, although it appears to have undergone oxygen isotopic exchange with country rocks. A small magmatic component is suggested by the moderately high temperatures, salinities, ΣS and CO_2 concentrations, and the low pH of inclusion fluids. Base metals were leached from both the Carmacks volcanics and older lithologies, and were transported in solution as chloride complexes, while gold was transported primarily as $Au(HS)_2^-$. The precipitation of base metal sulphides such as galena and sphalerite was caused by an increase in pH due to the loss of H^+ from initially acidic fluids during sericitic and argillic alteration of country rocks. The resultant and likely concurrent reduction in the ΣS concentration destabilized the gold-thio complexes.

Although the epithermal veins of the southern Dawson Range may generally be described as low sulphidation type, the lack of adularia alteration, the strong base metal character of the veins, the presence of high-sulphidation minerals, and moderately high fluid temperatures and Cl^-, ΣS, and CO_2 concentrations indicate that the veins are transitional between low and high sulphidation types. The transitional nature of the epithermal veins may reflect a system that was deeply emplaced but distal from the magmatic centre. Given the regional extent of the Carmacks hydrothermal event and the

fact that the deposition of gold and base metals was caused by the reaction of fluids with country rocks, it is likely that this type of vein deposit may be common throughout the Dawson Range.

4.11 References

Alderton, D. H. M., Thompson, M., Rankin, A. H., and Chryssoulis, S. L., 1982, Developments of the ICP-linked decrepitation technique for the analysis of fluid inclusions in quartz: Chemical Geology, v. 37, p. 203-213.

Anderson, G. M., 1973, The Hydrothermal Transport and Deposition of Galena and Sphalerite Near 100°C: Economic Geology, v. 68, p. 480-492.

Anderson, F., and Stroshein, R., 1998, Geology of the Flex gold-silver vein system, Mount Nansen area, Yukon: Yukon Exploration and Geology 1997, Exploration and Geological Services Division, Yukon, Indian and Northern Affairs Canada, p. 139-143.

Andrew, A., Godwin, C. I., and Sinclair, A. J., 1984, Mixing Line Isochrons, A New Interpretation of Galena Lead Isotope Data from Southeastern British Columbia: Economic Geology, v. 79, p. 919-932.

Arribas, A. Jr., 1995, Characteristics of high-sulfidation epithermal deposits, and their relation to magmatic fluid: Magmas, Fluids, and Ore Deposits, (ed.) J.F.H. Thompson, MAC Short Course, v. 23, p. 419-454.

Barrett, T. J., and Anderson, G. M., 1988, The solubility of sphalerite and galena in 1-5 m NaCl solutions to 300°C: Geochimica et Cosmochimica Acta, v. 52, p. 813-820.

Barton, P. B., and Skinner, B. J., 1979, Sulfide Mineral Stabilities: Geochemistry of Hydrothermal Ore Deposits, 2nd Edition, ed. H. L. Barnes, p. 278-403.

Beane, R. E., and Titley, S. R., 1981, Porphyry copper deposits, Part II, Hydrothermal Alteration and Mineralization: Economic Geology, 75th Anniversary Volume, p. 235-269.

Benning, L. G., and Seward, T. M., 1996, Hydrosulphide complexing of Au(I) in hydrothermal solutions from 150-400°C and 500-1500 bar: Geochimica et Cosmochimica Acta, v. 60, p. 1849-1871.

Bray, C. J., Spooner, E. T. C., and Thomas, A. V., 1991, Fluid inclusion volatile analysis by heated crushing, on-line gas chromatography; applications to Archean fluids: Journal of Geochemical Exploration, v. 42, p. 167-193.

Carlson, G. G., 1987, Geology of Mount Nansen (115-I/3) and Stoddart Creek (115-I/6) Map Areas, Dawson Range, Central Yukon: Indian and Northern Affairs Canada, Northern Affairs: Yukon Region Open File 1987-2.

Clowes, R. M. (ed.), 1997, Lithoprobe Phase V Proposal – Evolution of a Continent Revealed: Lithoprobe Secretariat, The University of British Columbia, Vancouver, B. C., 292 p.

Cumming, G. L., and Richards, J. R., 1975, Ore lead isotope ratios in a continuously changing Earth: Earth and Planetary Science Letters, v. 28, p. 155-171.

Czamanske, G., K., and Rye, R. O., 1974, Experimentally Determined Sulfur Isotope Fractionations between Sphalerite and Galena in the Temperature Range 600° to 275°C: Economic Geology, v. 69, p. 17-25.

Doe, B. R., and Stacey, J. S., 1974, The Application of Lead Isotopes to the Problems of Ore Genesis and Ore Prospect Evaluation: A Review: Economic Geology, v. 69, p. 757-776.

Doe, B. R., and Zartman, R. E., 1979, Plumbotectonics, The Phanerozoic, Chapter 2: Geochemistry of Hydrothermal Ore Deposits, (ed.) H. L. Barnes, p. 22-70.

Dubessy, J., 1984, Simulation des équilibres chimiques dans le système C-O-H. Conséquences méthodologiques pour les inclusions fluides: Bulletin de Minéralogie, v. 107, p. 155-168.

Engebretson, D. C., Cox, A., and Gordon, R. G., 1985, Relative motions between oceanic and continental plates in the Pacific Basin: Geological Society of America Special Paper 206, 59 p.

Francis, D. and Johnston, S. T., 1998, Isotopic constraints on lithospheric melting near the Yellowstone hotspot, Carmacks volcanics, Yukon: GSA Program with Abstracts, v. x, p. A-90.

Fritz, P., Drimmei, R. J., and Nowicki, V. K., 1974, Preparation of sulfur dioxide for mass spectrometer analyses by combustion of sulfides with copper oxide: Analytical Chemistry, v. 46, p. 164-166.

Gammons, C. H., and Williams-Jones, A. E., 1995a, Hydrothermal Geochemistry of Electrum: Thermodynamic Constraints: Economic Geology, v. 90, p. 420-432.

Gammons, C. H., and Williams-Jones, A. E., 1995b, The solubility of Au-Ag alloy + AgCl in HCl/NaCl solutions at 300°C: New data on the stability of Au (I) chloride complexes in hydrothermal fluids: Geochimica et Cosmochimica Acta, v. 59, p. 3453-3468.

Giggenbach, W. F., 1997, The Origin and Evolution of Fluids in Magmatic-Hydrothermal Systems: Geochemistry of Hydrothermal Ore Deposits, 3rd ed., (ed.) H. L. Barnes, p. 737-796.

Glasmacher, U., 1990, Petrogenetische und metallogeneitsche Entwicklung ausgewahlter Gebiete im 'Yukon – Tanana Terrane' und 'Stikine Terrane', (Yukon Territorium, Kanada) wahrend der Oberkreide und des Alttertiars: Mitteilungen zur Mineralogie und Lagerstattenkunde, Nr. 38, Aachen University Ph.D. Thesis, 605 p.

Godwin, C. I., 1975, Alternative interpretations for the Casino Complex and Klotassin Batholith in the Yukon Crystalline Terrane: Canadian Journal of Earth Sciences, v. 12, p. 1910-1915.

Godwin, C. I., 1976, Casino: Paper 35, Part B - Porphyry Copper and Copper-Molybdenum deposits of the Calc-Alkaline Suite: Porphyry Deposits of the Canadian Cordillera, CIM Special Volume 15, p. 344-354.

Godwin, C. I., and Sinclair, A. J., 1982, Average Lead Isotope Growth Curves for Shale-Hosted Zinc-Lead Deposits, Canadian Cordillera: Economic Geology, v. 77, p. 675-690.

Godwin, C. I., Gabites, J. E., and Andrew, A., 1984, Leadtable: A galena lead isotope data base for the Canadian Cordillera, with a guide to its use by explorationists: British Columbia Ministry of Energy, Mines and Petroleum Resources, Mineral Resources Division Paper 1988-4, 188 p.

Graney, J. R., and Kesler, S. E., 1995, Gas composition of inclusion fluid in ore deposits: is there a relation to magmas?: Magmas, Fluids, and Ore Deposits, (ed.) J.F.H. Thompson, MAC Short Course, v. 23, p. 221-245.

Grond, H. C., Churchill, S.J., Armstrong, R. L., Harakal, J. E., and Nixon, G. T., 1984, Late Cretaceous age of the Hutshi, Mount Nansen, and Carmacks groups,

southwestern Yukon Territory and northwestern British Columbia: Canadian Journal of Earth Sciences, v. 21, p. 554-558.

Hart, C. J. R., Johnston, S. T., Francis, D., Smuk, K., Wynne, J., and Enkin, J., 1998, Yellowstone in Yukon – a hotspot link to Late Cretaceous alkalic-associated Cu and Au mineralization: Cordilleran Roundup Meeting Abstract, Vancouver.

Hart, C. J. R., and Langdon, M., 1998, Geology and mineral deposits of the Mount Nansen camp, Yukon: Yukon Exploration and Geology 1997, Exploration and Geological Services Division, Yukon, Indian and Northern Affairs Canada, p. 129-138.

Hayashi, K, -I., and Ohmoto, H., 1991, Solubility of gold in NaCl- and H_2S-bearing aqueous solution at 259-350°C: Geochimica et Cosmochimica Acta, v. 55, p. 211-216.

Hayba, D. O., Bethke, P. M., Heald, P., and Foley, N.K., 1985, Geologic, Mineralogic, and Geochemical Characteristics of Volcanic-Hosted Epithermal Precious-Metal Deposits: Geology and Geochemistry of Epithermal Systems, Reviews in Economic Geology, v. 2, p. 129-167.

Haynes, F. M., Sterner, S. M., and Bodnar, R. J., 1988, Synthetic fluid inclusions in natural quartz. IV. Chemical analyses of fluid inclusions by SEM/EDA: Evaluation of method: Geochimica et Cosmochimica Acta, v. 52, p. 969-977.

Heald, P., Foley, N. K., and Hayba, D. O., 1987, Comparative Anatomy of Volcanic-Hosted Epithermal Deposits: Acid-Sulfate and Adularia-Sericite Types: Economic Geology, v. 82, p. 1-26.

Hedenquist, J. W., and Henley, R. W., 1985, The Importance of CO_2 on Freezing Point Measurements of Fluid Inclusions: Evidence from Active Geothermal Systems and Implications for Epithermal Ore Deposition: Economic Geology, v. 80, p. 1379-1406.

Hedenquist, J. W., Izawa, E., Arribas, A., and White, N. C., 1996, Epithermal gold deposits: Styles, characteristics, and exploration: Resource Geology Special Publication Number 1, 16 p.

Helgeson, H. C., Kirkham, D. H., and Flowers, G. C., 1981, Theoretical prediction of the thermodynamic behaviour of aqueous electrolytes at high pressures and temperatures. IV. Calculation of activity coefficients, osmotic coefficients, and

apparent molal and standard and relative partial molal properties to 600°C and 5 kb: American Journal of Science, v. 281,p. 1249-1516.

Hunt, P. A., and Roddick, J. C., 1991, A Compilation of K-Ar Ages, Report 20: Radiogenic Age and Isotopic Studies: Report 4, Geological Survey of Canada, Paper 90-2, p. 113-143.

INAC, 1990, Yukon Exploration 1989: Exploration and Geological Services Division, Yukon, Indian and Northern Affairs Canada, 182 p.

Irving, E., and Wynne, P. J., 1990, Palaeomagnetic evidence bearing on the evolution of the Canadian Cordillera: Philosophical Transactions of the Royal Society of London, A. 331, p. 487-509.

Johnson, J. W., Oelkers, E. H., and Helgeson, H. C., 1992, SUPCRT92: A software package for calculating the standard molal thermodynamic properties of minerals, gases, aqueous species, and reactions from 1 to 5000 bars and 0° and 1000°C: Computers and Geosciences, v. 18, p. 899-947.

Johnston, S. T., 1995, Geological Compilation with Interpretation from Geophysical Surveys of the Northern Dawson Range, Central Yukon (115 J/9 and 10, 115 I/12, 1:100 000 Scale Map): Exploration and Geological Services Division, Department of Indian and Northern Affairs Open File 1995-2(G).

Johnston, S. T., Wynne, P. J., Francis, D., Hart, C. J. R., Enkin, R. J., and Engebretson, D. C., 1996, Yellowstone in Yukon: The Late Cretaceous Carmacks Group: Geology, v. 26, p. 997-1000.

Journeay, J. M., and Williams, S. P., 1995, GIS Map Library: A Window on Cordilleran Geology: Geological Survey of Canada, Open File 2948 (v. 1.0).

Koehler, G. D., Chipley, D., and Kyser, T. K., 1991, Measurement of the hydrogen and oxygen isotopic compositions of concentrated chloride brines and brines from fluid inclusions in halite: Chemical Geology (Isotope Geoscience Section), v. 94, p. 45-54.

LeBarge, W. P., 1995, Sedimentology of Placer Gravels Near Mt. Nansen, Central Yukon Territory: Bulletin 4, Exploration and Geological Services Division, Indian and Northern Affairs Canada, Yukon Region, 155 p.

Le Couteur, P. C., and Templeman-Kluit, D. J., 1976, Rb/Sr ages and a profile of initial $^{87}Sr/^{86}Sr$ ratios for plutonic rocks across the Yukon Crystalline Terrain: Canadian Journal of Earth Sciences, v. 13, p. 319-330.

Manhès, G., Allègre, C. J., Dupré, B., and Hamelin, B., 1980, Lead isotope study of basic-ultrabasic layered complexes: speculations about the age of the Earth and primitive mantle characteristics: Earth and Planetary Science Letters, v. 47, p. 370-382.

Mariner, R. H., Kharaka, Y. K., Ambats, G., and White, L. D., 1992, Chemical composition and stable isotopes of thermal waters, Norris-Mammoth corridor, Yellowstone National Park, USA: Proceedings of the 7th International Symposium on Water-Rock Interaction – Low Temperature Environments, (ed.) Y.K. Kharaka and A.S. Maest, v. 1, p. 963-966.

McInnes, B. I. A., 1987, Geological and precious metal evolution at Freegold Mountain, Dawson Range, Yukon: unpublished M.Sc. thesis, McMaster University, 230 p.

McInnes, B. I. A., Goodfellow, W. D., Crocket, J. H., and McNutt, R. H., 1988, Geology, geochemistry and geochronology of subvolcanic intrusions associated with gold deposits at Freegold Mountain, Dawson Range, Yukon: Current Research, Part E, Geological Survey of Canada, Paper 88-1E, p. 137-151.

McInnes, B. I. A., Crocket, J. H., and Goodfellow, W. D., 1990, The Laforma deposit, an atypical epithermal-Au system at Freegold Mountain, Yukon Territory, Canada: Epithermal Gold Mineralization of the Circum-Pacific: Geology, Geochemistry, Origin and Exploration, II, (ed.) J.W. Hedenquist, N.C. White, and G. Siddeley, Journal of Geochemical Exploration, v. 36, p. 73-102.

Mikucki, E. J., 1998, Hydrothermal transport and depositional processes in Archean lode-gold systems: A review: Ore Geology Reviews, v. 13, p. 307-321.

Morin, J. A., 1981, Element distribution in Yukon gold-silver deposits: Yukon Geology and Exploration 1979-80, Exploration and Geological Services Division, Yukon, Indian and Northern Affairs Canada, p. 68-84.

Müller, D., and Groves, D. I., 1997, Potassic Igneous Rocks and Associated Gold-Copper Mineralization: Lecture Notes in Earth Science, v. 56, Springer-Verlag, 238 p.

Mutschler, F. E., and Mooney, T. C., 1993, Precious-metal Deposits Related to Alkalic Igneous Rocks: Provisional Classification, Grad-Tonnage Data and Exploration Frontiers: Mineral Deposit Modeling, (ed.) R. V. Kirkham, W. D. Sinclair, R. I. Thorpe, J. M. Duke, Geological Association of Canada, Special Paper 40, p. 479-520.

Ohmoto, H., 1972, Systematics of Sulfur and Carbon Isotopes in Hydrothermal Ore Deposits: Economic Geology, v. 67, p. 551-578.

Ohmoto, H., and Goldhaber, M. B., 1997, Sulfur and Carbon Isotopes: Geochemistry of Hydrothermal Ore Deposits, 3rd ed., (ed.) H. L. Barnes, p. 517-611.

Ohmoto, H., and Rye, R. O., 1979, Isotopes of sulfur and carbon: Geochemistry of Hydrothermal Ore Deposits, 2nd ed., (ed.) H. L. Barnes, p. 509-567.

Oppliger, G. L., Murphy, J. B., and Brimhall, G. H., 1997, Is the ancestral Yellowstone hotspot responsible for the Tertiary "Carlin" mineralization in the Great Basin of Nevada?: Geology, v. 25, p. 627-630.

Panteleyev, A., 1986, A Canadian Cordilleran Model for Epithermal Gold-Silver Deposits: Geoscience Canada, v. 13, p. 101-111.

Parry, W. T., and Bowman, J. R., 1990, Chemical and stable isotopic models for Boundary Creek warm springs, southwestern Yellowstone National Park, Wyoming: Journal of Volcanology and Geothermal Reasearch, v. 43, p. 133-157.

Paterson, C. J., Uzunlar, N., Groff, J., and Longstaffe, F. J., 1989, A View through an Epithermal-Mesothermal Precious Metal System in the Northern Black Hills, South Dakota; A Magmatic Origin for the Ore-Forming Fluids: The Geology of Gold Deposits: The Perspective in 1988, Economic Geology Monograph 6, p. 564-570.

Payne, J. G., Gonzalez, R. A., Akhurst, K., and Sisson, W. G., 1987, Geology of Colorado Creek (115-J/10), Selwyn River (115-J/9), and Prospector Mountain (115-I/5) Map Areas, Western Dawson Range, West-Central Yukon: Indian and Northern Affairs Canada, Northern Affairs: Yukon Region Open File 1987-3.

Potter, R. W., Clynne, M. A., and Brown, D. L., 1978, Freezing point depression of aqueous sodium chloride solutions: Economic Geology, v. 73, p. 284-285.

Reynolds, T. J., 1992, Fluid Inc. adapted U.S.G.S. gas-flow heating/freezing system instruction manual: Denver, Colorado, U.S. Geological Survey, 34 p.

Richards, J. P., 1995, Alkalic-type epithermal gold deposits – a review: Magmas, Fluids, and Ore Deposits, (ed.) J.F.H. Thompson, MAC Short Course, v. 23, p. 367-400.

Richards, J. P., 1992, Magmatic-epithermal transitions in alkalic systems: Porgera gold deposit, Papua New Guinea: Geology, v. 20, p. 547-550.

Roedder, E., 1984, Fluid Inclusions: Reviews in Mineralogy, v. 12, 644 p.

Ruaya, J. R., and Seward, T. M., 1986, The stability of chlorozinc(II) complexes in hydrothermal solutions up to 350°C: Geochimica et Cosmochimica Acta, v. 50, p. 651-661.

Saager, K., and Bianconi, F., 1971, The Mount Nansen Gold-Silver Deposit, Yukon Territory, Canada: Mineralium Deposita, v. 6, p. 209-224.

Saunders, C. R., 1980, Report on the Tawa Property, Mount Nansen Area, Yukon Territory: Dolmage Campbell & Associates (1975) Ltd. report for BRX Mining and Petroleum Corp., Whitehorse Assessment Office report #090692.

Salvi, S., 1994, Magma Degassing and Wall Rock Alteration in the Rare Metal-Rich Peralkaline Granite at Strange Lake, Quebec/Labrador: unpublished Ph.D. thesis, McGill University, 263 p.

Salvi, S., and Williams-Jones, A. E., 1997, Fischer-Tropsch synthesis of hydrocarbons during sub-solidus alteration of the Strange Lake peralkaline granite, Quebec/Labrador, Canada: Geochimica et Cosmochimica Acta, v. 61, p. 83-99.

Selby, D., 1998, Geochemistry of porphyry Cu-Au-Mo potassic ore fluids: A case study from the Yukon, Canada: SEG Newsletter, no. 35, p. 6.

Selby, D., and Nesbitt, B. E., 1998, Biotite chemistry of the Casino porphyry Cu-Mo-Au occurrence, Dawson Range, Yukon: Yukon Exploration and Geology 1997, Exploration and geological Services Division, Yukon, Indian and Northern Affairs Canada, p. 83-88.

Seward, T. M., 1984, The formation of lead(II) chloride complexes to 300°C: A spectrophotometric study: Geochimica et Cosmochimica Acta, v. 48, p. 121-134.

Shenberger, D. M., and Barnes, H. L., 1989, Solubility of gold in aqueous sulfide solutions from 150 to 350°C: Geochimica et Cosmochimica Acta, v. 53, p. 269-278.

Shock, E. L., 1998, Slop98.dat. SUPCRT92 1998 update: GEOPIG at Washington University, http://zonvark.wustl.edu/geopig/.

Smuk, K. A., Williams-Jones, A. E., and Francis, D., 1997, The Carmacks hydrothermal event: An alteration study in the southern Dawson Range, Yukon: Yukon Exploration and Geology 1996, Exploration and Geological Services Division, Yukon, Indian and Northern Affairs Canada, p. 92-106.

Souther, J. G., 1991, Volcanic Regimes, Chapter 14: Geology of the Canadian Cordillera, (ed.) H. Gabrielse, C.J. Yorath, Geological Survey of Canada, Geology of Canada, No. 4, p. 457-490.

Stacey, J. S., and Kramers, J. D., 1975, Approximation of terrestrial lead isotope evolution by a two-stage model: Earth and Planetary Science Letters, v. 26, p. 207-221.

Stevens, R. D., Delabio, R. N., and Lachance, G. R., 1982, Age determinations and geological studies: K-Ar isotopic ages, Report 16: Geological Survey of Canada, Paper 82-2, 52 p.

Taylor, H. P., Jr., 1974, The application of oxygen and hydrogen isotope studies to problems of hydrothermal alteration and ore deposition: Economic Geology, v. 69, p. 843-883.

Tempelman-Kluit, D. J., 1984, Geology of the Lebarge and Carmacks Map Sheets: Geological Survey of Canada, Open File 1101, map sheets with legends.

Tempelman-Kluit, D. J., and Wanless, R. K., 1975, Potassium-argon age determinations of metamorphic and plutonic rocks in the Yukon Crystalline Terrane: Canadian Journal of Earth Sciences, v. 12, p. 1895-1909.

Tempelman-Kluit, D. J., and Wanless, R. K., 1980, Zircon ages for the Pelly Gneiss and Klotassin granodiorite in western Yukon: Canadian Journal of Earth Sciences, v. 17, p. 297-306.

Thordsen, J. T., Kharaka, Y. K., Mariner, R. H., and White, L. D., 1992, Controls on the distribution of stable isotopes of meteoric water and snow in the greater Yellowstone National Park region, USA: Proceedings of the 7th International

Symposium on Water-Rock Interaction – Low Temperature Environments, (ed.) Y.K. Kharaka and A.S. Maest, v. 1, p. 591-595.

Tough, T. R., 1981, Interim report on the Tinta Hill Property, Whitehorse Mining Division, Y.T.: Report for Silver Tusk Mines Ltd. and Panther Mines Ltd., Whitehorse Assessment Office report #062119.

Umhoefer, P. J., 1987, Northward translation of "Baja British Columbia" along the Late Cretaceous to Paleocene margin of western North America: Tectonics, v. 6, p. 377-394.

Van Leeuwen, T. M., Leach, T, Hawke, A. A., and Hawke, M. M., 1990, The Kelian disseminated gold deposit, East Kalimantan, Indonesia: Epithermal Gold Mineralization of the Circum-Pacific: Geology, Geochemistry, Origin and Exploration, I, (ed.) J.W. Hedenquist, N.C. White, and G. Siddeley, Journal of Geochemical Exploration, v. 35, p. 1-61.

Williams-Jones, A. E., and Normand, C., 1997, Controls of Mineral Parageneses in the System Fe-Sb-S-O: Economic Geology, v. 92, p. 308-324.

Wynne, P. J., Enkin, R. J., Baker, J., Johnston, S. T., and Hart, C. J. R., 1998, The big flush: paleomagnetic signature of a 70 Ma regional hydrothermal event in displaced rocks of the northern Canadian Cordillera: Canadian Journal of Earth Sciences, v. 35, p. 657-671.

Yukon Minfile, 1996. Version 2.05, May 31, 1996: Exploration and Geological Services Division, Indian and Northern Affairs Canada.

Zartman, R. E., and Haines, S. M., 1988, The plumbotectonic model for Pb isotope systematics among major terrestrial reservoirs – A case for bi-directional transport: Geochimica et Cosmochimica Acta, v. 52, p. 1327-1339.

Chapter 5
Conclusions

This study has attempted to provide a metallogenic framework for epithermal vein mineralization in the southern Dawson Range, and makes some inferences as to the relative timing of associated porphyry-style mineralization. The results of whole rock geochemistry, mass-change studies, age dating, fluid inclusion microthermometry, gas chromatography, and oxygen, hydrogen, sulphur, and lead isotopic analyses suggest that there is a genetic relationship between Late Cretaceous Carmacks magmatism, alteration and epithermal mineralization in the southern Dawson Range.

Lavas, dykes, and stocks in the southern Dawson Range have been shown to belong to either the 105 Ma Mount Nansen or the 70 Ma Carmacks magmatic suites on the basis of their potassium content. The Carmacks group is a shoshonitic suite proposed to result from lithospheric melting above the Late Cretaceous Yellowstone hotspot (Johnston et al., 1996; Francis and Johnston, 1998; Wynne et al., 1998), while the Mount Nansen Group is a high-K, subduction-related calc-alkaline suite (Souther, 1991). Altered Mount Nansen dykes have been dated at between 94 and 61 Ma, ages that are interpreted to represent the resetting of Mount Nansen ages by a Carmacks-age hydrothermal event. The occurrence of a large-scale hydrothermal system is supported by the remagnetization of older units in the south-central Yukon to a remanent direction identical to that obtained for the Carmacks group (Johnston et al., 1996; Wynne et al., 1998). The close spatial relationship between mineralized veins and Mount Nansen dykes appears to be fortuitous, however, as porphyry-style mineralization in Mount Nansen stocks appears to be a 105 Ma event (Sawyer and Dickinson, 1976). Carmacks intrusions also host porphyry-style mineralization, and thus the existence of two mineralization events is well-established, regardless of the age of the epithermal veins. The results of this study have clarified previous confusion about the relationship between Au mineralization and the Mount Nansen and Carmacks magmatic events.

The most significant change during alteration of the dykes of both suites was an extreme loss of sodium, mineralogically reflected by the replacement of feldspar by sericite and clay minerals. This Na depletion is an effective guide to areas of intense

hydrothermal alteration and proximal mineralization. Other changes include the addition of Si and a slight depletion in K. Since the K change estimated for both suites of altered dykes is less than 20%, by their K content Carmacks dykes can be readily distinguished from Mount Nansen rocks. Altered dykes display general depletions in Pb, Zn and Cu, suggesting that these elements were mobilized during alteration and subsequently deposited in base metal veins. As and Sb are greatly enriched in all altered dykes, however, and are likely to have been introduced together with gold by hydrothermal solutions responsible for the mineralization.

Epithermal veins are dominated by base metal sulphides, in the approximate paragenetic order: pyrite, arsenopyrite, sphalerite, chalcopyrite, galena, enargite, (sulphosalts), and tetrahedrite. Gold occurs predominantly as submicroscopic inclusions within sulphide minerals. Fluid inclusion microthermometry, decrepitate analyses and gas chromatography of samples from the epithermal veins indicate that the mineralizing hydrothermal fluid had a temperature of approximately 300°C, was Na^+-dominated but also contained K^+ and Ca^{2+} in lesser proportions, had Cl^- and S^{2-} concentrations of approximately 0.99 *m* and 0.20 *m*, respectively, and was moderately CO_2 rich. Fluid inclusion data from the Mount Nansen-aged Revenue Au-Cu porphyry deposit indicate the existence of three hydrothermal episodes; an early porphyry-style mineralizing event (>400°C), a later epithermal event (~300°C), and a terminal low temperature event (<150°C) unassociated with mineralization.

The oxygen and hydrogen isotopic compositions of fluid inclusions in the ore minerals of five vein deposits of the southern Dawson Range indicate that the fluid is dominantly of meteoric origin, and most likely evolved through interaction with country rocks. A small contribution from magmatic water is suggested by the isotopic composition and other physicochemical parameters of the fluid, but is not unequivocally supported by the temperature-salinity relationships. The progressive shift of the three analyzed Dawson Range fluids from the meteoric water line towards heavier $\delta^{18}O$ can be correlated with their styles of mineralization, temperatures of deposition, and with their

CO_2 concentrations. There is a large difference between the δD value of present-day Dawson Range rainwater as measured by McInnes et al. (1990) and the δD values of Dawson Range vein ore, implying some degree of latitude change. If the δD shift is taken solely as an indication of latitude, data from the southern Dawson Range suggest that the veins were deposited at latitudes close to that of present-day Yellowstone.

Sulphur isotopic data suggest that the hydrothermal fluid had an igneous or magmatic source, and the similarity of the galena lead isotopes to the age-corrected whole rock Pb-isotopic composition of Carmacks volcanic rocks suggests that the Carmacks group was the main source of metals, although there was some contribution of metals from either Mount Nansen volcanics or some other lithology. The relatively high estimated chlorinity of the hydrothermal fluid favoured the transport of base metals as chloride complexes, and the accompanying high sulphur activity facilitated the deposition of these metals as sulphide minerals. The deposition of base metals from solution was likely caused by an increase in pH due to the consumption of H^+ during sericitic and argillic alteration of the host rocks. The resultant destabilization of gold-thio complexes due to the deposition of base metal sulphides promoted the coprecipitation of native gold. Since it is the country rock alteration that responsible for sulphide and gold deposition, areas that are intensely sericitically and argillically altered are favourable indicators of mineralized epithermal veins.

Certain characteristics of Dawson Range veins that differ from typical (Hedenquist et al., 1996; Arribas, 1995; Heald et al., 1987; Hayba et al., 1985) low sulphidation epithermal deposits include the presence of ore minerals such as enargite, (tennantite and barite), alteration minerals such as sericite and kaolinite, but little or no adularia, and fluids with low pH, high ΣS, and moderately high CO_2. The transitional nature of the epithermal veins could be explained in part by their close association with the shoshonitic Carmacks volcanics. In alkalic low sulphidation epithermal gold deposits, such as the well-known Cripple Creek, Black Hills, Porgera, Ladolam, and Emperor districts, evidence for a significant magmatic fluid component is well-established in the

form of high temperature (≤350°C), high salinities (≤10 wt.% NaCl equiv.), high CO_2, and heavy $\delta^{18}O$ in inclusion fluids (Richards, 1995; Paterson et al., 1989). Spatial and genetic associations between gold-copper mineral deposits and potassic igneous suites have been noted around the Circum-Pacific (Müller and Groves, 1997). Although the mechanism for the relationship is poorly understood, it seems to be a function of a high oxidation state and volatile contents of potassic magmas. Similarities exist between the Dawson Range veins and the Kelian low sulphidation Au deposit in Indonesia, for which comparably hot, saline, and CO_2-rich hydrothermal fluids, and depth of formation of ~1500 m, have been cited as evidence that the deposit is transitional between epithermal and porphyry styles of mineralization (Van Leeuwan et al., 1990; Hedenquist et al., 1996). If the Dawson Range epithermal veins are higher-level analogues of a porphyry system (Hayba et al., 1985; Panteleyev, 1986; Heald et al., 1987), they may correlate with the 70 Ma Casino Cu-Mo-Au deposit, and could have been emplaced below a low sulphidation, high-level vein system typical of hot spring deposits.

The results of this study provide evidence for a regional metallogenic event closely related to a Late Cretaceous shoshonitic magmatic event. Further insights could be obtained by extending the fluid inclusion and isotopic analyses to the porphyry deposits hosted by Mount Nansen and Carmacks intrusions, as well as to a greater number of epithermal veins in the southern Dawson Range. A larger set of fluid inclusion decrepitate or leachate data would better constrain the fluid chemistry and thus the fluid source and evolution. Further gas chromatographic analyses on ore minerals and possibly whole rock volcanic samples would add to the scant CO_2 data set, and confirm the link between volcanism and mineralization. Direct dating of a varied population of veins would provide unequivocal evidence for epithermal metallogenesis. A study of the geochemistry of placer gold in the southern Dawson Range, in comparison to that of lode gold in veins and porphyry bodies might identify the lode source of the extensive placer Au deposits. Lead isotope data from Dawson Range country rocks might define the other end-member of the lead mixing line (Fig. 4.6), and constrain the source of metals in the vein deposits. Although the "transitional" nature of the Dawson Range epithermal

mineralization has not been commonly reported in the literature, it may be a common feature of Au vein mineralization around the Circum-Pacific.

The most fundamental question is the nature of the mechanism linking Au mineralization to potassic or shoshonitic (loosely termed "alkalic") igneous rocks. High-K igneous rocks comprise between 5 and 10% of arc rocks, yet are known to be associated with 40% of the largest epithermal and porphyry deposits of the Circum-Pacific (Müller and Groves, 1997). The relationship between mineral deposits and potassic rocks in within-plate settings, i.e. generated by plumes or extensional tectonics, is not well established, nor well-documented (Müller and Groves, 1997; Mutschler and Mooney, 1993). Moreover, the recent suggestion that the Carlin gold trend may be genetically related to the Yellowstone plume (Oppliger et al., 1997), as has been suggested for the Carmacks group (Johnston et al., 1996; Francis and Johnston, 1998), invites comparison with gold mineralization along the North American Cordillera.

References

Arribas, A. Jr., 1995, Characteristics of high-sulfidation epithermal deposits, and their relation to magmatic fluid: Magmas, Fluids, and Ore Deposits, (ed.) J.F.H. Thompson, MAC Short Course, v. 23, p. 419-454.

Francis, D. and Johnston, S. T., 1998, Isotopic constraints on lithospheric melting near the Yellowstone hotspot, Carmacks volcanics, Yukon: GSA Program with Abstracts, v. x, p. A-90.

Hayba, D. O., Bethke, P. M., Heald, P., and Foley, N.K., 1985, Geologic, Mineralogic, and Geochemical Characteristics of Volcanic-Hosted Epithermal Precious-Metal Deposits: Geology and Geochemistry of Epithermal Systems, Reviews in Economic Geology, v. 2, p. 129-167.

Heald, P., Foley, N. K., and Hayba, D. O., 1987, Comparative Anatomy of Volcanic-Hosted Epithermal Deposits: Acid-Sulfate and Adularia-Sericite Types: Economic Geology, v. 82, p. 1-26.

Hedenquist, J. W., Izawa, E., Arribas, A., and White, N. C., 1996, Epithermal gold deposits: Styles, characteristics, and exploration: Resource Geology Special Publication Number 1, 16 p.

Johnston, S. T., Wynne, P. J., Francis, D., Hart, C. J. R., Enkin, R. J., and Engebretson, D. C., 1996, Yellowstone in Yukon: The Late Cretaceous Carmacks Group: Geology, v. 26, p. 997-1000.

McInnes, B. I. A., Crocket, J. H., and Goodfellow, W. D., 1990, The Laforma deposit, an atypical epithermal-Au system at Freegold Mountain, Yukon Territory, Canada: Epithermal Gold Mineralization of the Circum-Pacific: Geology, Geochemistry, Origin and Exploration, II, (ed.) J.W. Hedenquist, N.C. White, and G. Siddeley, Journal of Geochemical Exploration, v. 36, p. 73-102.

Müller, D., and Groves, D. I., 1997, Potassic Igneous Rocks and Associated Gold-Copper Mineralization: Lecture Notes in Earth Science, v. 56, Springer-Verlag, 238 p.

Mutschler, F. E., and Mooney, T. C., 1993, Precious-metal Deposits Related to Alkalic Igneous Rocks: Provisional Classification, Grad-Tonnage Data and Exploration

Frontiers: Mineral Deposit Modeling, (ed.) R. V. Kirkham, W. D. Sinclair, R. I. Thorpe, J. M. Duke, Geological Association of Canada, Special Paper 40, p. 479-520.

Oppliger, G. L., Murphy, J. B., and Brimhall, G. H., 1997, Is the ancestral Yellowstone hotspot responsible for the Tertiary "Carlin" mineralization in the Great Basin of Nevada?: Geology, v. 25, p. 627-630.

Panteleyev, A., 1986, A Canadian Cordilleran Model for Epithermal Gold-Silver Deposits: Geoscience Canada, v. 13, p. 101-111.

Paterson, C. J., Uzunlar, N., Groff, J., and Longstaffe, F. J., 1989, A View through an Epithermal-Mesothermal Precious Metal System in the Northern Black Hills, South Dakota: A Magmatic Origin for the Ore-Forming Fluids: The Geology of Gold Deposits: The Perspective in 1988, Economic Geology Monograph 6, p. 564-570.

Richards, J. P., 1995, Alkalic-type epithermal gold deposits – a review: Magmas, Fluids, and Ore Deposits, (ed.) J.F.H. Thompson, MAC Short Course, v. 23, p. 367-400.

Sawyer, J. P. B., and Dickinson, R. A., 1976, Mount Nansen: Paper 34, Part B - Porphyry Copper and Copper-Molybdenum deposits of the Calc-Alkaline Suite: Porphyry Deposits of the Canadian Cordillera, Canadian Institute of Mining and Metallurgy Special Volume 15, p. 336-343.

Souther, J. G., 1991, Volcanic Regimes, Chapter 14: Geology of the Canadian Cordillera, (ed.) H. Gabrielse, C.J. Yorath, Geological Survey of Canada, Geology of Canada, No. 4, p. 457-490.

Van Leeuwen, T. M., Leach, T, Hawke, A. A., and Hawke, M. M., 1990, The Kelian disseminated gold deposit, East Kalimantan, Indonesia: Epithermal Gold Mineralization of the Circum-Pacific: Geology, Geochemistry, Origin and Exploration, I, (ed.) J.W. Hedenquist, N.C. White, and G. Siddeley, Journal of Geochemical Exploration, v. 35, p. 1-61.

Wynne, P. J., Enkin, R. J., Baker, J., Johnston, S. T., and Hart, C. J. R., 1998, The big flush: paleomagnetic signature of a 70 Ma regional hydrothermal event in displaced rocks of the northern Canadian Cordillera: Canadian Journal of Earth Sciences, v. 35, p. 657-671.

Appendix I

Dawson Range Fluid Inclusion Microthermometric Data

Mount Nansen Camp

Deposit	Sample	T_h	T_f	T_e*	T_m	Salinity	Mineral
Huestis	MN 9D	283.5			-4.4	7.0	sphalerite
Huestis	MN 9D	277.6			-2.9	4.8	sphalerite
Huestis	MN 9D	281.2	-36.6	-5.5	-3.9	6.3	sphalerite
Huestis	MN 9D	283.4			-5.2	8.1	sphalerite
Huestis	MN 9D	260.1			-2.9	4.8	sphalerite
Huestis	MN 9D	263.2			-3.1	5.1	sphalerite
Huestis	MN 9D	271.5			-3.6	5.8	sphalerite
Huestis	MN 9D	274.2			-3.8	6.1	sphalerite
Huestis	MN 9D	290.0			-5.8	8.9	sphalerite
Huestis	MN 9D	291.0			-4.0	6.4	sphalerite
Huestis	MN 9D	289.0			-2.0	3.4	sphalerite
Huestis	MN 9D	288.0			-5.2	8.1	sphalerite
Huestis	MN 9D	287.0			-4.3	6.9	sphalerite
Huestis	MN 9D	279.0			-3.8	6.1	sphalerite
Huestis	MN 9D	283.0			-5.1	8.0	sphalerite
Huestis	MN 9D	298.8					sphalerite
Huestis	MN 9D	306.3					sphalerite
Huestis	MN 9D	273.1		-19.0	-1.4	2.4	sphalerite
Huestis	MN 9C	300.5					sphalerite
Huestis	MN 9F	289.8					sphalerite
Huestis	MN 9F	287.8					sphalerite
Huestis	MN 95-5	265.5					sphalerite
Huestis	MN 95-5	263.7					sphalerite
Huestis	MN 95-5	250.2					sphalerite
Huestis	MN 95-5	255.9	-42.9	-26.6	-4.1	6.6	sphalerite
Huestis	MN 95-5	267.7	-39.2		-1.9	3.2	sphalerite
Huestis	MN 95-5	250.4	-45.6		-2.5	4.2	sphalerite
Huestis	MN 95-5	250.3	-43.1		-4.2	6.7	sphalerite
Huestis	MN 95-5	242.1	-42.0		-5.1	8.0	sphalerite
Huestis	MN 95-5	235.9	-43.0		-5.1	8.0	sphalerite
Huestis	MN 95-5	239.2	-45.0		-5.1	8.0	sphalerite
Huestis	MN 95-5	238.8	-44.7		-5.1	8.0	sphalerite
Huestis	MN 95-5	241.2	-44.0		-5.1	8.0	sphalerite
Huestis	MN 95-5	231.2	-43.0		-5.1	8.0	sphalerite
Huestis	MN 95-5	270.0	-48.0	-23.0	-10.5	14.5	sphalerite
Huestis	MN 95-5	266.7	-48.0	-22.0	-10.0	14.0	sphalerite
Huestis	MN 95-5	272.6	-48.0	-23.0	-11.8	15.8	sphalerite
Huestis	MN 95-5	269.0	-48.0	-22.0	-10.0	14.0	sphalerite

Mount Nansen Camp

Deposit	Sample	T_h	T_f	T_e^*	T_m	Salinity	Mineral
Tawa	MN 95-10	296.1					sphalerite
Tawa	MN 95-10	210.9					sphalerite
Tawa	MN 95-10	288.8					sphalerite
Tawa	MN 95-10	339.0	-48.4	-13.4	-6.0	9.2	sphalerite
Tawa	MN 95-10	313.9					sphalerite
Tawa	MN 95-10	314.4					sphalerite
Tawa	MN 95-10	337.8					sphalerite
Tawa	MN 95-10	333.6					sphalerite
Tawa	MN 95-10	330.2					sphalerite
Tawa	MN 95-10	330.7					sphalerite
Tawa	MN 95-10	331.0					sphalerite
Tawa	MN 95-10	332.7					sphalerite
Tawa	MN 95-10	330.9					sphalerite
Tawa	MN 95-10	331.3					sphalerite
Tawa	MN 95-10	324.2					sphalerite
Tawa	MN 95-10	324.8					sphalerite
Tawa	MN 95-10	327.1					sphalerite
Tawa	MN 95-10	327.1					sphalerite
Tawa	MN 95-10	334.4					sphalerite
Tawa	MN 95-10	334.3					sphalerite
Tawa	MN 95-10	335.6					sphalerite
Tawa	MN 95-10	332.7					sphalerite
Tawa	MN 95-10	332.0					sphalerite
Tawa	MN 95-10	336.4					sphalerite
Tawa	MN 95-10	331.6					sphalerite
Tawa	MN 95-10	262.3					sphalerite
Tawa	MN 95-10	310.6	-35.2	-22.1	-3.9	6.3	sphalerite
Tawa	MN 95-10	319.7					sphalerite
Tawa	MN 95-10	350.2					sphalerite
Tawa	MN 95-10	344.7					sphalerite
Tawa	MN 95-10	330.0	-30.0		-4.1	6.6	sphalerite
Tawa	MN 95-10	337.0					sphalerite
Tawa	MN 95-10	339.0	-25.4		-6.0	9.2	sphalerite

Freegold Mountain Camp

Deposit	Sample	T_h	T_f	T_e^*	T_m	Salinity	Mineral
Emmons Hill	FG 95-7	138.0					sphalerite
Emmons Hill	FG 95-7	217.4					sphalerite
Emmons Hill	FG 95-7	209.1					sphalerite
Emmons Hill	FG 95-7	278.3					sphalerite
Emmons Hill	FG 95-7	239.0	-48.5	-19.8	-2.1	3.5	sphalerite
Emmons Hill	FG 95-7	243.1					sphalerite
Emmons Hill	FG 95-7	262.4					sphalerite
Emmons Hill	FG 95-7	258.4					sphalerite
Emmons Hill	FG 95-7	308.1					sphalerite
Emmons Hill	FG 95-7	253.8					barite
Emmons Hill	FG 95-7	337.0					barite
Emmons Hill	FG 95-7	262.8					barite
Emmons Hill	FG 95-7	281.3	-38.6		0.0	0.0	barite
Emmons Hill	FG 95-7	311.4	-40.4		-2.3	3.9	barite
Emmons Hill	FG 95-7	312.7	-45.0		-2.1	3.5	barite
Emmons Hill	FG 95-7	298.8	-40.0	-20.5	-3.2	5.2	barite
Emmons Hill	FG 95-7	228.8	-43.0		-2.3	3.9	barite
Emmons Hill	FG 95-7	334.5					barite
Emmons Hill	FG 95-7	324.2					barite
Emmons Hill	FG 95-7	344.6					barite
Emmons Hill	FG 95-7	326.2	-38.5		-4.9	7.7	barite
Emmons Hill	FG 95-7	266.1					barite
Emmons Hill	FG 95-7	290.9					barite
Emmons Hill	FG 95-7	302.1					barite
Emmons Hill	FG 95-7	303.7					barite
Emmons Hill	FG 95-7	317.9					barite

Freegold Mountain Camp

Deposit	Sample	T_h	T_f	T_e*	T_m	Salinity	Mineral
Tinta Hill	FG-TH2A1	306.9			-4.4	7.0	sphalerite
Tinta Hill	FG-TH2A1	292.2			-3.1	5.1	sphalerite
Tinta Hill	FG-TH2A1	275.5			-3.2	5.2	sphalerite
Tinta Hill	FG-TH2A1	283.9			-2.5	4.2	sphalerite
Tinta Hill	FG-TH2A1	270.1			-3.0	4.9	sphalerite
Tinta Hill	FG-TH2A1	290.0			-4.3	6.9	sphalerite
Tinta Hill	FG-TH2A1	280.7			-3.7	6.0	sphalerite
Tinta Hill	FG-TH2A1	288.4	-25.7	-4.2	-4.2	6.7	sphalerite
Tinta Hill	FG-TH2A1	189.6					sphalerite
Tinta Hill	FG-TH2A1	198.1					sphalerite
Tinta Hill	FG-TH2A1	264.7					sphalerite
Tinta Hill	FG-TH2A1	295.0			-4.3	6.9	sphalerite
Tinta Hill	FG-TH2A1	300.0			-3.6	5.8	sphalerite
Tinta Hill	FG-TH2A1	305.0			-4.6	7.3	sphalerite
Tinta Hill	FG-TH2A1	310.0			-4.5	7.2	sphalerite
Tinta Hill	FG-TH2A1	291.0			-4.3	6.9	sphalerite
Tinta Hill	FG-TH2A1	289.0			-4.2	6.7	sphalerite
Tinta Hill	FG-TH2A1	285.4	-44.4		-2.1	3.5	sphalerite
Tinta Hill	FG-TH2A1	275.8	-44.0	-11.1	-4.5	7.2	sphalerite
Tinta Hill	FG-TH2A1	272.3	-44.0		-4.8	7.6	sphalerite
Tinta Hill	FG-TH2A1	293.9		-18.3	-4.2	6.7	sphalerite
Tinta Hill	FG-TH2A1	292.1			-3.6	5.8	sphalerite
Tinta Hill	FG-TH2A1	289.9	-44.8		-4.1	6.6	sphalerite
Tinta Hill	FG-TH2A1	290.8			-5.3	8.3	sphalerite
Tinta Hill	FG-TH2A1	292.6			-6.6	10.0	sphalerite
Tinta Hill	FG-TH2A1	296.0			-6.6	10.0	sphalerite
Tinta Hill	FG-TH2A1	295.1			-6.1	9.3	sphalerite
Tinta Hill	FG-TH2A1	292.2			-5.6	8.7	sphalerite
Tinta Hill	FG-TH2A1	296.4					sphalerite
Tinta Hill	FG-TH2A1	297.8					sphalerite
Tinta Hill	FG-TH2A1	298.0					sphalerite
Tinta Hill	FG-TH2A1	298.4			-2.9	4.8	sphalerite
Tinta Hill	FG-TH2A1	295.9			-3.9	6.3	sphalerite
Tinta Hill	FG-TH2A1	304.6					sphalerite
Tinta Hill	FG-TH2A1	292.7					sphalerite
Tinta Hill	FG-TH2A1	300.1					sphalerite
Tinta Hill	FG TH-B	274.7		-25.0	-4.3	6.9	sphalerite
Tinta Hill	FG TH-B	268.2	-37.1	-14.5	-2.5	4.2	sphalerite
Tinta Hill	FG TH-B	264.2		-26.0	-8.7	12.5	sphalerite
Tinta Hill	FG TH-B	265.5	-39.0	-14.6	-3.5	5.7	sphalerite
Tinta Hill	FG TH-B	293.3	-64.8	-16.4	-5.7	8.8	sphalerite
Tinta Hill	FG TH-B	298.7					sphalerite
Tinta Hill	FG TH-B	301.1					sphalerite
Tinta Hill	FG TH-B	266.8		-21.8	-2.0	3.4	sphalerite
Tinta Hill	FG TH-B	250.7	-47.4	-14.2	-5.6	8.7	sphalerite
Tinta Hill	FG TH-B	298.2					sphalerite
Tinta Hill	FG TH-B	278.9	-46.0	-14.0	-1.8	3.1	sphalerite
Tinta Hill	FG TH-B	254.2					sphalerite

Freegold Mountain Camp

Deposit	Sample	T_h	T_f	T_e*	T_m	Salinity	Mineral
Tinta Hill	FG TH-B	258.9	-52.9	-18.4	-11.8	15.8	sphalerite
Tinta Hill	FG TH-B	279.3	-58.4	-14.5	-1.3	2.2	sphalerite
Tinta Hill	FG TH-B	280.7	-50.0	-13.4	-2.2	3.7	sphalerite
Tinta Hill	FG TH-B	320.6	-46.9	-18.4	-7.0	10.5	sphalerite
Tinta Hill	FG TH-B	297.1	-50.8	-16.8	-2.0	3.4	sphalerite
Tinta Hill	FG TH-B	310.7	-52.0	-11.4	-1.5	2.6	sphalerite
Tinta Hill	FG TH-B	311.6	-48.2	-21.2	-1.9	3.2	sphalerite
Tinta Hill	FG TH-B	256.7	-48.0	-16.4	-1.3	2.2	sphalerite
Tinta Hill	FG TH-B	273.3					sphalerite
Tinta Hill	FG TH-B	278.0					sphalerite
Tinta Hill	FG TH-B	300.1					sphalerite
Tinta Hill	FG TH-B	281.2	-47.1	-12.2	-6.0	9.2	sphalerite
Tinta Hill	FG TH-B	300.6	-49.8	-16.2	-2.4	4.0	sphalerite
Tinta Hill	FG TH-B	292.7	-51.7	-12.6	-1.6	2.7	sphalerite
Tinta Hill	FG TH-B	253.1	-49.8	-15.2	-2.1	3.5	sphalerite
Tinta Hill	FG TH-B	255.7		-18.5	-1.5	2.6	sphalerite
Tinta Hill	FG TH-B	290.3	-52.8	-14.5	-2.9	4.8	sphalerite
Tinta Hill	FG TH-B	288.3	-53.7	-13.3	-1.0	1.7	sphalerite
Tinta Hill	FG TH-B	289.6	-48.1	-12.5	-2.0	3.4	sphalerite
Tinta Hill	FG TH-B	277.2					sphalerite
Tinta Hill	FG TH-B	287.2	-52.2	-12.1	-1.6	2.7	sphalerite
Tinta Hill	FG TH-B	257.7					sphalerite
Tinta Hill	FG TH-B	252.3					sphalerite
Tinta Hill	FG TH-B	264.2					sphalerite
Tinta Hill	FG TH-B	268.9					sphalerite
Tinta Hill	FG TH-B	277.8					sphalerite
Tinta Hill	FG TH-B	279.0					sphalerite
Tinta Hill	FG TH-B	298.0					sphalerite
Tinta Hill	FG TH-B	292.1					sphalerite
Tinta Hill	FG TH-B	288.2					sphalerite
Tinta Hill	FG TH-B	288.9					sphalerite
Tinta Hill	FG TH-B	306.6					sphalerite
Tinta Hill	FG TH-B	292.1					sphalerite
Tinta Hill	FG TH-B	283.8					sphalerite
Tinta Hill	FG TH-B	301.1					sphalerite
Tinta Hill	FG TH-B	297.7					sphalerite
Tinta Hill	FG TH-B	303.0					sphalerite
Tinta Hill	FG TH-B	293.2					sphalerite
Tinta Hill	FG TH-B	297.1					sphalerite
Tinta Hill	FG TH-B	281.7					sphalerite
Tinta Hill	FG TH-B	283.1					sphalerite
Tinta Hill	FG TH-2C	128.0	-35.8	-15.8	-1.3	2.2	sphalerite
Tinta Hill	FG TH-2C	116.1	-35.0	-14.8	-1.2	2.1	sphalerite
Tinta Hill	FG TH-2C	117.0			-1.0	1.7	sphalerite
Tinta Hill	FG TH-2C	116.0			-1.4	2.4	sphalerite
Tinta Hill	FG TH-2C	115.0			-1.2	2.1	sphalerite
Tinta Hill	FG TH-2C	115.5			-1.3	2.2	sphalerite
Tinta Hill	FG TH-2C	116.5			-1.1	1.9	sphalerite
Tinta Hill	FG TH-2C	116.3			-1.4	2.4	sphalerite

Freegold Mountain Camp

Deposit	Sample	T_h	T_f	T_e*	T_m	Salinity	Mineral
Tinta Hill	FG TH-2C	115.8			-1.2	2.1	sphalerite
Tinta Hill	FG TH-2C	120.0	-41.0		-2.0	3.4	sphalerite
Tinta Hill	FG TH-2C	232.3					sphalerite
Tinta Hill	FG 95-15	296.3	-45.1	-29.2	-4.2	6.7	sphalerite
Tinta Hill	FG 95-15	298.0	-49.2		-5.5	8.5	sphalerite
Tinta Hill	FG 95-15	294.8	-47.6	-24.7	-5.6	8.7	sphalerite
Tinta Hill	FG 95-15	297.7	-49.0		-5.5	8.5	sphalerite
Tinta Hill	FG 95-15	295.1					sphalerite
Tinta Hill	FG 95-15	298.9					sphalerite
Tinta Hill	FG 95-15	298.7			-5.7	8.8	sphalerite
Tinta Hill	FG 95-15	289.6	-48.1	-15.1	-2.9	4.8	sphalerite
Tinta Hill	FG 95-15	281.9			-3.0	4.9	sphalerite
Tinta Hill	FG 95-15	283.0			-2.8	4.6	sphalerite
Tinta Hill	FG 95-15	285.0			-3.1	5.1	sphalerite
Tinta Hill	FG 95-15	287.0			-2.7	4.5	sphalerite
Tinta Hill	FG 95-15	300.0	-46.6		-6.4	9.7	sphalerite
Tinta Hill	FG 95-15	301.0	-46.6		-6.4	9.7	sphalerite
Tinta Hill	FG 95-15	299.6	-47.8	-20.2	-5.5	8.5	sphalerite
Tinta Hill	FG 95-15	303.3					sphalerite
Tinta Hill	FG 95-15	300.0			-5.8	8.9	sphalerite
Tinta Hill	FG 95-15	249.2	-46.3	-20.7	-4.4	7.0	sphalerite
Tinta Hill	FG 95-15	246.2	-41.0		-7.2	10.7	sphalerite
Tinta Hill	FG 95-15	255.8	-42.0		-6.4	9.7	sphalerite
Tinta Hill	FG 95-15	242.3	-46.3		-4.4	7.0	sphalerite
Tinta Hill	FG 95-15	249.2	-44.3		-4.4	7.0	sphalerite
Tinta Hill	FG 95-15	241.6	-42.0		-6.4	9.7	sphalerite
Tinta Hill	FG 95-15	246.3	-42.0		-6.4	9.7	sphalerite
Tinta Hill	FG 95-15	249.5	-32.5				sphalerite
Tinta Hill	FG 95-15	260.5					sphalerite
Tinta Hill	FG 95-15	247.8					sphalerite
Tinta Hill	FG 95-15	298.6			-5.8	8.9	sphalerite
Tinta Hill	FG 95-15	289.3					sphalerite
Tinta Hill	FG 95-15	294.6	-47.1		-5.4	8.4	sphalerite
Tinta Hill	FG 95-15	278.8	-45.0				sphalerite
Tinta Hill	FG 95-15	283.8	-47.1	-22.6	-4.2	6.7	sphalerite
Tinta Hill	FG 95-15	296.8					sphalerite
Tinta Hill	FG 95-15	283.1					sphalerite
Tinta Hill	FG 95-15	283.6					sphalerite
Tinta Hill	FG 95-15	282.6					sphalerite
Tinta Hill	FG 95-15	284.5					sphalerite
Tinta Hill	FG 95-15	291.4					sphalerite
Tinta Hill	FG 95-15	259.5					sphalerite
Tinta Hill	FG 95-15	293.7		-24.8	-3.8	6.1	sphalerite
Tinta Hill	FG 95-15	286.6	-44.4	-20.4	-5.7	8.8	sphalerite
Tinta Hill	FG 95-15	268.5	-40.9		-4.8	7.6	sphalerite

Prospector Mountain Camp

Deposit	Sample	T_h	T_f	T_e*	T_m	Salinity	Mineral
Frog	PR 95-18	384.1					quartz
Frog	PR 95-18	340.9					quartz
Frog	PR 95-18	344.6					quartz
Frog	PR 95-18	298.7			-2.8	4.6	quartz
Frog	PR 95-18	305.7			-3.4	5.5	quartz
Frog	PR 95-18	303.2			-2.8	4.6	quartz
Frog	PR 95-18	299.1	-42.0		-3.1	5.1	quartz
Frog	PR 95-18	304.7	-40.6		-2.1	3.5	quartz
Frog	PR 95-18	284.2	-42.5		-0.3	0.5	quartz
Frog	PR 95-18	264.6			-5.2	8.1	quartz
Frog	PR 95-18	318.2					quartz
Frog	PR 95-18	318.7					quartz
Frog	PR 95-18	317.7					quartz
Frog	PR 95-18	318.2					quartz
Frog	PR 95-18	325.4	-39.0		-4.3	6.9	quartz
Frog	PR 95-18	299.6	-44.2		-1.9	3.2	quartz
Frog	PR 95-18	243.5			-3.9	6.3	quartz
Frog	PR 95-18	303.2	-42.6		-3.8	6.1	quartz
Frog	PR 95-18	301.9	-43.8		-3.8	6.1	quartz
Frog	PR 95-18	302.5	-43.0		-3.8	6.1	quartz
Frog	PR 95-18	303.0	-43.0		-3.8	6.1	quartz
Frog	PR 95-18	302.9	-43.0		-3.8	6.1	quartz
Frog	PR 95-18	286.0	-45.1		-3.0	4.9	quartz
Frog	PR 95-18	304.3	-42.6		-2.3	3.9	quartz
Frog	PR 95-18	298.3		-21.4	-3.8	6.1	quartz
Lilypad	*LP-4*	*330.0*			*-2.0*	*3.7*	*quartz*
Lilypad	*LP-4*	*306.0*			*-2.0*	*3.7*	*quartz*
Lilypad	*LP-4*	*281.0*			*-2.5*	*4.7*	*quartz*
Lilypad	*LP-4*	*303.0*			*-2.1*	*3.9*	*quartz*
Lilypad	*LP-4*	*327.0*			*-2.2*	*4.1*	*quartz*
Lilypad	*LP-4*	*313.0*			*-2.6*	*4.9*	*quartz*
Lilypad	*LP-4*	*299.0*		*-20.0*	*-3.0*	*5.7*	*quartz*
Lilypad	*LP-4*	*310.0*		*-18.0*	*-3.2*	*6.1*	*quartz*
Lilypad	*LP-4*	*313.0*		*-18.0*	*-3.3*	*6.3*	*quartz*
Lilypad	*LP-4*	*313.0*		*-18.0*	*-3.1*	*5.9*	*quartz*
Lilypad	*LP-4*	*297.0*		*-18.0*	*-3.6*	*6.9*	*quartz*
Lilypad	*LP-4*	*331.0*		*-17.0*	*-3.4*	*6.5*	*quartz*
Lilypad	*LP-4*	*304.0*		*-19.0*	*-3.3*	*6.3*	*quartz*
Lilypad	*LP-4*	*312.0*		*-16.0*	*-3.2*	*6.1*	*quartz*

The above italicized data are from Hart and Selby

NB: T_e* in most cases is not the accurate T_e but the temperature of first visible change, usually vapour bubble movement